Università degli Studi di Padova

Dipartimento di Scienze Biomediche

CORSO DI DOTTORATO DI RICERCA IN SCIENZE BIOMEDICHE

XXXIV CICLO

CFTR correctors as a novel pharmacological approach for sarcoglycanopathies

Coordinatore: Chiar.mo Prof. Fabio Di Lisa

Supervisore: Chiar.ma Prof.ssa Dorianna Sandonà

Dottoranda: Dott.ssa Martina Scano

CONTENTS

ABSTRACT

Sarcoglycanopathies or LGMDR3-6 are rare autosomal recessive disease, affecting mainly the limb proximal musculature that are still without a cure. The onset occurs in childhood, the disease is progressive, very often forcing affected subjects to the wheelchair, even though mild forms may present with late onset and slow progression. Sarcoglycanopathies are caused by mutations in genes coding for sarcoglycans (SG). SG are four glycoproteins forming a tetramer in skeletal and cardiac muscle, located at the sarcolemma that plays a crucial role in protecting the membrane from damages due to muscle contraction. It has been observed that missense mutations, the majority of the reported cases, result in a folding defective, even though potentially functional protein, that is recognized and prematurely discarded by the cell quality control (QC). Lacking one subunit, the SG-complex is disrupted, and the consequent loss of function leads to progressive muscle degeneration. To counteract this harmful process, we proposed to help SGs folding using small molecules, called CFTR correctors, developed to correct mutated cystic fibrosis transmembrane regulator (CFTR) channel, defective in folding and trafficking.

The effective rescue of different SG mutants has been proved for some of such molecules by using cell models and, importantly, myogenic cells from LGMDR3 patients. In these pathological cells we evidenced the possibility to combine correctors to gain an additive or even synergic effect in LGMDR3 myotubes. Furthermore, thanks to the availability of myogenic cells from a LGMDR4 subject, we had the possibility to verify the efficacy of CFTR correctors in the other forms of sarcoglycanopathy. Lastly, once correctors have been successfully tested *in vitro*, there was the need for animal models in which proving efficacy and safety of this pharmacological approach. To this intent and to overcome the unsuitability of the already existing sarcoglycanopathy murine models, we generated a novel mouse model of LGMDR3. This model is characterized by humanized hind limbs, resulting from the injection of the human α-SG sequence, either wild-type or carrying a missense mutation, via adeno associated virus 1 (AAV1). The transduction was performed in the background of *sgca*-null newborn mice to assure muscle development in the presence of either the wild-type or mutated human protein and to induce tolerance toward the transgene. Mice expressing R98H α-SG in hind limbs, well mimicking the human pathologic phenotype, were used to test the efficacy of the most promising, according to *in vitro* data, CFTR corrector, C17. The systemic and chronic administration of the C17 molecule successfully rerouted the SG-complex containing the human α-SG R98H mutant to the sarcolemma, with a clear amelioration of the dystrophic phenotype. Notably, the force of the C17 treated muscle was fully recovered, reaching levels almost identical to the WT, healthy muscles. In addition, the preliminary C17 pharmacokinetic characterization evidenced a large blood stability, in *in vitro* experiments, and the resistance to metabolization from both cytochromes P450 (CYPs) and UDP glucuronosyltransferases (UGTs), enzymes present in extracted liver microsomes.

Altogether, the *in vitro* and *in vivo* data, are the proof of concept of C17 efficacy in LGMDR3 cases, opening a new way of therapeutic intervention for the forms of sarcoglycanopathy characterized by missense mutation.

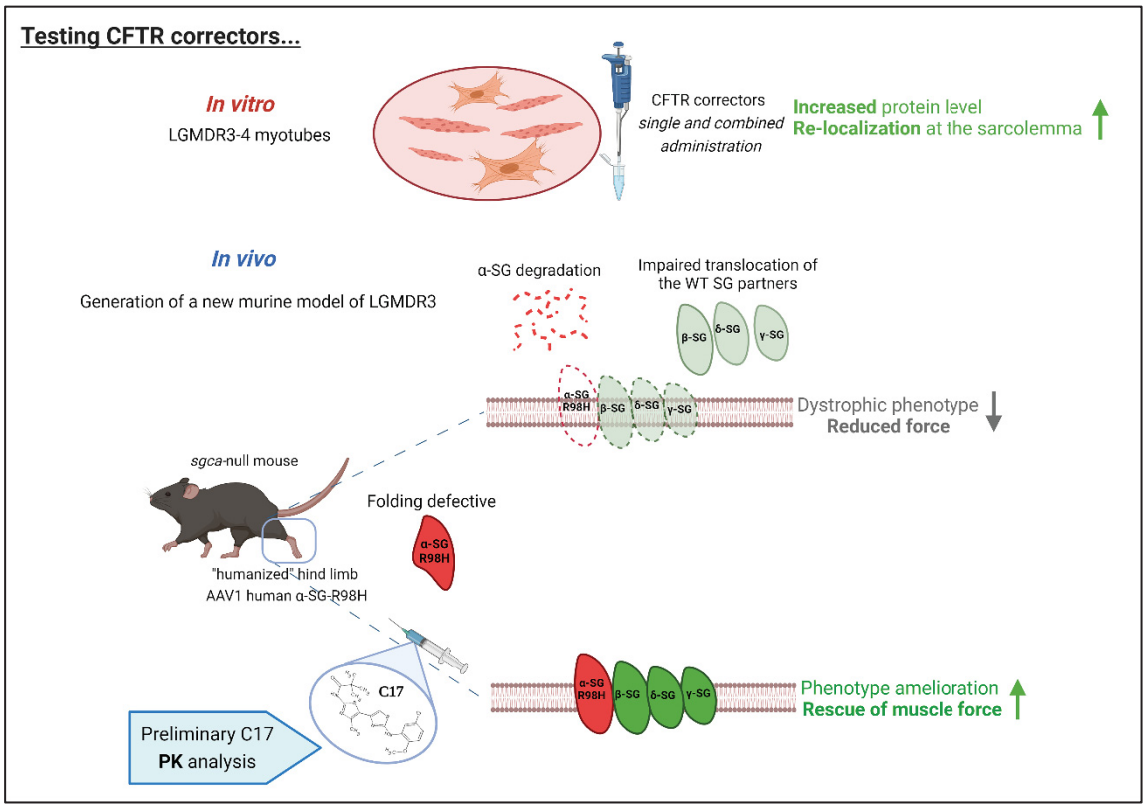

Graphical abstract. Pipeline of the strategy utilized to test the efficacy of CFTR correctors, either *in vitro* and *in vivo*. Created with Biorender.com

RIASSUNTO

Le sarcoglicanopatie o LGMDR3-6 sono rare malattie autosomiche recessive incurabili che colpiscono principalmente i muscoli prossimali degli arti. L'esordio avviene in età infantile, la malattia è progressiva, costringendo molto spesso i soggetti alla sedia a rotelle. Sono note anche forme più lievi con esordio tardivo e lenta progressione. Le sarcoglicanopatie sono causate da mutazioni nei geni codificanti i sarcoglicani (SG). I SG sono quattro glicoproteine che formano un tetramero nel muscolo scheletrico e cardiaco, localizzato nel sarcolemma, cruciale nella protezione della membrana dallo stress meccanico dovuto alla contrazione muscolare. È stato osservato che le mutazioni missenso, che rappresentano la maggior parte dei casi riportati, producono una proteina con un "folding" difettoso che, anche se potenzialmente funzionale, viene riconosciuta e degradata dal sistema di controllo qualità della cellula. A causa della mancanza di una subunità, il complesso del SG viene distrutto e la conseguente perdita di funzione determina danni al sarcolemma con progressiva degenerazione muscolare. Per contrastare questo processo, il nostro approccio intende aiutare il corretto ripiegamento dei SG utilizzando piccole molecole sviluppate per correggere la proteina CFTR (cystic fibrosis transmembrane regulator) che quando mutato può presentare difetti nel ripiegamento e nella corretta localizzazione.

L'efficacia di alcuni correttori del CFTR nel recupero di diversi mutanti del SG è stata provata utilizzando modelli cellulari e cellule miogeniche provenienti da pazienti LGMDR3. Usando queste cellule abbiamo qui verificato l'uso combinato dei correttori ottenendo un effetto additivo o addirittura sinergico. Inoltre, grazie alla disponibilità di cellule miogeniche di un soggetto LGMDR4, abbiamo provato l'efficacia dei correttori del CFTR nelle altre forme di sarcoglicanopatia. Infine, una volta valutato l'effetto dei correttori *in vitro*, era necessario validare l'efficacia *in vivo*. A questo scopo e per superare l'inadeguatezza dei modelli murini di sarcoglicanopatia esistenti abbiamo generato un nuovo modello di LGMDR3, caratterizzato da arti posteriori umanizzati, esprimenti la sequenza umana di α-SG. La sequenza umana, wild-type o mutata, è stata trasdotta con il virus adeno-associato di sierotipo 1 (AAV1). La trasduzione è stata effettuata nel background dei topi *sgca*-null neonati che non presentano il gene dell'α-SG murino che viene così rimpiazzato dalla proteina umana veicolata dal virus. La precoce trasduzione assicura che il muscolo si sviluppi in presenza del sarcoglicano umano, wild-type o mutato, e che insorga tolleranza immunologica verso il transgene. I topi con arti posteriori umanizzati esprimenti l'α-SG con la mutazione R98H hanno sviluppato e riprodotto con alta fedeltà la patologia umana. Di conseguenza, sono stati utilizzati per testare l'efficacia del correttore del CFTR più promettente, il C17, secondo i dati raccolti *in vitro*. La somministrazione sistemica in cronico della molecola C17 ha reindirizzato con successo il complesso del SG al sarcolemma, inducendo un forte miglioramento del fenotipo distrofico. È importante sottolineare che la forza dei muscoli dei topi trattati ha raggiunto livelli quasi identici a quelli di muscoli WT.

Inoltre, la preliminare caratterizzazione farmacocinetica *in vitro* della molecola C17 ha evidenziato un'ampia stabilità nel sangue e la resistenza alla metabolizzazione da parte dei citocromi P450 (CYP) e dagli UDP glucuronosiltransferasi (UGT), enzimi presenti nei microsomi estratti da fegato murino.

Complessivamente, i dati *in vitro* ed *in vivo* sono il "proof of concept" dell'efficacia del C17 nei casi di LGMDR3, e aprono nuove possibilità di intervento terapeutico per tutte le forme di sarcoglicanopatia caratterizzate da mutazione missenso.

1. INTRODUCTION

Muscular dystrophies (MDs) are a heterogeneous group of genetically inherited degenerative disorders sharing clinical features of progressive muscle weakness and dystrophic pathological appearance on muscle biopsy.

Molecular genetic tools have allowed the identification of more than 40 genes involved in muscular dystrophies, including very rare variants (Mercuri et al., 2019).

MDs can be classified as X-linked diseases, autosomal recessive diseases or autosomal dominant diseases. The classification comprises conditions affecting daily-life activities, with different degree of severity of symptoms, age of onset, extent and distribution of muscle weakness, family history and genetic cause.

Among the different classification, they can be divided on the bases of the major group of conditions, and the genes responsible for their causation, together with function of the responsible proteins (Mercuri et al., 2019).

Congenital muscular dystrophies are typically due to mutations in proteins located in the extracellular matrix, or external membrane proteins or enzymes involved in post translational modification of such proteins. Mutations in nuclear proteins typically result in Emery- Dreifuss muscular dystrophy whereas defects in sarcolemmal and sarcomeric proteins mostly cause limb girdle muscular dystrophies (figure 1). Additional common variants are Duchenne muscular dystrophy, Becker muscular dystrophy, facioscapulohumeral muscular dystrophy, oculopharyngeal muscular dystrophy, which were already recognised and clearly described because of their unique features and high incidence.

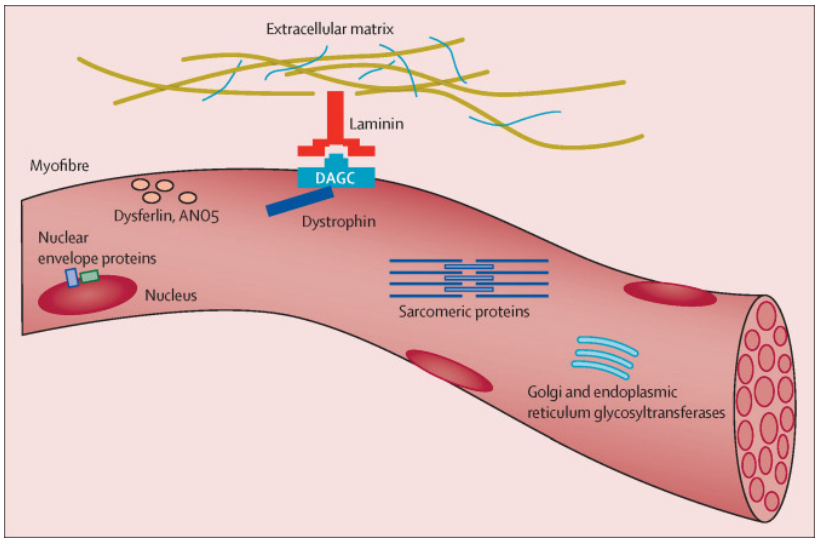

Figure 1. **Schematic representation of the major classes of proteins involved in muscular dystrophies *(Mercuri, Bonnemann et al., 2019).*** DAGC=dystrophin-associated glycoprotein complex. ANO5=anoctamin 5 protein.

John Walton and Frederick Nattrass in 1954 used for the first time the definition "*Limb Girdle Muscular Dystrophy*", abbreviated in "*LGMD*" to identify a genetic disorder as a separated pathophysiological entity from the Duchenne and Becker MDs. Even though the various forms of LGMD do not share a common pathophysiological mechanism (figure 2), there are few common features. Indeed, except for autosomal inheritance, which could be dominant or recessive, LGMD are characterized by onset usually in the first, second or third decade, muscular weakness in either the shoulder and pelvic girdle, relatively slow course, which however leads to severe disablement and often premature death (Thompson & Straub, 2016).

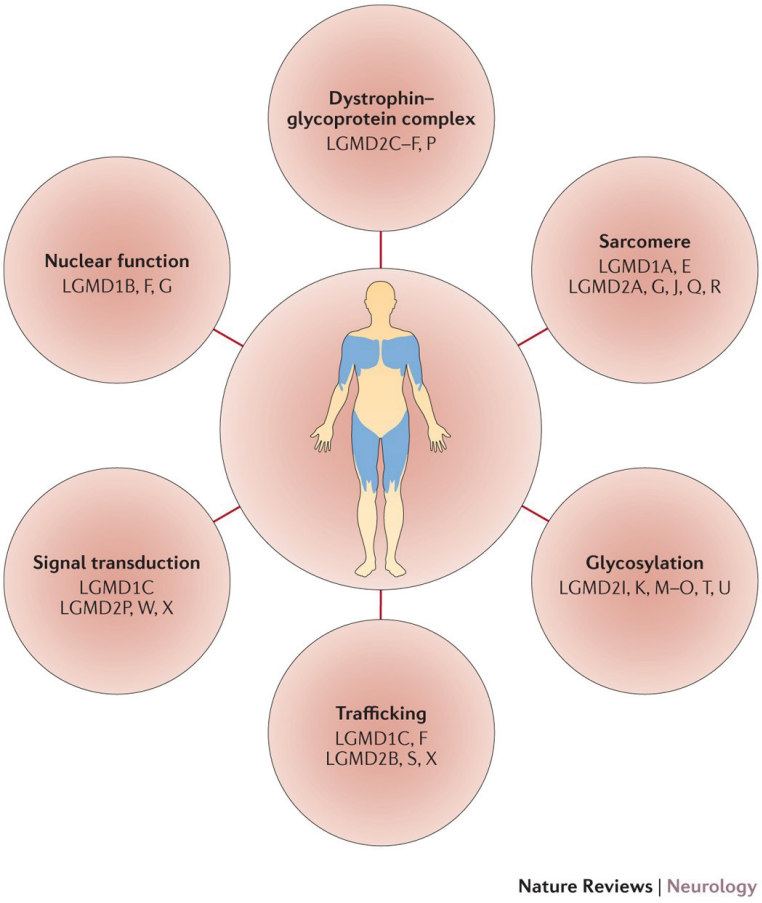

Figure 2. The primary events in LGMD forms are different and may affect several aspects of muscle physiology (Thompson & Straub, 2016).

1.1 Sarcoglycanopathies

All forms of LGMD are rare, and all are autosomal inherited. They are classified into dominant forms (LGMD-D) and recessive forms (LGMD-R) (Straub, Murphy et al., 2018). Recessive forms are characterized by both higher number of subtypes and prevalence, with regional variation owing to founder effects in some cases. Some of the rarest forms affect only few families in the world (Thompson & Straub, 2016).

The term ‘rare disease’ is used to describe conditions that affect a small proportion of the population; in the USA they are described as affecting fewer than 200 000 people and in Europe as affecting fewer than one in 2000. Although the terms are often used interchangeably, “orphan diseases” are defined as diseases that are underappreciated or ignored by the medical community and do not have an effective cure (Pogue, Cavalcanti et al., 2018).

Even if they are individually rare, these conditions affect up to 10% of the worldwide population representing a significant impact on health. For this reason, it is important to be aware of the resources that exist to support their diagnosis, management, and treatment (Pogue et al., 2018).

The term “sarcoglycanopathies” identifies a subgroup of rare autosomal recessive LGMD due to mutations in the genes coding for one of the four proteins composing the sarcoglycan (SG) complex, located at the sarcolemma of skeletal and cardiac muscle. As summarized in table 1, according to this classification, we distinguish α-sarcoglycanopathy (LGMDR3), β-sarcoglycanopathy (LGMDR4), γ-sarcoglycanopathy (LGMDR5), δ-sarcoglycanopathy (LGMDR6).

This nomenclature is in accordance with the update of (Straub et al., 2018) and replaces the previous one (reported in brackets).

DISEASE	***GENE***	***PROTEIN***	***LENGHT (aa)***
LGMDR3 (LGMD2D)	*SGCA*	α-SG	387
LGMDR4 (LGMD2E)	*SGCB*	β-SG	318
LGMDR5 (LGMD2C)	*SGCG*	γ-SG	291
LGMDR6 (LGMD2F)	*SGCD*	δ-SG	290

Table 1. Classification of sarcoglycanopathy forms according to the mutated gene.

The name and the amino acidic length of the protein encoded by the mutated gene responsible for the development of the disease are also reported.

The prevalence of LGMDR3–6 varies among different populations. For example, the prevalence in Northern England has been estimated in 0.27/100 000 while the prevalence is approximately 0.56/100 000 in Northeastern Italy (Carotti et al., 2017).

Despite this, LGMDR3 is the most frequently reported form of sarcoglycanopathy in most countries, followed by LGMDR5 (which, however, is the most frequent form in Maghreb, India, and European Rom gypsy population) and by LGMDR4 and LGMDR6.

From a clinical point of view, sarcoglycanopathies are a group of heterogeneous diseases in which the proximal musculature of pelvic and shoulder girdles undergoes a progressive wasting.

Most cases are characterized by early onset and rapid progression, with patients becoming wheelchair bound during adolescence. Milder phenotypes characterized by late onset and preserved ambulation until adulthood are also reported (Alonso-Perez, Gonzalez-Quereda et al., 2020, Gonzalez-Quereda, Gallardo et al., 2018, Oliveira Santos, Coelho et al., 2020, Tarakci & Berger, 2016).

On average, the earlier the onset, the more rapid the progression, even if in some cases the progression could not be linear. Interestingly, symptoms variability has been reported among members of the same family and even between siblings (Angelini, Fanin et al., 1998, Takano, Bonnemann et al., 2000). This could be due to both genetic (i.e. intragenic polymorphisms, modifier genes) and non-genetic factors (i.e. nutrition, sport activity, body mass index, use of drugs, infections, inflammatory processes) (Angelini & Fanin, 2016).

In various populations, the frequency of severe childhood-onset LGMD ranges between 22 to 69% of cases, whereas LGMD adult-onset is only 4-8%. This is also related to the fact that severe childhood-onset LGMD patients have a higher probability of obtaining a molecular diagnosis than adult ones (Angelini & Fanin, 2016).

Despite the time of onset, the disease is invariably progressive, and muscle weakness eventually involves the respiratory muscle, with the patient's need for respiratory support.

Cardiomyopathy may occur in all forms, although rarely in LGMDR3, while cognitive impairment has never been reported. Other features of sarcoglycanopathy are elevated levels of serum creatine kinase (more than 10 times the upper limit in the first phases of the disease), calf hypertrophy, and scapular winging. Contractures and scoliosis commonly develop during the disease because of increasing weakness and fibrotic degeneration of skeletal muscles (Bushby, Finkel et al., 2010, Carotti et al., 2017). Currently, a treatment for sarcoglycanopathy is not available. Cell and gene therapy-based approaches are under investigation, even if few published cell-therapy clinical trials in DMD have not demonstrated substantial recovery (Biressi, Filareto et al., 2020, Negroni, Bigot et al., 2016). In addition, although interesting and promising results have been obtained with the gene therapy (Mendell, Chicoine et al., 2019), it still must overcome several challenges to become a productive strategy. Among others, there is the difficult of delivering the gene to skeletal muscle, which is the most abundant tissue of human body, the problem of immunogenicity of the viral vector and of the transgene (if the protein is totally absent in the patient), etc. Thus, presently, the unique pharmacological intervention is based on the use of corticosteroids to alleviate symptoms and possibly delay the course of the disease. Furthermore, patients require supportive care, such as physiotherapy, which should start immediately after diagnosis to prevent joint deformity, and constant medical surveillance to support respiration and prevent cardiac failure (Carotti et al., 2017).

1.2 Cytoskeleton of skeletal muscle: dystrophin associated protein complex

Skeletal muscle has an elaborate network of proteins responsible for translating the shortening of the sarcomeres into force capable of moving bones to permit locomotion and any other activity. These proteins, collectively known as the dystrophin associated protein complex (DAPC), link the actin cytoskeleton to laminin in the extracellular matrix (ECM).

Furthermore, the DAPC protects the muscle fiber from damage stabilizing the sarcolemma during repeated cycles of contraction and relaxation.

There is also evidence that the DAPC is involved in cell signalling via its interactions with calmodulin, Grb2 and nNOS (Rando, 2001). Almost all the members of the DAPC are implicated in muscle diseases, evidencing the role of this complex in the maintenance of muscle integrity (figure 3).

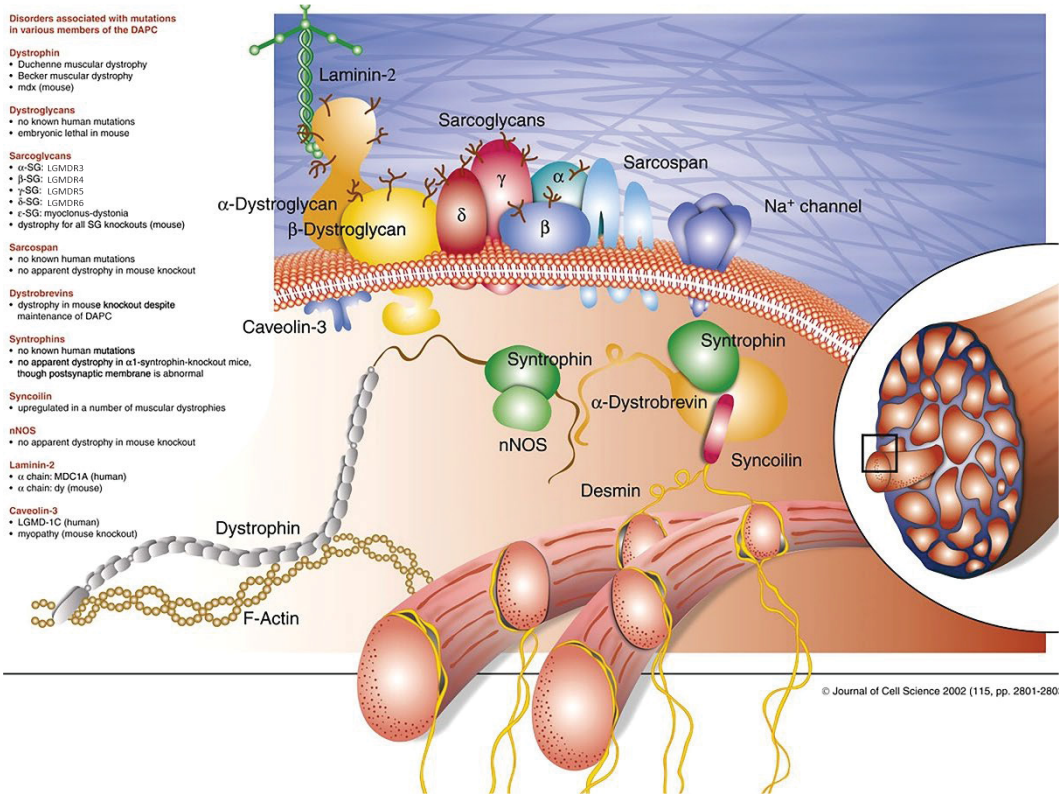

Figure 3. The dystrophin-associated protein complex (DAPC). Adapted from (Ehmsen, Poon et al., 2002).

Major known proteins that constitute the DAPC and the disorders associated by their mutations.

1.2.1 Structure and composition of the DAPC

The members of this complex, whose composition depends on the muscle type, are:

1. *Dystrophin*: a large intracellular protein of 427 kDa that binds to actin through the N-terminal domain. It is characterized by a cysteine-rich C-terminus region allowing binding to β-dystroglycan and the assembly of the DAPC and a long central domain (rod domain) containing several spectrin-like repeats. Dystrophin deficiency results in loss of the associated protein complex and severe muscular dystrophy called Duchenne muscular dystrophy (DMD). A mild phenotype (Becker muscular dystrophy, BMD) may develop when the N- and C-termini of dystrophin are preserved because of in frame deletions in the rod-domain (Ehmsen et al., 2002).
2. *Dystroglycans* (DGs). They make up the core of the DAPC, establishing the transmembrane link between laminin-2 and dystrophin.

The widely expressed α- and β-DG are produced from a single polypeptide which is post-translationally cleaved. They are highly glycosylated prior to being sorted to their respective extracellular and transmembrane locations.

These glycosylation patterns are largely correlated to the tissues of expression (Winder, 2001). The deletion of DG in mouse is embryonically lethal, suggesting that it is indispensable for survival. Hypoglycosylation of α-dystroglycan has been linked to muscular dystrophy phenotypes, with variable degrees of cognitive impairments, collectively termed dystroglycanopathies. The disease can be distinguished in primary dystroglycanopathy, when defects are on *DAG1,* the gene coding for dystroglycans, secondary or tertiary when mutations are on gene coding for glycosyltransferases or enzymes involved in the synthesis of the carbohydrate building blocks (Brancaccio, 2019, Sheikh, Halmo et al., 2017).

3. *Sarcoglycans (SGs)*. In the skeletal muscle, four subunits constitute the SG subcomplex interacting with DG, sarcospan and dystrophin. Dystrophin and γ-SG can interact directly, and δ sarcoglycan appears to be coordinated to the DG complex (Chan, Bonnemann et al., 1998). Mutations impairing the expression of any one of the SGs cause the loss or strong reduction of the other subunits from the sarcolemma, causing four recessive limb girdle muscular dystrophy forms (Bushby, 1999).
4. *Dystrobrevin*: Alternative splicing produces five α-dystrobrevin isoforms, differing as C-terminal truncations. Three of them are found in muscle, but only α-dystrobrevin-2 is abundantly expressed at the sarcolemma. As dystrobrevin contains several tyrosine-kinase consensus sites, protein-protein interactions may also be regulated by tyrosine phosphorylation. Dystrobrevin and dystrophin associate via coiled-coil interactions, but an independent link with the SG/sarcospan complex might also exist. Indeed, dystrobrevin and syntrophin can bind to the DAPC in the absence of the C-terminal region of dystrophin. Interestingly, dystrobrevin-knockout mice present a DMD-like phenotype.
5. *Synthrophins*. They are intracellular DAPs (dystrophin-associated proteins) that interacts to the dystrophin C-terminus and to dystrobrevins. Syntrophins may function as modular adaptors in recruiting signalling proteins to the sarcolemma and DAPC (Rando, 2001). α1-Syntrophin mutations, the most abundant isoform in heart, have been associated with long QT syndrome (Ueda, Valdivia et al., 2008, Wu, Ai et al., 2008).
6. *Neuronal nitric oxide synthase (nNOS*). The production of nitric oxide (NO) by nNOS is important for increasing local blood flow to match the increased metabolic load of contracting muscles. This protein interacts through PDZ domain with syntrophin. Abolishing nNOS expression alone in mice does not cause dystrophy. However, the loss of nNOS could cause functional ischemia contributing to skeletal and cardiac muscle cell injury in DMD, even though the underlying pathophysiology and extent of effects are still unknown (Dombernowsky, Olmestig et al., 2018, Zhao, Yang et al., 2019).

7. *Sarcospan*. Sarcospan is a 25 kDa membrane protein with four transmembrane domains and intracellular N- and C-termini. It's tightly associated with the SG complex. No human disease is currently associated with sarcospan deficiency.

1.3 Sarcoglycan complex: structure and biogenesis

As already mentioned, in striated muscle, the SG complex is part of the DAPC and it contributes to connect the intracellular cytoskeleton to the ECM, having a role in protecting sarcolemma from possible damage elicited during muscle contraction.

1.3.1 Sarcoglycans structure

SGs are four glycosylated proteins (α, β, γ, and δ) with a large extracellular domain, a transmembrane helix and a short cytosolic tail expressed primarily in skeletal and cardiac muscle. α -SG (50 kDa) is a type I membrane protein, whereas β-(43 kDa), γ-(35 kDa), and δ-SG (35 kDa) are type II membrane proteins together forming a heterocomplex by unitary stoichiometry (figure 4). Furthermore, two additional SGs have been identified, ε- SG and ζ-SG. The former is homologous to α-SG (43% identical), whereas the second is closely related to δ- and γ-SG (62% of similarity) (Wheeler, Zarnegar et al., 2002). Both are nonstriated- muscle SGs that are primarily expressed in smooth muscle, the brain, and the cerebellum (Ettinger, Feng et al., 1997, Wheeler et al., 2002). ε- SG is expressed in skeletal muscle too, however at a low concentration in comparison to α-SG (Imamura, Mochizuki et al., 2005, Liu & Engvall, 1999).

Even though SGs have no homology with other known proteins, as a proof of their important role during evolution, they share some features. Indeed, a cysteine cluster is present in the extracellular domain of all SGs which could be important for the tertiary structure of the protein and for complex assembly. All four SGs possess putative phosphorylation sites in the intracellular domain, indicating a possible post-translational modulation of the protein or complex.

Moreover, α-SG has a cadherin-like domain and Ca^{2+}-binding pockets, which have also been described in α-DG, suggesting a possible Ca^{2+}-dependent heterotypic adhesion between the two proteins (Dickens, Beatson et al., 2002).

α -SG has also a putative ATP-binding site in the extracellular domain, which is conserved in all species and presumably it is involved in the modulation of the extracellular ATP concentration (Betto, Senter et al., 1999, Sandona, Gastaldello et al., 2004).

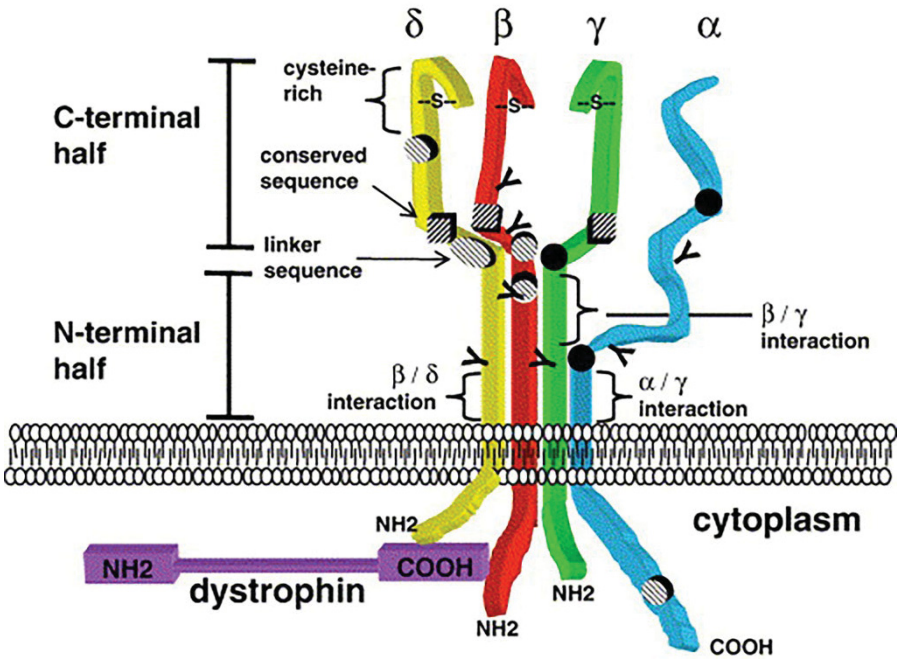

Figure 4. Sarcoglycan complex structure (Chen, Shi et al., 2006).

1.3.2 Sarcoglycan complex biogenesis

Sarcoglycans are co-translationally translocated in the endoplasmic reticulum (ER), where they undergo folding and maturation with glycosylation and disulphide-bond formation (Sandona & Betto, 2009).

Several studies, carried out with both myogenic cells endogenously expressing SGs or cellular models ectopically expressing SGs suggested that the SG complex assembly occurs as a stepwise process. Firstly, β- and δ-SG form a tight core complex to which γ-SG and α-SG subsequently bind. Once assembled, the tetramer leaves the ER and, moving through the Golgi apparatus reaches the sarcolemma where, in the DAPC, interacts mainly with the dystroglycan heterocomplex and sarcospan, as well as dystrophin (Draviam, Shand et al., 2006, Noguchi, Wakabayashi et al., 2000) (figure 5).

Both glycosylation and disulphide bridge formation seem to be essential to allow complex formation, traffic, and interaction with the dystroglycan complex, while the intracellular tails of β- and δ- SG are thought to be crucial for the interaction with dystrophin (Chen et al., 2006, Holt & Campbell, 1998).

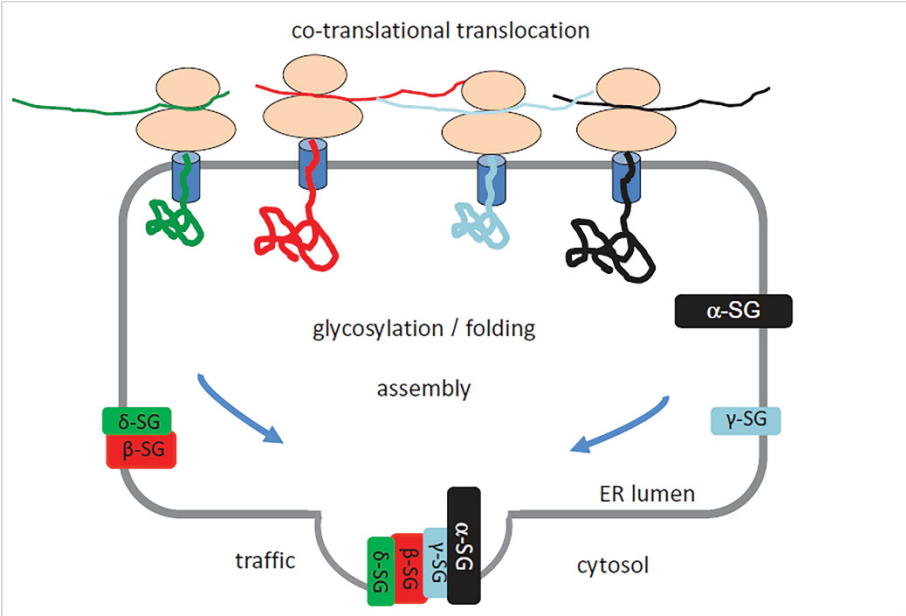

Figure 5. Sarcoglycan-complex biogenesis (Carotti, Fecchio et al., 2017).

Sarcoglycans are co-translationally translocated into the ER, where they undergo glycosylation and folding until they reach their native conformation. When properly folded, a βδ-SG core forms to which γ-SG and α-SG subsequently interact to form a tetramer. Once assembled, the SG complex leaves the ER and through the Golgi apparatus moves towards the sarcolemma.

1.4 Molecular pathogenesis of sarcoglycanopathy

Correct assembly, trafficking and targeting of the SG complex to the sarcolemma is of vital importance, and mutations that severely perturb tetramer formation and localisation lead to sarcoglycanopathy. Gene defects in one of the four SG can also cause the loss or the reduction of the other subunits.

1.4.1. Consequences of SG complex deficiency

The SG complex integrity is crucial for the sarcolemma stability. A destabilized DAPC, because of SG complex loss, is unable to guarantee protection from contraction induced sarcolemma lesions, causing uncontrolled cytoplasmic Ca^{2+} ions influx. This activates a cascade of events that terminates in cell death (Matsumura & Campbell, 1993, Straub & Campbell, 1997). Beside the structural role in membrane stability, SG complex also participates in bidirectional signal transduction with integrins, links filamin-2 in cytoskeletal signalling, and provides an additional anchorage site for neuronal nitric oxide synthase (nNOS), through dystrobrevin and syntrophin (Angelini & Fanin, 2016).

With these premises, the absence/strong reduction of SGs from the sarcolemma reported in patients with sarcoglycanopathy, leads to the progressive degeneration of myofibers, which are consequently replaced by adipose and fibrotic tissue.

The general assumption about the pathogenetic mechanism of sarcoglycanopathy is that SG mutants are unable to either correctly integrate into the DAPC or reach the sarcolemma from the ER being therefore rapidly degraded in the cytoplasm.

The loss of SG complex in the smooth vasculature of coronary arteries seems to be an important pathogenic factor in the cardiomyopathy associated with deficiency of β-SG and δ-SG (Araishi, Sasaoka et al., 1999, Coral-Vazquez, Cohn et al., 1999, Durbeej, Cohn et al., 2000). Furthermore, SG deficiency in the vascular smooth muscle could lead either to structural changes or to an impairment of metabolic and signaling pathways involving altered nNOS stability (Fanin, Tasca et al., 2009).

The entire SG complex tends to be affected as a unit. Indeed, as reported in figure 6, mutations in any SG can have deleterious consequences not only on the mutated protein but also on wild-type partners, resulting in strong reduction or even absence of the complex from the sarcolemma (Barresi, Confalonieri et al., 1997, Duggan, Gorospe et al., 1997, Vainzof, Passos-Bueno et al., 1999). However, immunohistochemistry of muscle biopsies suggested that the immunoreactivity of some components may appear nearly normal. For example, in α- and γ-sarcoglycanopathy, the mutated proteins are strongly reduced while the other subunits may be preserved or mildly affected (Higuchi, Kawai et al., 1998). By contrast, in β- and δ-sarcoglycanopathies, the entire complex is severely reduced or completely absent from the sarcolemma (Dincer, Bonnemann et al., 2000, Draviam et al., 2006) (figure 7).

Different studies suggested that residual expression of α-SG may correlate with milder clinical phenotypes (Alonso-Perez et al., 2020, Angelini, Fanin et al., 1999, Eymard, Romero et al., 1997), even if the complete absence of the protein has been also reported with milder phenotypes in γ-sarcoglycanopathy (McNally, Passos-Bueno et al., 1996).

The variability in the severity of the phenotype may depend by the different type of mutations, Indeed, nonsense and frameshift mutations, as well as those affecting the glycosylation status, seem to have a major impact on the SG complex, therefore resulting in a more severe clinical outcome. On the other hand, those mutations, such as missense mutations or small in frame deletion that seem to preserve a residual amount of protein at the sarcolemma may result in a milder phenotype (Sandona & Betto, 2009).

The gene encoding human α-SG maps on chromosome 17p21, and it is constituted by 10 exons. The others SGs genes, *SGCB* (β), *SGCG* (γ), *SGCD* (δ) maps on chromosomes 4q12, 13q12, and 5q33 and are constituted by 6, 8, and 9 exons, respectively.

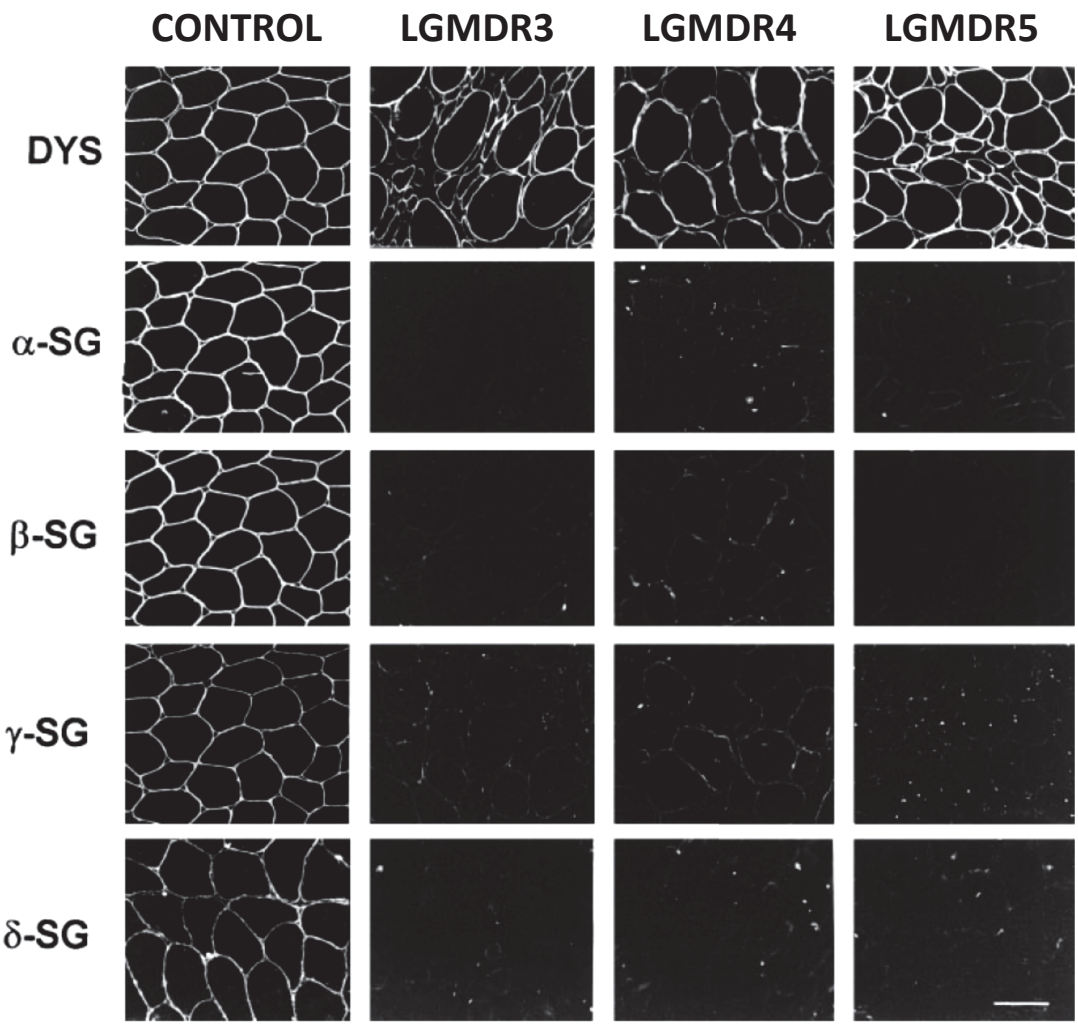

Figure 6. SGs deficiency in LGMDR3-5. Adapted from (Jung, Duclos et al., 1996).

Immunofluorescence of human control, LGMDR3, LGMDR4 and LGMDR4 patients muscle biopsies. Deltoid muscles stained with affinity-purified anti-dystrophin (DYS), α-SG, β-SG, γ-SG and δ-SG antibodies. It suggests that a mutation in any SG leads to instability of the remaining WT SGs, while dystrophin is less affected.

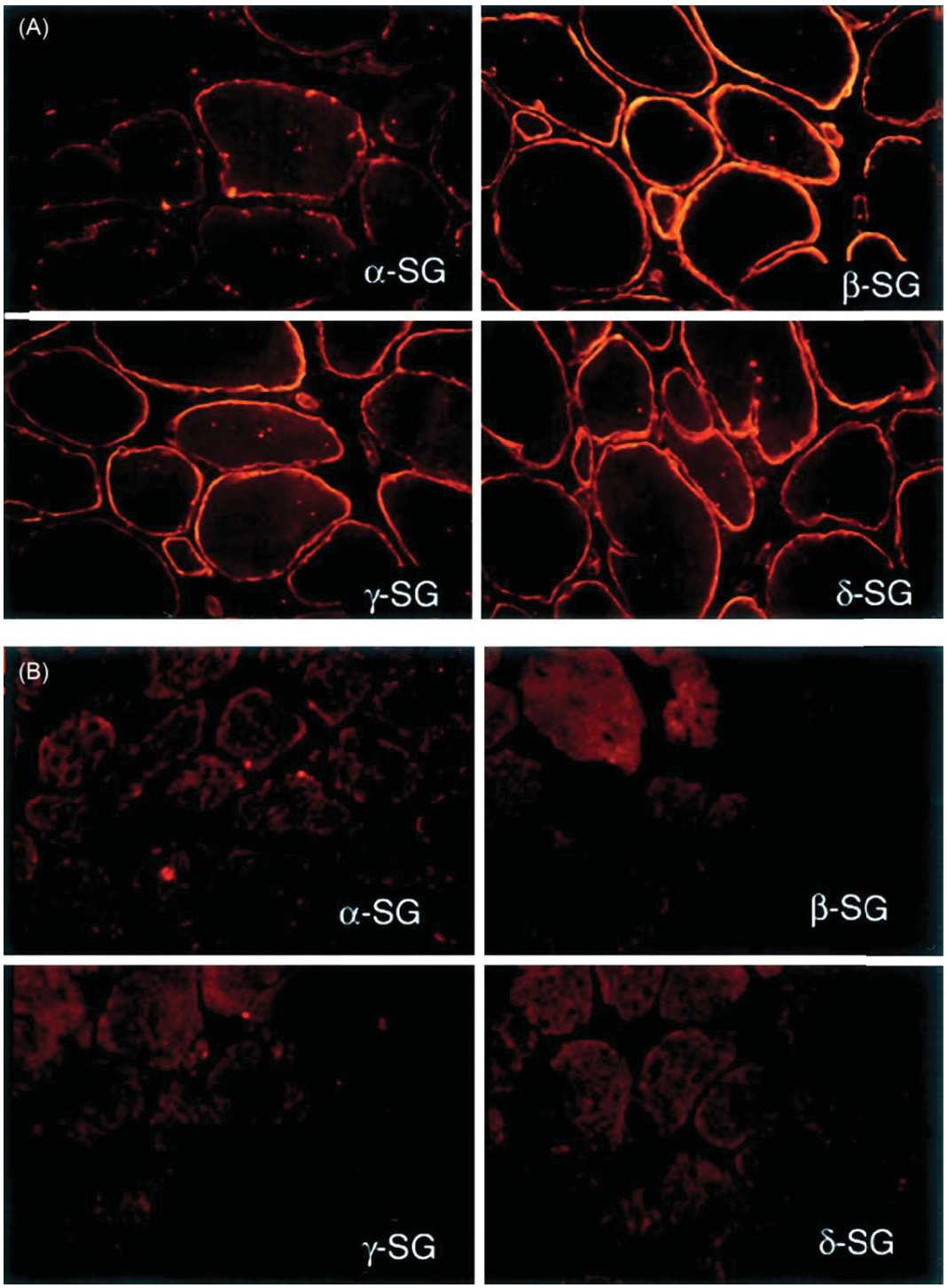

Figure 7. SG immunohistochemistry of skeletal muscle biopsies (Mohassel & Bönnemann, 2015).

(A) α-sarcoglycanopathy: strong reduction of α-SG with preservation of the other SGs.
(B) β-Sarcoglycanopathy: complete loss of membrane localization of all four SGs.

1.4.1.1 α-SG variants

In 1993 the locus for LGMDR3 was mapped on chromosome region 17q21 and is composed by 6 exons (McNally, Yoshida et al., 1994, Roberds, Anderson et al., 1993, Roberds, Leturcq et al., 1994) and the first mutations in the gene encoding α-SG were identified in French patients (Roberds et al., 1994).

LGMDR3 is the most common form of sarcoglycanopathies in many countries. The phenotype is the most variable, ranging from severe to mild, and asymptomatic patients with only hyperCKemia have also been described (Angelini & Fanin, 2016).

The frequency of the different mutations in *SGCA* is reported below and graphed in figure 8:

- 7.1 % null,
- 23.8% frame-shift,
- 65.5% missense,
- 3% in-frame deletion, insertion, and duplication.

Most mutations are of the missense type, possibly explaining the tendency of a more benign phenotype of LGMDR3 as compared to the other sarcoglycanopathies. The amino acid substitution R77C is the most frequently reported, followed by R284C and V247M. The mutation p.R77C, located at the level of the cadherin-like domain on the extracellular portion of the glycoprotein is the most common mutant allele in different world populations (Angelini et al., 1999, Duggan et al., 1997, Moreira, Vainzof et al., 2003), and especially in Europe, where it accounts for 24-32% of all the reported cases; it is associated with variable severity that seems to correlate with the residual protein present at the sarcolemma.
Mutations involving the most distal portion of the gene (e.g. p.V247M, p.R284C) seem to be associated with a milder form of the disease. Notably, symptoms variability is observable among members of the same family and even between siblings with the same mutation. (Angelini & Fanin, 2016, Carrie, Piccolo et al., 1997, Morandi, Barresi et al., 1996, Moreira et al., 2003).

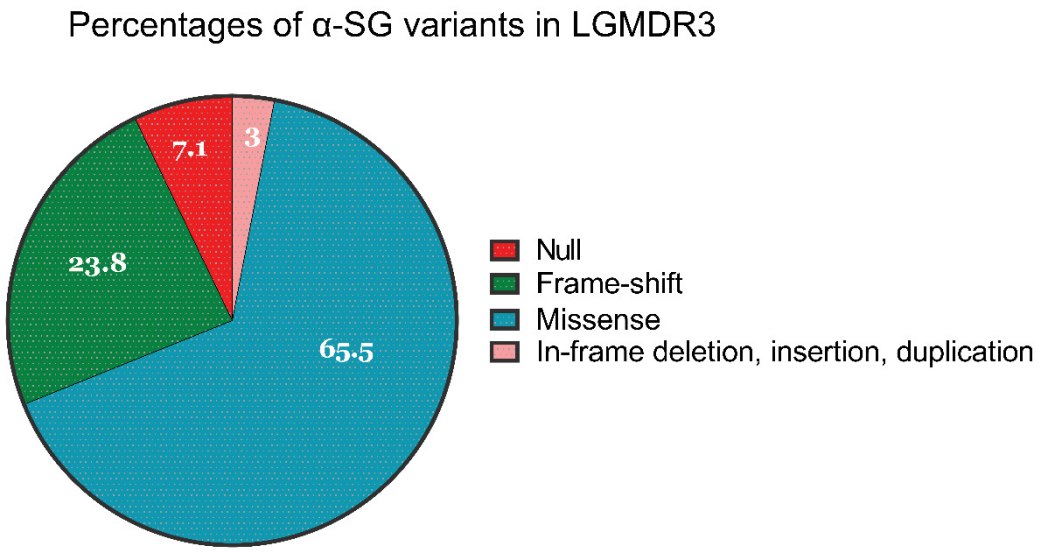

Figure 8. Frequency of α-SG variants in LGMDR3.

1.4.1.2 β-SG variants

The locus for LGMDR4 was mapped on chromosome 4q2, is composed by 8 exons (Lim, Duclos et al., 1995) and the first mutations on the gene encoding β-SG was identified in Amish patients (Lim et al., 1995) and one Italian patient (Bonnemann, Modi et al., 1995). The clinical phenotype in the majority of patients is severe LGMD, with childhood-onset, rapid loss of ambulation, and usually severe form of dilated cardiomyopathy. Of the 29 different known β-SG variants, the S114F amino acid substitution accounts for approximately the 45%.

The frequency of the different mutations in *SGCB* is reported below and graphed in figure 9:

- 13.7% null
- 25.5% frame-shift
- 56.9% missense
- 4% in-frame deletion, insertion, and duplication

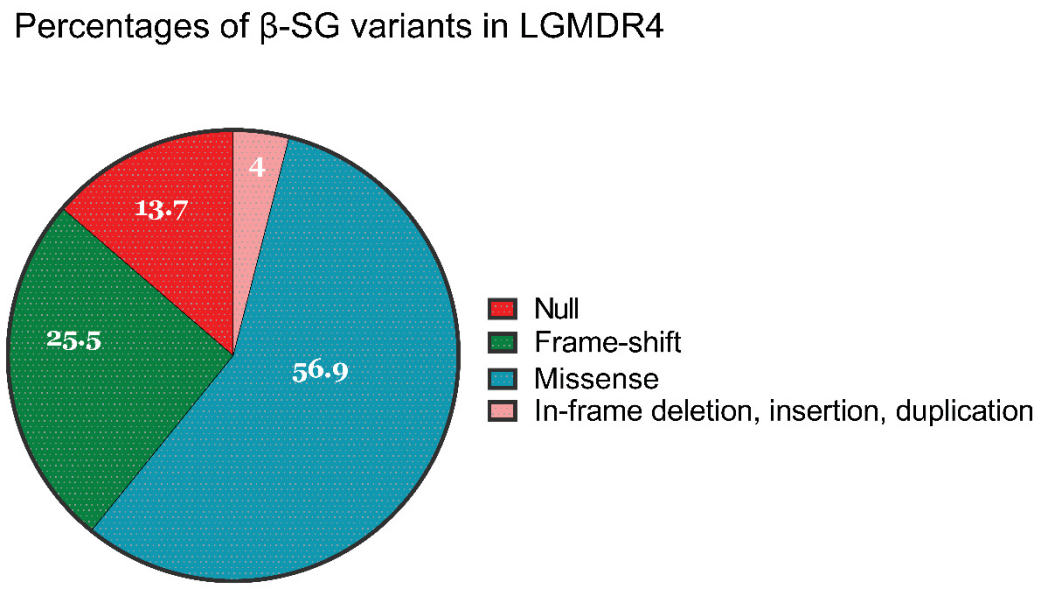

Figure 9. Frequency of β-SG variants in LGMDR4.

1.4.1.3 Other SG variants

SGCG and *SGCD* genes map on chromosomes 13q12, and 5q33 respectively and are constituted by 9 exons. The prevalent types of variants are the missense mutations, 40% and 57.2% respectively, followed by frame-shift variants for the *SGCG* gene (30.8%) and null variants for the *SGCD* gene (21.4%).

The mutation C283Y is responsible for half of all reported LGMDR5 cases. Only eight different amino acid substitutions are known for δ-SG, with two variants (A31P and R97N) together accounting for more than half of the reported cases of LGMDR6 (Carotti et al., 2017).

Mutations in the gene *SGCE* coding for the ε-SG are linked to the myoclonus dystonia syndrome, while in contrast the ζ-SG, encoded by the *SGCZ* gene, has been associated with no disease yet.

In addition, many patients are compound heterozygotes because of the presence of different mutations on the two alleles of the defective SG gene.

1.4.2 The cell quality control system and the degradative pathway

The absence of SGs from muscles of patients with sarcoglycanopathy can be easily explained when the mutation impairs either transcription or affects splicing sites, resulting in the production of aberrant transcripts. However, null, out-of-frame, in-frame insertions/deletions and missense mutations are also responsible for the loss/strong reduction of the affected protein.

Even though in some cases (null and out-of-frame mutations) the polypeptide synthesis is interrupted due to a premature stop codon activating the nonsense-mediated mRNA decay (NMD), in most cases, the defect leads to the production of a full-length protein with a single amino acid substitution (missense mutations).

It is thought that this last case may result in the formation of misfolded or folding defective SGs that, although potentially functional, are rapidly degraded.

Indeed, each newly synthesized protein is scrutinized by a quality control (QC) system that can discriminate between properly folded and folding-defective polypeptides. The first one can proceed in the biosynthetic pathway, whereas the latter are discarded to avoid the accumulation of potentially harmful proteins (Amm, Sommer et al., 2014).

SGs, which are destined to the plasma membrane, are thought to undergo QC surveillance inside the ER. In this organelle, a complex group of molecular chaperones, glycosylating and modifying enzymes helps proteins to reach the proper 3D structure. Among these, there are modifying enzymes, such as oligosaccharyltransferase, glucosidase I and II, lectin chaperones (calnexin and calreticulin), and folding-mediating enzymes (oxidoreductases of the PDI family and peptidyl-prolyl cis/trans isomerases). If the protein does not reach the native state, the enzyme UDP-glucose:glycoprotein glucosyltransferase (UGGT) reattaches one glucose molecule, causing the molecule reintroduction into the calnexin-calreticulin-mediated folding cycle (Sandona & Betto, 2009).

By contrast, properly folded proteins are not recognized by UGGT and the mannosidase I trims terminal mannoses, impeding the glucose re-addition for the reintroduction in the CNX-CRT cycle. Thus, the proteins can continue their maturation process, which, in the case of SGs, consists in the assembly with the other proteins of the complex, the trafficking and the insertion in the membrane. However, if the native conformation is not reached, even after repeated folding cycles, the defective polypeptides become substrates of the endoplasmic reticulum-associated protein degradation (ERAD) pathway (Bartoli, Gicquel et al., 2008, Gastaldello et al., 2008). In this pathway, a primary role is played by the dislocon. Dislocon is a macromolecular complex composed by ER-associated E2-E3 ubiquitin ligases, including primarily UbE2J1 and HRD1, which are responsible for the poly-ubiquitination, with the support of cofactors such as Derlin1 and Sel1L. The latter two cofactors, thanks to the driving force generated by the AAA-ATPase p97, also mediate the retro-translocation of the modified entity into the cytoplasm, where the 26S proteasome-mediated degradation occurs (Bianchini et al., 2014). The premature degradation of a mutated SG precludes its possibility to assemble with the other partners and to reach the sarcolemma (Carotti et al., 2017) (figure 10). While the first evidence was related to α-SG mutants (Bartoli et al., 2008, Gastaldello et al., 2008), further studies, latterly confirmed the ERAD involvement in the degradation of all SGs carrying a missense mutation (Soheili, Gicquel et al., 2012).

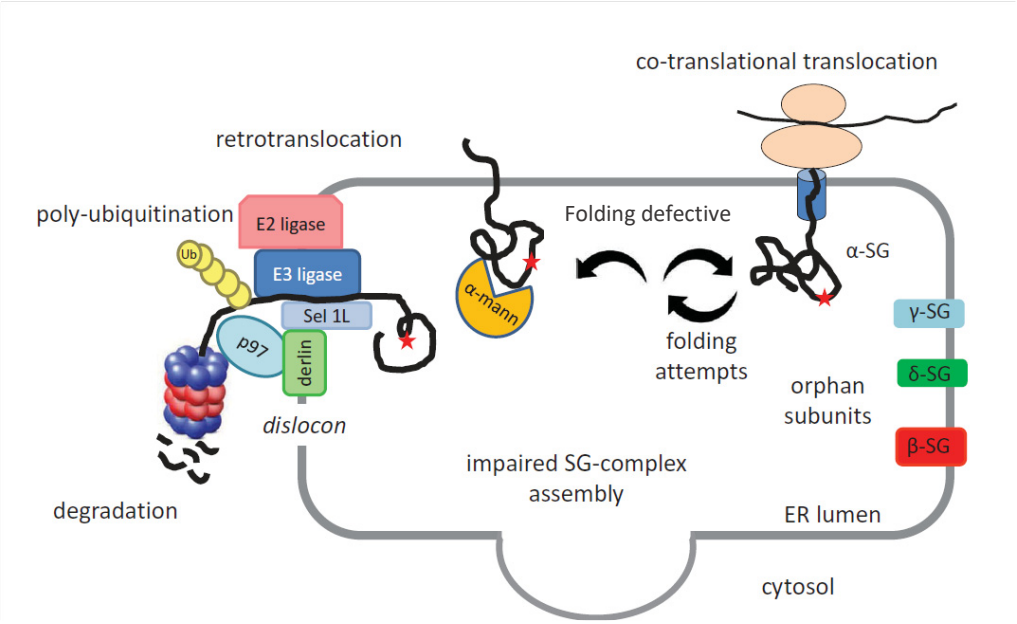

Figure 10. Graphical representation of the ER associated degradation of folding defective α-SG mutants. Adapted from (Carotti et al., 2017).

During the biosynthetic process, SGs undergo careful screening by the QC system of the ER. When a mutation (red star) impairs α-SG from reaching the native conformation, the α-mannosidase I enzyme terminates the maturation process and delivers the folding defective α-SG to the dislocon. Dislocation into the cytosol occurs via E2-E3 enzymes (UbE2J1 and HRD1), which are responsible for the poly-ubiquitination of the mutant and co-factors that help both ubiquitination and retrotranslocation, such as Sel1L and Derlin1.The AAA ATPase p97 on the cytosolic side provides the driving force for the membrane eradication of α-SG. Once in the cytosol, the α-SG mutant is degraded by the 26S proteasome. SG partners, as orphan subunits, are thought to be also degraded, with the consequent impairment of complex assembly and trafficking towards the sarcolemma.

1.5 Therapeutic approaches for sarcoglycanopathy

Until now, there are no available therapies to treat sarcoglycanopathies. Thus, unveiling the pathological mechanism(s) responsible for the disease was the major driving force in searching and identifying new druggable targets.

In particular, the recognition of the ubiquitin-proteasome system as the responsible for SG degradation, and the identification of the single ERAD elements directly interacting with the mutated α-SG (Bianchini et al., 2014, Gastaldello et al., 2008) allowed the identification of new possible therapeutic strategies for sarcoglycanopathies. Indeed, the outcome of the inhibition of different steps of the degradative pathway was the relocalization of the SG mutants at the cell surface, suggesting that the primary defect in these forms of sarcoglycanopathy is the loss of function due to the premature disposal of a folding-defective but potentially functional SG. On these premises, the first approach deals with in the inhibition of the protein degradation pathway by blocking either the proteasome, the ubiquitin ligase HRD1 or the mannosidase I (Bartoli et al., 2008, Bianchini et al., 2014, Gastaldello et al., 2008, Soheili et al., 2012). Conversely, the second strategy, aims at “repairing” the folding defective SG by using small molecules acting as protein folding correctors.

1.5.1 ERAD pathway inhibition-based approaches

1.5.1.1 Proteasome activity inhibition

Gastaldello et al. (2008) evidenced that the ubiquitin-proteasome system is responsible for the mutated SGs degradation allowing authors to hypothesize a possible therapeutic approach, consisting in preventing degradation (through proteasome inhibition) to push the mutants toward additional rounds of folding, thus forcing mutated α-SG rescue.

For this purpose, it was generated a heterologous cellular system that relied on human embryonic kidney cells (HEK293) which constitutively expressed the β-, γ- and δ-SG.
This cellular model (βγδ-HEK) reproduced the same organization of the SG complex of skeletal muscle present in pathological conditions. Indeed, the absence of the α-SG hampered the complex formation.
However, once the wild-type (WT) form of α-SG was transfected, the complex was formed and localized at the plasma membrane as in healthy muscle. Conversely, when βγδ-HEK cells were transfected with the mutated α-SG (R77C, D97G, R98H, P228Q, and V247M) the tetrameric complex failed to form and localize on the cellular membrane because the amount of the mutants was dramatically reduced in comparison to the WT.
Thus, the inhibition of the proteasomal activity was investigated by testing proteasome inhibitors such as MG132, lactacystin and bortezomib.
The treatment of βγδ-HEK293 with MG132 resulted in the increase of the content of the mutants (figure 11), suggesting that the ubiquitin-proteasome system has a key role in the pathogenesis of LGMDR3. Notably, after the proteasome inhibition most of the rescued mutants (D97G, R98H, P228Q, and V247M) reached the cell membrane (figure 12).
By contrast the mutant R77C, although showing a high level of expression in βγδ-HEK cells, was barely detectable at the cell surface. Of note, this mutant formed aggregosomes that remained entrapped into the ER.

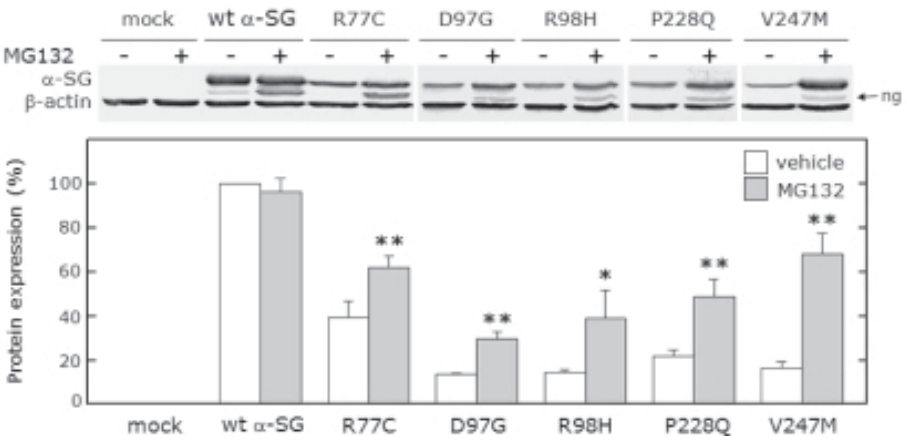

Figure 11. Western blot and densitometric analyses of βγδ -HEK cells transfected with either wild-type or mutated α-SG (as indicated) (Gastaldello et al., 2008).

Either the proteasome inhibitor MG132 or the sole vehicle were applied to transfected cells. Actin was used as an internal marker to normalize cell protein content.

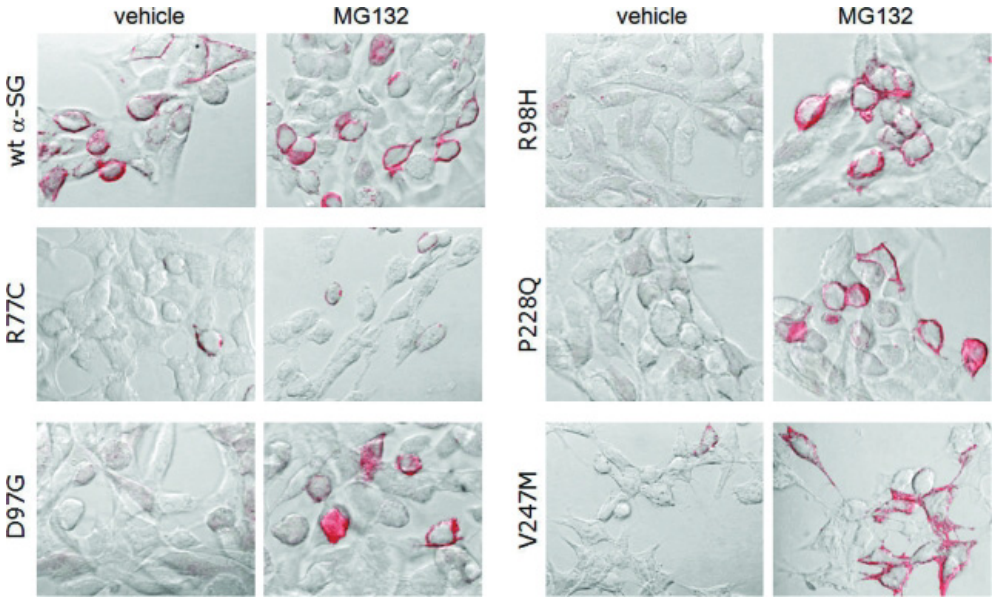

Figure 12. Confocal immunofluorescence analysis of βγδ -HEK cells transfected with either wild-type or mutated α-SG (as indicated) (Gastaldello, D'Angelo et al., 2008).

Transfected cells were treated with proteasome inhibitor MG132 or with vehicle. Non permeabilized cells were decorated with the antibody specific for α-SG.

1.5.1.2 Mannosidase I inhibition

An alternative approach was based on the correction of the basic trafficking defect of sarcoglycan mutants, by interfering with the first events of the ERAD pathway instead of inhibiting the last step (the proteasome) (Bartoli et al., 2008, Soheili et al., 2012). In these studies, kifunensine was the mannosidase I inhibitor used.

Mannosidase I is the enzyme that ends the process of folding of glycosylated proteins determining their exit from the CNX-CRT cycle. Kifunensine treatments were able to rescue the membrane localization of α-SG mutants (Bartoli et al., 2008) as well as of β-, γ- and δ-SG mutants (Soheili et al., 2012).

This molecule is mainly effective on proteins carrying a mutation that moderately affected the polypeptide structure. However, it seems of benefit for the R77C mutants of α-SG as evaluated in both HER911 cells co-transfected with β-, γ- δ-SGs and in mice transduced with adeno-associated virus (AAV) expressing the human mutated sequence (Bartoli et al., 2008, Soheili et al., 2012).

1.5.1.3 HRD1 inhibition

In Bianchini *et al.* (2014), one particular mutation responsible for LGMDR3 has been studied: the V247M mutation of α-SG.

The aim of this study was the characterization of the ERAD degradative pathway by unveiling the different components that can be envisaged as possible pharmacological targets. The authors evidenced the role of two E3 ligases, HRD1, and RFP2 as essential for the ubiquitination and for the delivery of defective α-SG to the proteasome.

Thus, small molecules LS-101 and LS-102 that are selective inhibitors of HRD1 and already proposed for the treatment of rheumatoid arthritis (Yagishita, Aratani et al., 2012) have been tested. Experiments were conducted on HEK293 cells expressing human V247M-α-SG (V247M cells), and in primary skeletal muscle cells derived from a LGMDR3 patient, carrying the L31P and V247M mutations on the *SGCA* alleles.

Results evidenced the capability of these inhibitors to induce an increase of the α-SG V247M content in the cellular model and, most importantly, the rescue of the SG complex on the sarcolemma of pathological myotubes (figure 13).

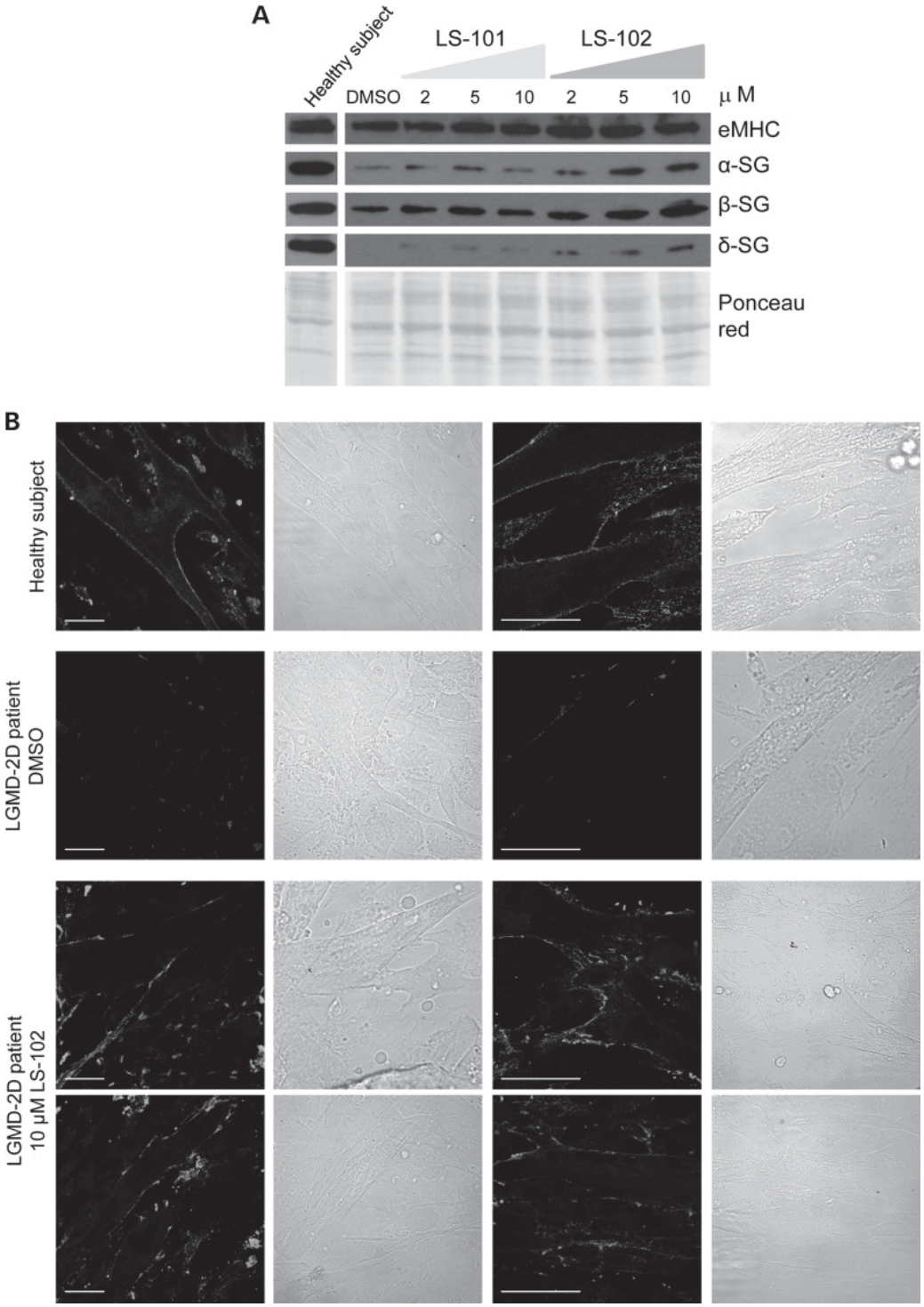

Figure 13. Inhibition of the E3 ubiquitin ligase HRD1 induced SG rescue in LGMDR3 myotubes (Bianchini, Fanin et al., 2014).

(A) Myotubes at 5 days of differentiation were incubated for 48 h with either DMSO, used as negative control, or increasing concentration of LS-101 and LS-102. At the end of incubation, they were lysed to analyse the expression of *α*-SG, β-SG and δ-SG by western blotting. To verify the differentiation homogeneity of the different samples the expression of embryonic myosin heavy chain (eMHC) was measured. By comparison, the expression of the same proteins was evaluated in 7-day old myotubes derived from a healthy subject. To normalize the results, the Ponceau red staining of the membranes is reported.
(B) Myotubes were grown on glass coverslips and differentiated for 7 days. At the fifth day of differentiation, either the negative control (DMSO) or 10 μM LS-102 were added. Two days later, not permeabilized myotubes were immunodecorated with the rabbit polyclonal antibody specific for an extracellular epitope of α-SG. As positive control, myotubes derived from a healthy subject were used.

1.5.2 Protein folding correctors to recover folding defective SG

The elucidation of the pathogenic mechanism behind sarcoglycanopathy forms caused by missense mutations and the identification of many ERAD elements involved in the degradative route of mutated SG opened new avenues for therapeutic intervention (Bartoli et al., 2008, Bianchini et al., 2014, Gastaldello et al., 2008, Soheili et al., 2012).

However, the proposed inhibition of the steps involved in the degradative pathway can impair the protein homeostasis equilibrium, increasing the concentration of many other defective proteins, possibly responsible for cell side effects. On the other hand, evidence suggests also that, although mutated, SG proteins retain their functionality and the development of novel therapeutic strategies, aiming to reduce the disposal of this folding defective mutants, would be of benefit for patients.

Protein misfolding, caused by different mechanisms, is involved in hundreds of genetic diseases, including cystic fibrosis, retinitis pigmentosa, Gaucher's disease, hypogonadotropic hypogonadism (Chaudhuri & Paul, 2006, Valastyan & Lindquist, 2014). The molecules proposed to revert this condition are also numerous.

Such compounds can directly act on the improperly folded protein, as *pharmacological chaperones*, or indirectly as *proteostasis regulators* by increasing the proteostasis network capacity (Chaudhuri & Paul, 2006, Powers, Morimoto et al., 2009, Wang, Di et al., 2014).

Among them, several compounds known as correctors of the cystic fibrosis transmembrane regulator (CFTR) protein are also included. CFTR correctors have been developed for their ability to recover at the cell surface type II mutants of the chloride channel defective in folding and trafficking (Bell, De Boeck et al., 2015, Pedemonte, Lukacs et al., 2005). Since missense mutants of CFTR and SGs share a similar pathogenetic mechanism, it seems reasonable to hypothesise that some CFTR correctors, if acting as proteostasis regulators, may be active also on mutated SGs. Indeed, very promising results have been collected by treating cell models and primary myotubes from a LGMDR3 patient with several of these compounds (Carotti et al., 2018).

Twelve CFTR correctors were tested in HEK293 cells transiently expressing the α- SG mutants R98H or D97G, as well as in a population of HEK293 cells, constitutively expressing the V247M-α-SG and compared with cells expressing the wild-type α-SG.

Many of the tested CFTR correctors (C5, C6, C4, C13, C14, C17 and C15) were effective in inducing the α-SG protein increase and the correct localization at the plasma membrane.

To validate these data, the efficacy of CFTR correctors was assessed directly in sarcoglycanopathy myotubes carrying the L31P and V247M mutations on the *SGCA* alleles. In figure 14, immunofluorescence staining of myotubes with and without the indicated corrector treatment is reported. The figure shows that in the absence of the treatment (vehicle), the signal

of SG on the sarcolemma was extremely weak. By contrast, the signal of α- and δ-SG on the sarcolemma increased considerably after incubation with C5, C6 or C17 correctors, suggesting the successful rescue of the SG complex and the localization at the cell membrane.

The C17 effect seems specific for the mutated protein, indeed, incubation with C17 10 µM of LGMDR3 myotubes resulted in a statistically significant increase of the α-SG mutant level, while no variation in the wild-type α-SG content was observed in myotubes from a healthy subject after 48h of incubation with even a higher concentration of the corrector (C17 15 µM) (figure 15). These results suggest that C17 acts directly on the α-SG mutants and/or on cellular pathways specifically handling the mutant (Carotti et al., 2018).

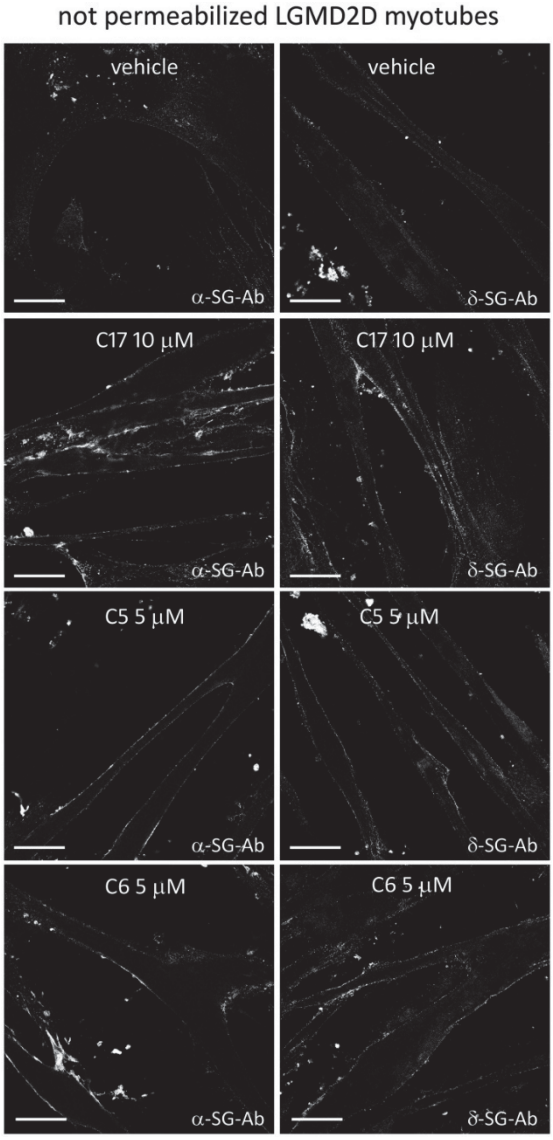

Figure 14. CFTR correctors rescued the SG complex in LGMDR3 myotubes (Carotti, Marsolier et al., 2018).

CFTR correctors rescued the SG complex in LGMDR3 myotubes. Myogenic cells from a patient carrying the L31P/V247M α-SG mutations were grown and differentiated for 7 days and treated for the last 48 h with 1‰ DMSO (vehicle) or the indicated CFTR correctors. At the end of incubation intact myotubes (not permeabilized) were labelled with antibodies recognizing an extracellular epitope of either α-SG (on the left) or δ-SG (on the right) to mark the membrane resident SGs only.

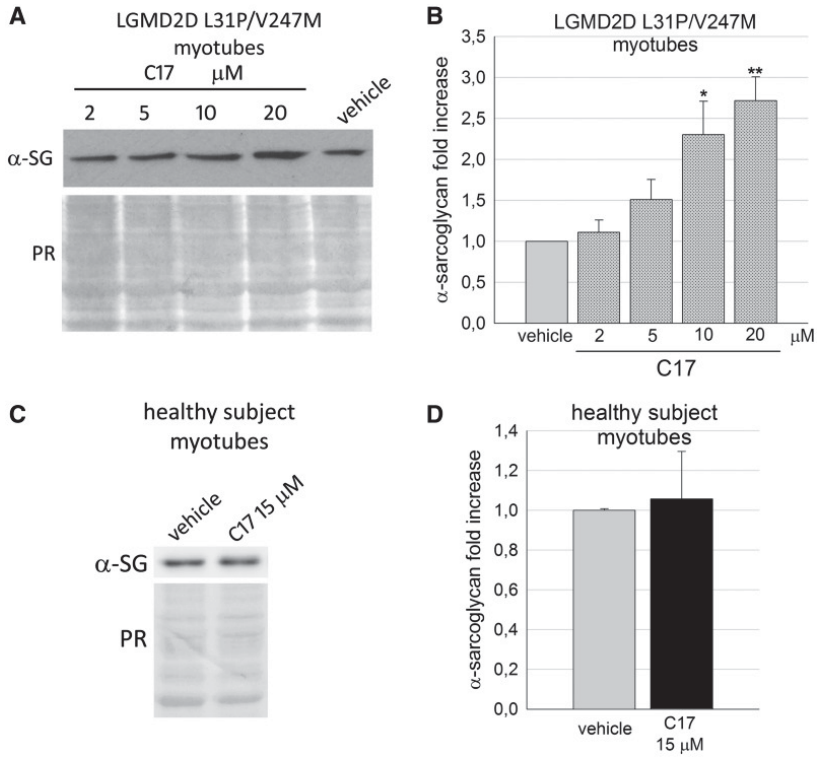

Figure 15. Corrector C17 induced a dose dependent increase of α-SG mutant in LGMDR3 myotubes (Carotti et al., 2018).

(A) representative western blot of total protein lysates of myogenic cells grown and differentiated for 7 days and treated for the last 48 h with either 1‰ DMSO (vehicle) or increasing concentrations of corrector C17, as indicated. α-SG protein was revealed with specific primary antibody, the Ponceau red staining (PR) was utilized to normalize the total amount of proteins loaded in each lane.
(B) quantification by densitometric analysis of α-SG protein bands
(C) myogenic cells from a healthy subject were grown and differentiated for 7 days and treated for the last 48 hours with either 1‰ DMSO (vehicle) or 15 µM C17. Total protein lysates were analysed by Western blot as described in **(A)**.
(D) quantification by densitometric analysis of wild-type α-SG protein bands.

Moreover, the *in vitro* protein recovery of α-SG mutants increased with longer incubation with C17 whereas no sign of toxicity was evident at the two tested concentrations (10 and 15 µM). Indeed, differentiated LGMDR3 cells did not present alterations in the morphology or signs of cytotoxicity, like membrane blebbing or cells detaching from the plate, even after 96 h of incubation (figure 16).

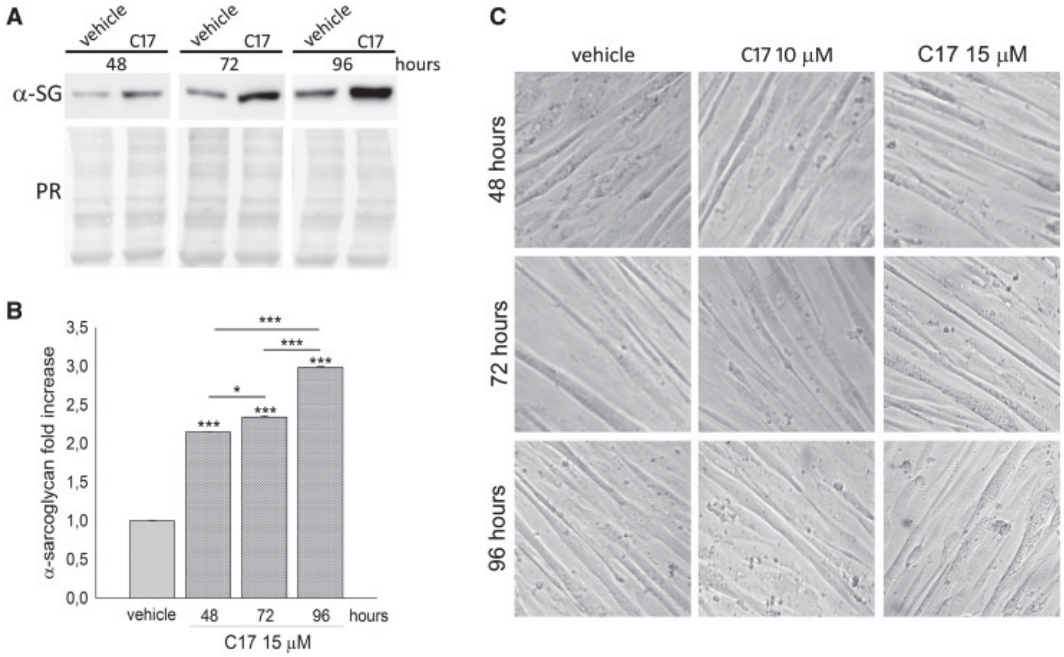

Figure 16. Corrector C17 induced a time dependent increase of mutated α-SG, without toxicity, in LGMDR3 myotubes (Carotti et al., 2018).

(A) Representative western blot of total protein lysates of myogenic cells grown and differentiated for 7 days and treated for the last 48 h with either 1‰ DMSO (vehicle) or 15 μM C17 for the indicated time intervals. α-SG protein was revealed with specific primary antibody, the Ponceau red staining (PR) is utilized to normalize the total amount of proteins loaded in each lane.
(B) quantification by densitometric analysis of α-SG protein bands.
(C) Phase contrast images of myotubes treated with DMSO (vehicle) and C17 at the indicated concentrations and time intervals.

To confirm from a functional point of view the efficacy of the application of CFTR correctors, the creatine kinase (CK) release from myotubes upon exposition to osmotic stress was measured. CK is a cytosolic enzyme and a widely used marker for muscle damage as its release is typically 10-fold higher in patient with LGMD with respect to healthy individuals.

The treatment with correctors evidenced an elevated reduction of the released CK because of the rescue of the SG complex localization, which conferred stability to the sarcolemma. Figure 17 illustrates as healthy subject myotubes released very low levels of CK, if compared to LGMDR3 patients myotubes (treated with the vehicle). It is evident the increased CK release from pathological myotubes as the test conditions worse. On the contrary, the CK release from myotubes pre-treated with C17 was considerably reduced if compared with untreated samples, nearly approaching the healthy-subject myotubes levels. Thus, this result suggests the functional improvement at the level of the sarcolemma when the SG complex is rescued by C17 CFTR corrector treatment.

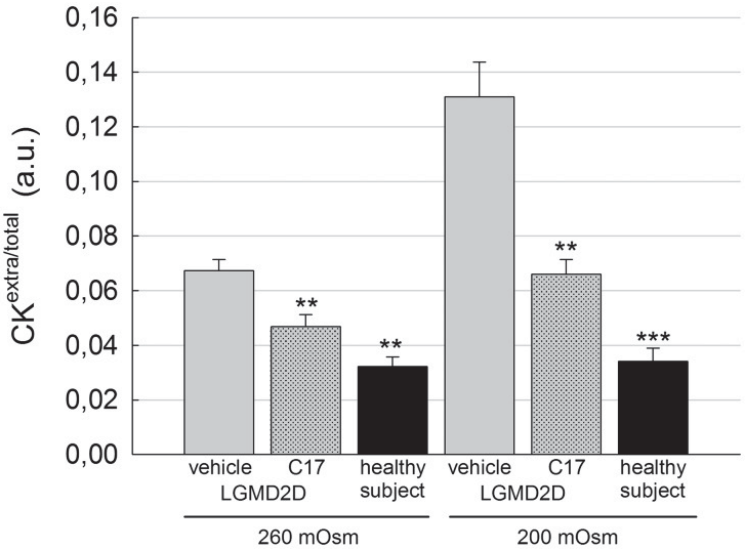

Figure 17. The treatment *in vitro* with the corrector C17 recovered the functionality of patient myotubes (Carotti et al., 2018).

Myogenic cells were grown and differentiated for 7 days and treated for the last 96 h with 1‰ DMSO (vehicle) or 15 μM C17. At the end of the treatment, myotubes were incubated for 20 min in hypo-osmotic solutions as indicated. Then, the cytosolic protein CK was measured in the supernatant of myotubes, whereas the intracellular level of the protein was determined after cell lysis. Ratio between extra and total CK values were plotted.

It is generally known that a combination of two or more molecules will be required to achieve a significant clinical benefit (Clancy, Rowe et al., 2012, de Wilde, Gees et al., 2019, Okiyoneda, Veit et al., 2013). This concept has recently been strengthened by the clinical data generated by Vertex pharmaceuticals in which the addition of a next generation CFTR corrector (such as VX440, VX152, VX659 or VX445) to cystic fibrosis patients chronically treated with Symdeko® (combination of Ivacaftor or VX770 and Tezacaftor or VX661) led to an improvement in patient outcome (Vertex, 2017).

To this intent and thanks to the promising results obtained with the CFTR corrector C17 in recovering folding defective α-SG, the combined administration of this molecule with other correctors was evaluated (Carotti, Scano et al., 2020). Results highlighted the additive and even potential synergistic activity of such compounds, with the possibility to scale down the dose of the tested molecules conserving the maximum effect. Moreover, the collected data provided preliminary information on the possible mechanism of action of the correctors. The data published in Carotti *et al*, 2020 are attached in the results section because part of this PhD project.

1.5.2.1 Insights on CFTR correctors mechanism of action

Cystic fibrosis (CF) is caused by ~2 000 mutations in the *CFTR* gene with a wide range of disease severity. Currently, six major classes of mutations are distinguished on the basis of their primary biological defect (Veit, Avramescu et al., 2016):

- Class I include frameshift, splicing, or nonsense mutations that introduce premature termination codon, resulting in severely reduced or absent CFTR expression.
- Class II mutations lead to misfolding, premature degradation by the endoplasmic reticulum (ER) quality-control system, and impaired protein biogenesis, severely reducing the number of CFTR molecules reaching the cell surface.
- Class III mutations impair the regulation of the CFTR channel, resulting in abnormal gating characterized by a reduced open probability.
- Class IV mutations alter the channel conductance by impeding the ion conduction pore;
- Class V mutations alter its abundance by introducing promoter or splicing abnormalities;
- Class VI mutations destabilize the channel in post-ER compartments and/or at the plasma membrane.

Defining the cellular and molecular pathology of CFTR mutations was fundamental for the development of small-molecule compounds targeting a specific defect in CF, grouped under the name of CFTR modulators. Depending on their effects on CFTR mutation they have been classified into five main groups, including correctors, potentiators, stabilizers, read-through agents, and amplifiers (Lopes-Pacheco, 2019).

Particularly, CFTR correctors are a subgroup of modulators able to enhance or even restore, through different mechanisms, the expression, function, and stability of type II CFTR mutants.

Although correctors may act by distinct mechanisms, they usually enhance protein conformational stability during the ER folding process. They could act directly by binding to the misfolded protein as *pharmacological chaperones,* (PC) stabilizing some conformations. Other CFTR correctors are thought to act indirectly as *proteostasis regulators* (PR) by modulating the function, composition or concentration of elements of the proteostasis network itself. In both cases, they enable the passage of the mutated CFTR through the ER quality control checkpoints.

Particularly, in the case of PR, it would be interesting to tailor and employ such compounds in order to pharmacologically manipulate folding and proteostasis in a wider range of misfolding diseases, such as sarcoglycanopathy.

Indeed, different works suggested that CFTR correctors could be a significant pharmacological option for many orphan diseases, such as intrahepatic cholestasis and many other diseases characterized by protein folding and trafficking defects (Sampson, Lam et al., 2013, van der Woerd, Wichers et al., 2016).

From the studies of Carotti *et al*, 2018, 2020, a potential lead compound was identified, which upon optimization for efficacy and safety, could represents a promise for the development of treatments for sarcoglycanopathy.

The corrector C17, name IUPAC N-(2-(5-chloro-2-methoxy phenyl amino)-4'-methyl-4, 5'-bithiazol-2'-yl) pivalamide, is a molecule of the family of methylbithiazoles, characterized by a central bithiazolic group, linked to a chloro-methoxy-benzene group and via an amidic bond to a tert-butyl group (figure 18).

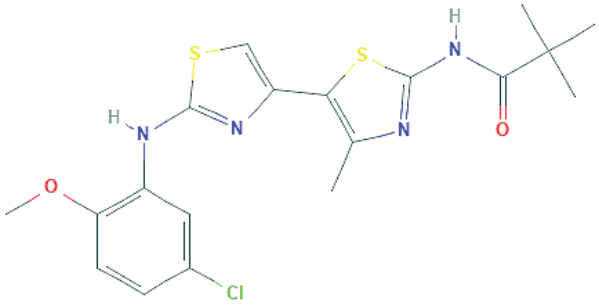

Figure 18. Chemical structure of the CFTR corrector C17.

In structural studies with ΔF508 CFTR, bithiazolic compounds like C4 and, in minor extent, C17, seem to contact CFTR either by binding to an *in silico* predicted site in the intracellular Nucleotide Binding Domains (NBD) of CFTR or by stabilizing the Transmembrane Domains (TMD) (Loo, Bartlett et al., 2013).

Such structural studies however, are not possible with α-SG since the structure of the protein has not been yet fully elucidated (Dickens et al., 2002) and only recently a predicted 3D structure has been defined (Jumper et al., 2021) (figure 19). In any case SGs and CFTR are quite different in terms of both structure and function, therefore, we can just draw some hypothesis based mainly on the fact that examples of CFTR correctors' efficacy on proteins different from the chloride channel are growing (Sampson et al., 2013, van der Woerd et al., 2016). Therefore, it is possible that in the presence of a mutated protein, correctors act mainly modulating the function, composition or concentration of proteostasis network elements. Consequently, the perspective that different correctors may act on different targets, offers the opportunity to develop combined treatments also for sarcoglycanopathy.

Thus, in the absence of further structural studies, the most accredited hypothesis is that the C17 molecule acts as a proteostasis regulator, helping the maturation of α-SG mutants and promoting the assembly with the other WT subunits indirectly.

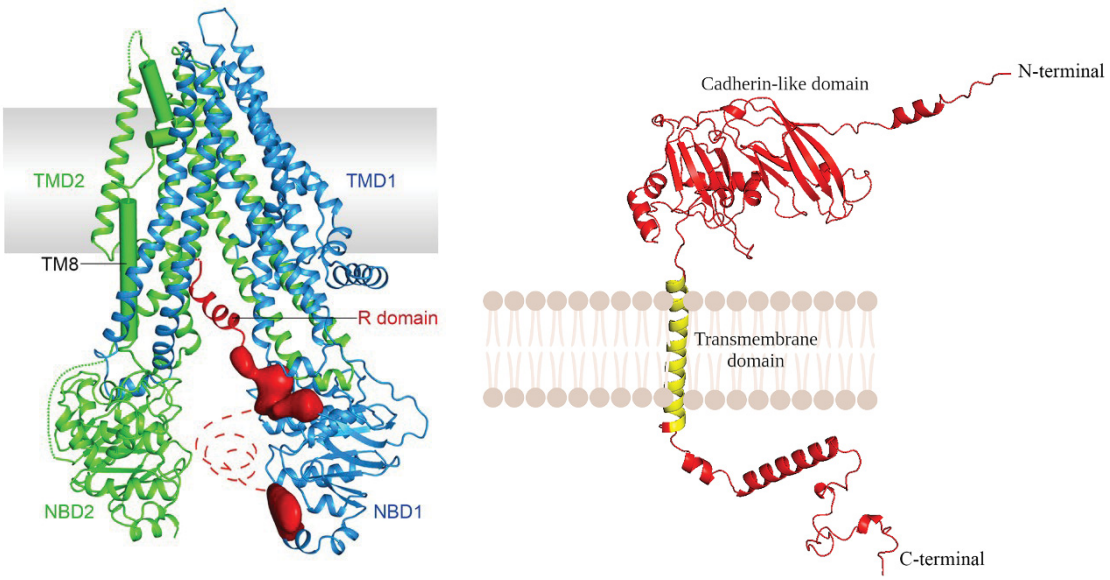

Figure 19. CFTR channel molecular structure (Liu, Zhang et al., 2017) and α-SG predicted molecular structure (Jumper, Evans et al., 2021).

Ribbon diagram of human CFTR in the dephosphorylated, ATP-free conformation obtained by Cryo-Electron Microscopy (Cryo-EM) is reported on the left. Nucleotide binding domains (NBD1 and 2) and transmembrane binding domains (TMD1 and 2) are indicated. The EM densities shown in red correspond to unstructured regions of the R domain which insert between the cytoplasmic extension of the TMDs and packs along NBD1. Regions not resolved in the structure are shown as dashed lines.
On the right it is reported the predicted structure of human α-SG protein obtained with the AlphaFold protein structure database. The transmembrane domain, the cadherin-like domain, the N- and the C-termini are indicated.

1.6 *In vivo* studies to assess C17 corrector efficacy

In vitro studies are crucial, and although the results described by Carotti *et al*, 2018, 2020 are very promising, the development of new drugs is a long and difficult process. Studies in animals are important first steps and should not be undervalued, because many drugs that show promising results in cells do not work properly in animals or may show unpredictable adverse effects. A new drug showing potential activity in cells needs a long range of animal tests before moving toward clinical trials in humans. Indeed, studies in animals add more valuable data not only about the efficacy of the drug but also concerning its pharmacodynamics (mechanism, safety, tolerability, etc) and pharmacokinetic (ADME events, i.e. absorption, distribution, metabolism and excretion), explaining why many years are needed to translate a drug into a treatment. Considering all these aspects, to validate the finding collected *in vitro*, an animal model expressing an α-SG missense mutant is mandatory.

1.6.1 Available animal models of sarcoglycanopathy

Animal models for each of the four sarcoglycanopathies exist and they mimic well the human pathological condition (Sandona & Betto, 2009). The BIO14.6 hamster strain was established in 1962 and is recognized as the first animal model of sarcoglycanopathies (Homburger, Baker et al., 1962). However, it was not considered until the discovery of the causative mutation in LGMDR6 patients (Nigro, Piluso et al., 1996).

In addition to the hamster model, 4 types of knockout (KO) mice were generated. Each of them lacks one of the four SG proteins. Mice is very similar from a genetic and a physiological point of view to humans, making them a valuable experimental system to study the pathophysiology of human diseases. Among them, the first murine model for sarcoglycanopathy is the α-SG *null* mouse, which allowed analysing the biological role of SGs in the pathophysiology of LGMDR3. The total absence of α-SG in muscles leads to progressive skeletal muscle degeneration, with the mice developing histopathological features of muscular dystrophy shortly after birth with progressive worsening until nine months of age (Duclos, Straub et al., 1998). As for the human pathology, this KO model shows the reduction of the entire SG complex, sarcospan and the other elements of the DAPC. Furthermore, from a functional point of view, these mice present also high serum levels of CK compared to control animals (Duclos et al., 1998). In addition, KO models for the other SGs are also available. β-SG deficient mice exhibit progressive muscular dystrophy with extensive degeneration and regeneration and typical β-sarcoglycanopathy muscular hypertrophy. The deficiency of β-SG also causes loss of all of the other SGs as well as of sarcospan at the sarcolemma (Araishi et al., 1999). γ-SG KO mice show pronounced dystrophic muscle in early life, with the development of cardiomyopathy and premature death. The loss of γ-SG produces secondary reduction of β and δ-SG with partial retention of α-SG (Hack, Ly et al., 1998). Finally, the KO model for the δ-SG is characterized by either muscular dystrophy and severe cardiomyopathy with focal areas of myocardial ischemic-like lesions as the characteristic histopathological feature (Coral-Vazquez et al., 1999).

However, even if these murine models mimic well the LGMDR3-6 dystrophic phenotypes, they do not produce the protein and hence they are not suitable to test CFTR correctors aiming at recovering the folding defective but synthetized protein.

Besides the KO, also two knock-in (KI) mouse models were generated. The first one was a KI for α-SG carrying the missense mutation H77C and was generated in independent manner by two distinct laboratories (Bartoli et al., 2008, Kobuke, Piccolo et al., 2008). It has a missense mutation that leads to a histidine-to-cysteine substitution at the codon for the residue 77 (H77C), in order to reproduce the most frequently reported human mutation R77C. The second KI model carried the T153R substitution on β-SG protein (Henriques, Patissier et al., 2018).

In both models, the mutant protein is expressed at normal levels at the sarcolemma, and no sign of muscular pathology are present. One possible explanation for the α-SG KI mice could be represented by the two different amino acids in position 77 of the protein: in the human α-SG there is an arginine (R), while the murine protein presents a histidine (H). This may modify the local organization of the protein, leading to a lower structural impact of the murine QC system.

Thus, considering a possible lower impact of this substitution on the protein folding compared to substitutions in more conserved regions, the β-SG KI model has been generated. In this case the substituted residue is identical in human and mouse and it is located in a highly conserved region. Unfortunately, also this KI model does not present any dystrophic phenotype. The explanation for the different outcome of missense mutations in SG between human and mouse is still obscure. However, it is possible to hypothesize that the mouse quality control system is more permissive and more tolerant than the human one, allowing a fraction of the mutated protein to escape degradation and assemble into a functional complex that localizes at the sarcolemma. Thus, the bi-allelic expression of the protein, as in the KI animals, should result in a much higher synthesis of the protein, which, even though mutated, can escape the murine QC.

Indeed, in the case of human missense mutation, the mechanism of the loss of function is not related to the function of the protein but to its premature degradation and deficient trafficking toward the sarcolemma. Therefore, understanding the species differences in protein quality control pathways will give possible explanations why mouse models keep failing in recapitulate the human pathological phenotypes. In addition, this suggests also that to obtain a mouse model of the disease it is perhaps important to strictly control the amount of the produced protein.

As previously mentioned, the existence of an animal model expressing a missense mutant of any *SGC* gene and developing the typical pathologic signs of human sarcoglycanopathy is fundamental for the study of the disease and for the development of possible novel therapeutic approaches aiming at recovering the mutated SG. To this purpose and to overcome the unsuitability of already existing murine models, we developed a novel model of the disease, in which the hind limbs of *sgca*-null mice have been transduced (immediately after birth) by adeno associated viruses (AAVs) expressing the human α-SG sequences wild-type (WT) or mutated. Mice with the *mutated humanized* hind limbs allowed us to show the *in vivo* efficacy of C17 CFTR corrector.

1.6.2 Adeno-associate virus (AAV) serotype 1

Adeno-associated viruses (AAVs) belong to the genus *Dependoparvovirus* within the family *Parvoviridae,* and their life cycle depends on the presence of a helper virus, the adenovirus. They are non-enveloped viruses and are composed by a capsid of about 26 nm and a single-stranded DNA genome of about 4.7 kb (Naso et al., 2017).

The genome is essentially composed by three genes: *rep*, *cap* and *aap*. The *rep* gene encodes four proteins essential for viral replication: Rep78, Rep68, Rep52 and Rep40. The *cap* gene encodes three capsid subunits, VP1, VP2 and VP3, and a third gene, the *aap* gene, encodes the assembly activating protein (AAP). Today, recombinant AAVs (rAAVs) are used as platform for *in vivo* delivery of gene therapies. In the application of gene delivery, the AAV genome vectors are devoid of all the protein-coding sequence and the only sequences of viral origin are the inverted terminal repeats (ITRs), which are essential to guide genome replication and packaging during vector production (figure 20).

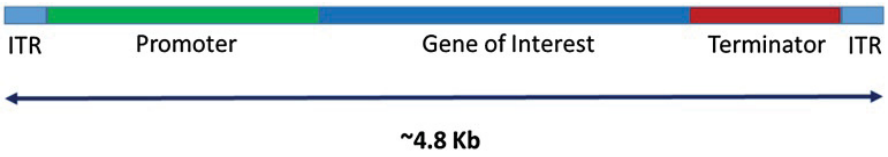

Figure 20. Schematic representation of the basic components of a gene of interest packaged inside recombinant AAV gene vector (Naso, Tomkowicz et al., 2017).

AAV: adeno-associated virus, *ITR:* inverted terminal repeat

Nowadays, AAVs are very common vectors for clinical trials use, because of the long-term transgene expression with relative low immune response and toxicity in animal models. Moreover, they persist in the nucleus as episomes that do not integrate in the host cell genome eliminating the risk of DNA damage and unpredictable consequences. Eleven serotypes of AAVs have been identified so far: serotypes differ in their tropism making AAV a very useful system for preferentially transducing specific cell types. In addition, recombinant techniques involving capsid shuffling, directed evolution, and random peptide library insertions can be used to derive variants of known AAVs with unique attributes and specifically targeting a cell type.

The chosen AAV serotype in this PhD thesis, used to deliver the human α-SG sequence in *sgca* null mice, was the AAV1 as it showed a good tropism for the skeletal muscle (Hauck & Xiao, 2003, Zincarelli, Soltys et al., 2008). Its specificity for the skeletal muscle was further enhanced with the insertion of a promoter specific for striated muscle, the tMCK (muscle creatine kinase) promoter, controlling the expression of the *SGCA* gene. The tMCK promoter ensures sustained long-term expression of the α-SG for up to 12 weeks in the absence of evident cytotoxicity (Rodino-Klapac, Lee et al., 2008). Thus, when the AAV1 is injected intramuscularly (IM) the vector is expressed only at the site of interest, avoiding potential ectopic expression in case of the vector spill over. Moreover the i.m. injection of the AAV1 vector on new-born mouse (1-2 days of life) allows to establish tolerance towards the human sequence (Vitiello, Faraso et al., 2009). In this way, a sequence that should be recognized as nonself from the immune system, can be expressed and maintained as a self- protein and mouse skeletal muscle can develop in the presence of the exogenous protein. Indeed, the human α-SG should follow the proper biosynthetic and maturation process, leading to the development of either healthy or dystrophic hind limbs, depending on the sequence of the human protein injected.

1.7 Studies to characterize a lead compound

When a compound, as in the case of the C17 molecule, shows promising effects both *in vitro* and *in vivo*, a deepening investigation on its features is required also to better understand the behaviour of the molecule inside the organism. The development of a new therapeutic compound always involves a preclinical analysis stage. Throughout this stage the preliminary pharmacokinetic, pharmacodynamic, and toxicological properties of the drug candidate are investigated.

ADME studies are conducted with *in vitro*, *in vivo* or *in silico* models and an appropriate experimental scheme is needed (figure 21). *In vitro* models allow to evaluate many ADME parameters, including apparent permeability, metabolic stability, protein binding, blood-to-plasma partitioning, inhibition and induction of cytochromes P450 (CYP), cytotoxicity.

In vivo models of animals and healthy human subjects provide information such as drug oral bioavailability, exposures, distribution, clearance, and duration of exposure for a drug and its metabolites. Finally, *in silico* models predict drug behaviours based on physicochemical properties of drug candidates in combination with crystal structures of a protein, if available (Zhang et al., 2012). Several simple stability tests allow the assessment of the "drug-ability" of a compound or chemical template. For example, if a compound is highly unstable in a tissue (liver, for example) or fluid (blood, for example) consequently its therapeutic activity could be low. Among the different experiment that could be performed, blood and microsomal stability could be simple but highly informative assays (Vrbanac & Slauter, 2017).

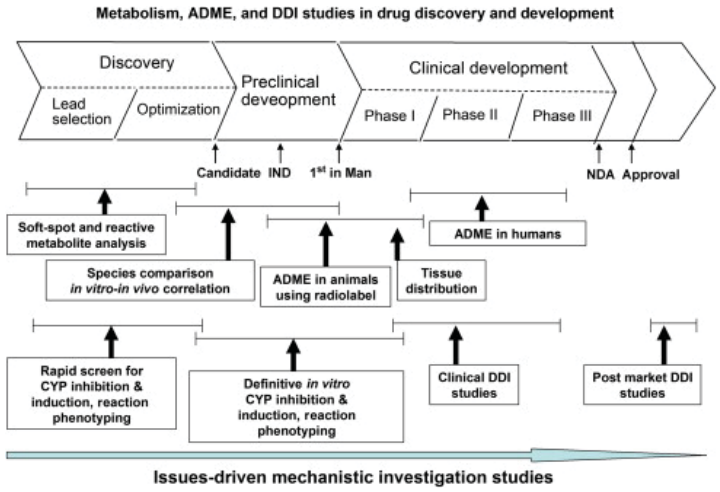

Figure 21. Typical model systems used in drug discovery and development stages (Zhang, Luo et al., 2012).

1.7.1 Blood stability studies

A thorough understanding of the pharmacokinetics of a drug or a molecule is the basis for defining the most appropriate dose, route of administration, and intervals between doses to provide the therapeutic effect.

A preliminary characterization of a drug/molecule pharmacokinetics can start by analysing drug stability in the blood. Indeed, in the blood a molecule can undergo to chemical, metabolic or physical modifications generating an inactive molecule or metabolites that can be potentially harmful. Metabolic instability occurs when the molecules are metabolized in blood cells or in the fluid compartment of blood, either serum or plasma, while chemical instability is due to oxidative, hydrolytic isomerization reactions depending on the physicochemical properties of the tested analyte. In addition, there is also the possibility of compound aggregation, precipitation or interaction with matrix components (non-covalent) or with the surface of the container, and this type of reactions are known as physical instability (Reed, 2016).

Blood stability determination is a simple widely used test that can quickly determine the withdrawal of compounds in drug discovery screenings. As already stated above, the drug discovery/development process involves not only the identification of drug targets and demonstration of desirable activities in model systems, but also the elimination of compounds that must, by definition, fail in the clinic. To determine the stability in blood, typically an appropriate concentration of a compound is incubated in collected blood under physiological temperature (37°C) for 30–60 min. Its stability is determined by an appropriate analytical method, such as LC-UV or LC-MS. Viable drug candidates should be "relatively" stable under these conditions.

1.7.2 Biotransformation studies

Biotransformation is broadly defined as the transformation of chemical compounds within living systems. Understanding the biotransformation of drugs is a key element of the modern drug discovery, both in later stage of development and early in the discovery phase. The metabolism of a xenobiotic or drug has the potential of modifying the properties that will improve or reduce its chances of advancing through the discovery and development processes, eventually becoming a useful therapeutic. The metabolism hence allows the elimination of the drug or xenobiotic from the body, but may also convert the drugs to toxic substances, including highly reactive carcinogenic, mutagenic, or teratogenic molecules. Thus, bioactivation is the aspect of the overall risk/benefit assessment ensuring the advancement of a drug candidate into development. (Vrbanac & Slauter, 2017). However, decades of research have failed to yield a unique chemistry strategy responsible for the generation of reactive metabolites. Indeed, reactive metabolites formation in a chemical reaction cascade should also consider alternative metabolic pathways, competing detoxification pathways, and an estimation of the human dose based on pharmacokinetic/pharmacodynamic studies in preclinical species (Spracklin, Kalgutkar et al., 2013). The biotransformation of drugs as well as of xenobiotics and endogenous molecules takes place in several tissues, with the liver as the principal organ, but also kidney, gut, lungs, nasal epithelium, skin, can be involved.

The liver is the largest internal organ of the human body and is strategically located between the digestive tract and the other parts of the body (Brandon, Raap et al., 2003). Biotransformation is divided into two types of reactions: phase I reactions (hydrolysis, oxidation, reduction) and phase II reactions (conjugation). The biotransformation pathway of a drug is mediated by phase I, phase II, or a combination of both (figure 22). The term phase I or phase II is a conventional name given to the type of reactions that can occur to a compound, but they did not correspond to the order by which they occur. Indeed, a molecule can undergo modification by phase II enzymes and hence followed by phase I reactions. The cytochrome P450 (CYP) enzyme superfamily plays a dominating role in the phase I biotransformation and is mainly present in the liver. CYP enzymes, heme-containing proteins, are involved in the biosynthesis and metabolism of steroids, fatty acids, bile acids, prostaglandins, leukotrienes, various carcinogens, and environmental pollutants and they can also convert a non-toxic compound into reactive intermediates that are toxic or carcinogenic. Many CYP isoforms have been characterized and they are grouped based on their sequence. Phase II enzymes (e.g., uridine diphosphoglucuronosyl transferase (UGT), N-acetyl transferase (NAT), glutathione S-transferase (GST), and sulfotransferase (ST) also have an important role in the detoxification and/or excretion rate of xenobiotics (Asha & Vidyavathi, 2009). The elucidation of the entire human biotransformation pathway, both phase I and phase II biotransformation, is essential in the early development of a candidate drug.

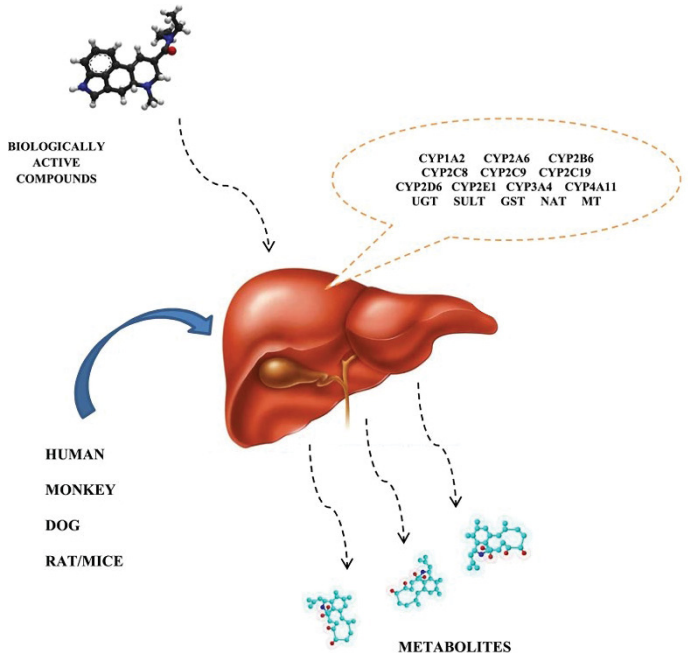

Figure 22. Scheme of phase I and II reactions responsible for a molecule biotransformation, occurring mainly in the liver. Adapted from (Szultka-Mlynska & Buszewski, 2016).

Although the use of transgenic animals facilitates understanding the role of drug-metabolizing enzymes in the organism, animal studies cannot entirely replace clinical studies in predicting all responses in human, particularly because of pronounced species differences between humans and common laboratory animals. However, as the risk for human volunteers that participate in early clinical studies should be minimized, a variety of *in vitro* metabolism studies can be introduced (Dudda & Kuerzel, 2013).

Common *in vitro* metabolism systems include hepatocytes, the S9 fraction, microsomes, and the soluble fraction. All of them have both advantages and disadvantages which are summarized in table 2 and must be selected case by case.

In vitro system	Pros	Cons
Perfused organs	All metabolic active enzymes for phases I and II present including cofactors, whole metabolic profile observed, best correlation to in vivo	Expensive, ex vivo animal trial, complex methodology, high technical effort, batch variability, more complicated than enzyme-only system, quality control, limited use for multiple compounds
Slices	All metabolic active enzymes for phases I and II present including cofactors, whole metabolic profile observed, good correlation to in vivo	Expensive, ex vivo animal trial, diffusion controlled, complex methodology, high technical effort, batch variability, more complicated than enzyme-only system, quality control, limited use for multiple compounds
Cells in primary culture (e.g., hepatocytes)	All metabolic active enzymes for phases I and II present including cofactors, whole metabolic profile, population pools for cryopreserved hepatocytes possible, good correlation to in vivo	Expensive, batch variability, quality control, complex methodology, high technical effort, limited use for multiple compounds
S9 fraction	Easy to use, cheap, phases I and II present, whole metabolic profile observed	Addition of cofactors, lower enzyme activity than microsomes/supersomes
Microsomes	Easy to use, cheap, "population" pools	Addition of cofactors, only membrane-bound metabolizing enzymes such as CYPs, FMOs, and UGTs partial metabolic profile
Cytosol	Easy to use, cheap	Addition of cofactors, only soluble metabolizing enzymes such as alcohol dehydrogenases, sulfotransferases, glutathione *S*-transferase, *N*-acetyl transferases partial metabolic profile
Supersomes	Easy to use, moderately cheap, single enzyme only	Currently only CYPs, FMOs, UGTs, GSTs, and SULTs, single enzyme only, different CYP: oxidoreductase molar ratio, accuracy of kinetics questionable

Table 2. Comparison of *in vitro* test systems to study biotransformation (Dudda & Kuerzel, 2013).

Microsomes are widely and commonly used as the first-choice *in vitro* model method since they provide a simple and affordable way to obtain a good indication of the CYPs and UGTs metabolic profile. They are derived from the smooth endoplasmic reticulum (SER) and are commonly used as an enzyme source for the measurement of metabolic stability (Knights, Stresser et al., 2016).

Microsomes are obtained through steps of differential centrifugation (Pelkonen, Kaltiala et al., 1974) and they express the major drug-metabolizing enzymes (DMEs) CYPs and UGTs along with others that contribute to drug metabolism. The former group of enzymes needs NADPH as cofactor, while the latter one requires of alamethicin and UDPGA to perform its catalytic activity.

The activity of liver microsomes can vary substantially between different organisms, even if within the same species, because of ontogeny, genetic polymorphisms, or environmental factors.

However, this last problem can be successfully solved by the application of pooled microsomes obtained by the extraction from several livers.

The evaluation of a metabolic stability profile of a compound can be performed in higher throughput especially due to the development of more sensitive HPLC/UV or HPLC-MS instruments and the possibility to analyse more analytes in parallel.

2. AIM OF THE PROJECT

This PhD thesis belongs to a project aiming at investigating, both *in vitro* and *in vivo*, small molecules, called CFTR correctors, able to help the protein folding of defective sarcoglycans (SG). Mutated SGs are the primary cause of a group of diseases called sarcoglycanopathies, presently incurable.

Sarcoglycanopathies are rare autosomal recessive myopathies, belonging to the family of limb girdle muscular dystrophies (LGMDR3-6). Sarcoglycanopathies, because of mutations in *SGCA*, *SGCB*, *SGCD* and *SGCG* genes coding for α-, β-, δ- and γ-SG, respectively, result in progressive muscular weakness. SGs assemble into a single tetrameric unit within the dystrophin-associated protein complex (DAPC) of skeletal and cardiac muscle, playing a key role in assuring sarcolemma stability during muscle contraction. The most frequently reported defects in sarcoglycanopathies are missense mutations. The presence of a single amino acid substitution results in a folding defective protein recognized by the QC machinery and prematurely degraded by the ubiquitin-proteasome system. However, although structurally defective, most of the SG mutants are still functional. Indeed, by assisting/promoting their folding and trafficking by CFTR correctors, the SG complex can reach the sarcolemma, strengthening its function. The proof of concept of the CFTR correctors efficacy has been established *in vitro,* treating LGMDR3 myotubes (Carotti et al., 2018).

The study described in this thesis is first devoted to the consolidation of this important finding by using myogenic cells isolated from sarcoglycanopathy subjects, the closest *in vitro* model of the disease. In the second part, major efforts were dedicated to the generation of an animal model faithfully mimicking the forms of sarcoglycanopathy due to a missense mutation. Once characterized, the novel animal model was successfully used to prove efficacy and safety of the most promising CFTR corrector *in vivo*.

It is generally known that a combination of two or more molecules could give an improvement in the achievement of a significant clinical benefit. Therefore, to further establish the therapeutic value of CFTR correctors in sarcoglycanopathies, we tested the combined administration of these small molecules. Assuming that correctors belonging to different chemical families could act on different steps of the folding process, CFTR corrector C17, the most effective identified so far, was combined with other correctors to treat LGMDR3 myotubes. Simultaneously, to verify how broaden is the panel of SG missense mutants rescuable by CFTR correctors, the efficacy of the C17 molecule was checked on LGMDR4 patient's myotubes, carrying a missense mutation on the *SGCB* alleles. These findings may allow enlarging the cohort of patients that could benefit from this therapeutic approach in the future.

In vitro studies to assess the efficacy of a molecule are crucial, however, as the development of a new drug is a long and difficult process, studies in animals should not be undervalued.

Once the therapeutic strategy based on CFTR correctors has been validated *in vitro,* the step forward aims validating the most promising compounds *in vivo*. KO models were generated for all SG, however as they do not express the protein, they are unsuitable to test the efficacy of CFTR correctors aiming at recovering a folding defective but synthetized protein. On the other hand, the two conventional KI mice generated in the last years by introducing a pathogenic missense mutation in either the *sgca* or *sgcb* genes failed to develop the dystrophic phenotype expected on the basis of the equivalent human mutations. Therefore, to bypass this bottleneck, the second main aim of this PhD project, was the generation of a valuable model of LGMDR3 by the AAV transduction of the hind limbs of the *sgca*-null mouse with the human α-SG sequence. Upon characterization, the resulting humanized mice expressing the endogenous β, γ-, δ-SG, and the human α-SG carrying the missense mutations were chronically treated with the corrector C17, to eventually evidence its efficacy at the molecular, histological and functional point of view and its safety.

As final goal, initial pharmacokinetic and toxicological studies started to evaluate the behaviour of the molecule C17 in the organism. To this intent, we checked the C17 blood stability and its biotransformation mediated by phase I and major phase II enzymes present in liver microsomes.

Overall, we are confident that our results will strengthen the hypothesis that CFTR correctors, such as C17, are effective in recovering mutated sarcoglycans, i.e. proteins structurally unrelated to CFTR, but sharing similar fate when a missense mutation impairs their folding and/or trafficking. Moreover, considering the absence of toxicity observed until now, we expect the CFTR correctors become a valid pharmacological approach not only for cystic fibrosis but for sarcoglycanopathies as well.

3. MATERIALS AND METHODS

3.1 *In vitro* experiments

3.1.1 Cell culture and CFTR correctors treatment

Primary human myogenic cells from a LGMDR4 patient were isolated from a bioptic fragment from the Telethon Genetic Bio-Bank facility. Myogenic cells were grown in Dulbecco's modified Eagle's medium (DMEM) supplemented with 20% FBS (Gibco, Thermo Fisher Scientific, Waltham, MA, USA). To induce differentiation, myoblasts, grown at confluence, were incubated with DMEM supplemented with 2% Horse Serum (Euroclone), 10 mg/ml human recombinant insulin (Sigma-Aldrich), 100 mg/ml human Apotransferrin (Sigma-Aldrich) and adenovirus carrying the MyoD ORF at a multiplicity of infection (MOI) of 50. Differentiation was carried on for seven days. C17 CFTR corrector was added 48 hours before lysis. After treatments, cells were washed twice with ice cold PBS and lysed with RIPA buffer supplemented with complete protease inhibitor (Sigma-Aldrich, St. Louis, MO, USA).

3.1.2 Biotinylation of surface proteins

The biotinylation reaction was conducted according to (Carotti et al., 2020). At the end of the experiments, e.g. after 48 hours of treatment with C17 molecule, myotubes were incubated at 4°C for at least 10 min and all the procedures were performed at this temperature to slow down all cellular processes and in particular cell membrane protein recycling. Cells were then washed three times with ice cold PBS supplemented with calcium and magnesium and incubated under gentle agitation with a solution of 0.5 mg/mL biotin (EZ-Link Sulfo-NHS-LC-Biotin, Thermo Fisher Scientific, Waltham, MA, USA) in PBS for 20 min at 4 °C. The biotinylation reaction was stopped washing the cells twice with 100 mM glycine in PBS (each wash 5 min), and twice with PBS. Cells were lysed with RIPA buffer, and lysates were centrifuged at 15,000 g at 4 °C for 30 minutes. The supernatants were quantified by BCA assay, and 50 µg of proteins were incubated with streptavidin agarose beads (Thermo Fisher Scientific, Waltham, MA, USA) (20 µL of resin for each sample) over night at 4 °C under gentle rotation. The streptavidin-resin was washed three times with RIPA buffer, and bound proteins were eluted with Laemmli sample buffer for the western blot analysis. As negative control, lysates of non-biotinylated cells were incubated with the streptavidin resin and analyzed by western blot to exclude nonspecific binding to the streptavidin resin.

3.1.3 Immunofluorescence

Primary human myogenic cells grown on poly-lysine coated coverslips were stained according to the following protocol:

- incubation for 30 min at 4°C;
- 2 gentle washings with ice-cold PBS;
- incubation with the primary antibody against β-SG diluted 1:1000 in 0.5% BSA in PBS for 5 h at 4°C;
- 3 gentle washings with ice-cold PBS;
- incubation with the secondary antibody Alexa Fluor488 anti-rabbit IgG diluted 1:200 in in 0.5% BSA in PBS for 2 h at 4°C;
- 3 gentle washing with PBS;
- fixation for 15 min with 4% paraformaldehyde in PBS (PFA);
- blocking with 10 mM ammonium chloride
- mounting and observation with a Leica SP5 laser scanning confocal microscope.

3.2 Adeno associated virus production

The R98H or V247M mutation were introduced in the full-length, tag-less wild-type sequence of the human α-SG cloned in the pcDNA vector described in (Sandona et al., 2004) by the subcloning of the BamHI fragment excised from the expressing vectors described in (Gastaldello et al., 2008). The WT and mutated cDNA sequences were subsequently cloned between the two inverted terminal repeats (ITRs) of the adeno associated virus type 1 (AAV1) vector, under the muscle specific tMCK promoter using the NheI and XhoI sites. All constructs were controlled by DNA sequencing. The cloning process, production and *in vivo*-grade purification of recombinant AAV1 stocks were carried out by the Applied Biological Materials (ABM) Inc (Richmond, BC, Canada).

3.3 Animal experiments

All *in vivo* experiments were performed in accordance with the European guidelines and regulations for the human care and use of experimental animals. The protocol has been authorized by the Public Veterinary Health Department of the Italian Ministry of Health (Authorization n° 24/2020-PR, 10/01/2020).

C57BL/6 and *sgca*-null mice were bred in the animal facility of the Department of Biomedical Sciences, provided with water and food ad libitum and were housed in a thermally controlled room at 20–24°C with a 12-h light/dark cycle. *Sgca*-null mice were previously characterized (Liu & Engvall, 1999). Both male and female mice were used for this study. For viral transduction, 1-2-day-old pups of *sgca*-null mouse were injected in hind limbs with 10 µl of AAV1 ($9x10^{11}$ genome copies/ml) carrying either the WT or mutated (R98H and V247M) human *SGCA*

sequence. Neonate *sgca*-null pups were anesthetized by induced hypothermia; a 30G needle micro-syringe was used to deliver intramuscularly the AAV1 particles suspended in phosphate buffer ($9x10^{11}$ genome copies/ml). Two injections of 5µL each were performed in the muscles below the knee. After injection, warmed pups returned to their mother, until weaning.

For transduced muscle characterization, 10 weeks upon viral injection, mice were sacrificed by cervical dislocation and muscles of the hind limbs were explanted and quickly frozen in liquid nitrogen-cooled isopentane. For drug treatment, 7 weeks upon viral injection, mice were daily injected intraperitoneally with either C17 (25mg/kg) dissolved in 5% DMSO, 5% Kolliphor-EL in physiological solution or vehicle, for 21 or 35 days.

3.4 Muscle physiology

For in vivo force measurement procedure, the animal was deeply anesthetized with an intraperitoneal injection of Ketamine 100mg/kg Xylazine 10mg/kg and, a few minutes later, an intramuscular injection of Altadol 5-10mg/kg as a pain relief treatment. A small incision was made on the side of the knee to the direction of the hip, exposing the common peroneal nerve. A TeflonTM-coated seven-stranded steel wire (AS 632; Cooner Wire Company, Chatsworth, CA, USA) was sutured with 5-0 silk thread at each side of the nerve. Upon electrical stimulation, torque production of the tibialis anterior muscle is measured using a lever system (Model 305B; Aurora Scientific, Aurora, ON, Canada). The electrical stimulation has been performed on a S88 stimulator (Grass Instrument, Warwick, RI, USA) using the following protocol: train duration 200ms, pulse width 500 µsec, amplitude 1-2V and stepwise increase frequencies from a single pulse to 20Hz, 40Hz, 55Hz, 75Hz, 100Hz and 150Hz; each train is performed every 30s to avoid effects due to fatigue.

TA muscles from C57BL/6 and sgca-null mice of similar age and weight were used as positive and negative control, respectively. After force measurements, mice were sacrificed by cervical dislocation, and muscles were dissected, weighed and frozen in isopentane precooled in liquid nitrogen for further analyses.

3.5 Explant, fixing, paraffine inclusion and slice-preparation of mouse kidney and liver

Immediately upon sacrifice, liver and kidneys were explanted and immersed in 4% buffered neutral paraformaldehyde at 4°C for 48 hours. To promote fixative penetration in the tissue, each liver was cut in 6 pieces and each kidney in 2 pieces. Subsequently, organs were extensively washed with phosphate-buffered saline (PBS, 0.1 M, pH 7.4) and finally immersed in 70% ethanol for conservation and/or further processing. For histological analysis, tissue fragments were dehydrated through a graded series of ethanol and embedded in paraffin.

3.6 Histological, morphometric and immunofluorescence analyses

From paraffine-embedded livers and kidneys, sections (5 µm thick) were cut in a microtome and were stained with haematoxylin and eosin (H&E).

From frozen muscle explants, transverse cross sections (8 µm thick) were cut in a cryostat microtome (Leica CM1850) set at -24 ± 1°C. H&E staining was performed to examine the general morphology of tissues. Sections are stained for 5 min each in hematoxylin and eosin, dehydrated with ethanol and xylenes, mounted and examined by light microscopy.

To easily determine the cross-sectional area (CSA) of individual muscle fibers, immunostaining was performed using an antibody against laminin to visualize the basal lamina according to (Mouisel, Vignaud et al., 2010). Briefly, muscle cryo-sections were blocked with 5% normal goat serum in PBS and subsequently incubated for 1 hour at 37°C with the rabbit polyclonal antibody specific for laminin diluted 1:150 in 5% fetal bovine serum. The primary antibody was revealed with an anti-rabbit Alexa-Fluor-488 diluted 1:200 in PBS incubated for 1 hour at 37°C. Nuclei were counterstained with DAPI (Abcam, Cambridge, UK).

Muscle sections were examined with a Leica RD100 fluorescence microscope equipped with a digital camera. Muscle fiber CSA was measured on digital photographs using ImageJ software (Scion, Frederick, MD).

Immunofluorescent staining of α- β- and δ-SG was carried out to assess the cytolocalization of the proteins. Muscle cryo-sections were washed and blocked with 10% normal goat serum, 0.5% bovine serum albumin (BSA) in PBS for 1 hour at room temperature. Muscle sections were incubated overnight at 4°C with the primary antibodies (all raised in rabbit) specific for α- β- and δ-SG diluted respectively 1:2000, 1:100 and 1:500 in 0.5% BSA. Protein signals were revealed with an anti-rabbit Alexa-Fluor-488 diluted 1:500 in 0.5% BSA in PBS incubated for 2 hours at room temperature. Nuclei were counterstained with DAPI (Abcam, Cambridge, UK). As negative controls, immunostaining with the sole secondary antibodies was performed. Muscle sections were examined with a Leica DMR fluorescence microscope equipped with a digital camera.

3.7 Western blot analysis

For western blot analysis, about 10 mg of TA mouse muscle were incubated in lysis buffer containing 3% SDS, 0.1 mM EGTA supplemented with complete protease inhibitors cocktail, Sigma-Aldrich (St. Louis, MO, USA) and homogenized with the TissueLyser II instrument (Quiagen, Hilden, Germany). Both cell and muscle lysates were resolved by SDS-PAGE, blotted onto a nitrocellulose membrane and probed with selected primary antibodies.
Secondary antibodies were horseradish peroxidase-conjugated, and blots were developed with ECL chemiluminescent substrate (Genetex, Alton Pkwy Irvine, CA, USA), signals were digitally

acquired with Alliance Mini HD9 Imaging System (Uvitec, Cambridge, UK). Densitometry was performed with the ImageJ software. The intensities of sarcoglycan bands were normalized for the intensity of the housekeeping protein GAPDH.

3.8 Quantitative Real Time PCR

Total DNA was extracted from 10 mg of TA muscle with MyTaq Extract-PCR kit (Meridian Bioscience) according to manufacturer's protocol. DNA concentration, upon RNAse treatment, was determined at the Nanodrop 2000 spectrophotometer (Thermo Scientific, Wilmington, DE); 500 ng of each sample were used for the PCR reactions.

Serial 10-fold dilutions starting from 10^9 genome copies/mL of the viral vector were used to prepare the standard curve by plotting the vector copy number logarithm against the measured threshold cycle (Ct) values, as reported in (Cui, Shi et al., 2018). The amount of DNA quantified for each sample was expressed as a number of genome copies per mL.

The PCR parameters were: initial denaturation at 95°C for 10 min followed by 40 cycles of 10 s at 95°C and 30 s at 60°C for acquisition of fluorescence signal. A melting curve was generated by the iQ5 software at the end of the final cycle for each sample to confirm the specificity of the amplified product.
The PCR reactions was performed in triplicate in 10 µL final volume in IQ5 Thermal Cycler (Bio-Rad, Hercules, CA, USA) using Biorad iQ Sybr green supermix. Primer sequences were as follows: human α-SG forward primer 5'- CCCCAGACCGTGACTTCTTG-3', human α-SG reverse primer 5'- TCTCTTCAGCCTTCCCTCCC-3'.

3.9 Blood stability assay

The blood stability assay was performed according to the protocol described and schematically reported below:

- Blood was collected from C57BL/6 mouse (1 ml for each experiment);
- C17 was added to the blood to reach a concentration of 25 µM. The solution was incubated at 37°C under agitation (370 rpm);
- 100 µL of blood containing the compound, was collected at different time points (0', 30', 1h, 2h, 4h);
- the blank solution was prepared with 100 µL of blood to determine the background in the analysis of the UHPLC data;
- five volumes of acetone were added to the blood fractions, the suspension was sonicated for 2 min, 5 volumes of acetonitrile + 0.1% trifluoroacetic acid were added and the solution was sonicated again for 5 min;

- each fraction was centrifuged at 4°C for 7 min at 15’000 g;
- supernatants were analysed at the UHPLC.

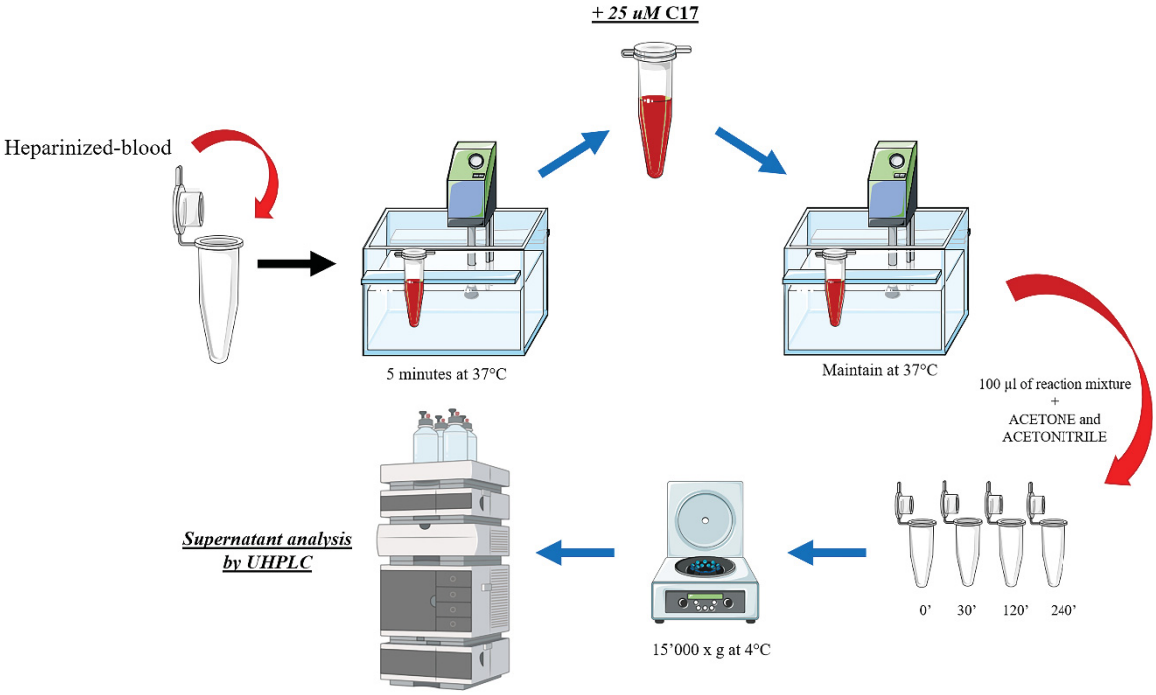

Figure 23. Schematic representation of C17 blood stability experiment protocol (created with smart.servier.com and Biorender.com).

3.10 Biotransformation assays

3.10.1 Liver microsomes isolation from mouse livers, adapted from (Pelkonen et al., 1974)

An appropriate number of livers were harvested from *sgca*-null mice and immediately frozen in liquid nitrogen. This organ can be stored at -80°C until further processing.

The livers were homogenized initially in the homogenization buffer (sucrose 250 mM, HEPES 50 mM, KCl 25 mM, MgCl 5 mM, EDTA 0.1 mM, pH 7.4) after the addition of PMSF 0.1 M in EtOH (0.25 µL/mL), a serine protease inhibitor. Homogenate is obtained by using the Ultra Turrax T25 at 20’500 rpm times for 30 seconds at 4°C. Homogenates were centrifuged at 700 x g for 10 minutes at 4°C and then 10’000 x g for 10 minutes at 4°C. The pellet was discarded, and the supernatant was then centrifuged at 15’000 x g for 20 minutes at 4°C.

The pellet was discarded again, and homogenates were re-centrifuged at 105’000 x g for 1 hour at 4°C with ultracentrifuge (Optima max-XP, Beckman Coulter, Brea, California, Stati Uniti).

Following this high-speed step, the supernatant was discarded, and the pellet was resuspended in the homogenization buffer and centrifuged again at 105’000 x g for 1 hour at 4°C.

The supernatant was again discarded, the remaining pellet, corresponding to the microsomal fraction, was resuspended in the homogenization buffer.

The BCA assay was performed to determine microsome-proteins concentration. Microsomes were stored at -80°C until use. A representative scheme of the experimental workflow is reported below.

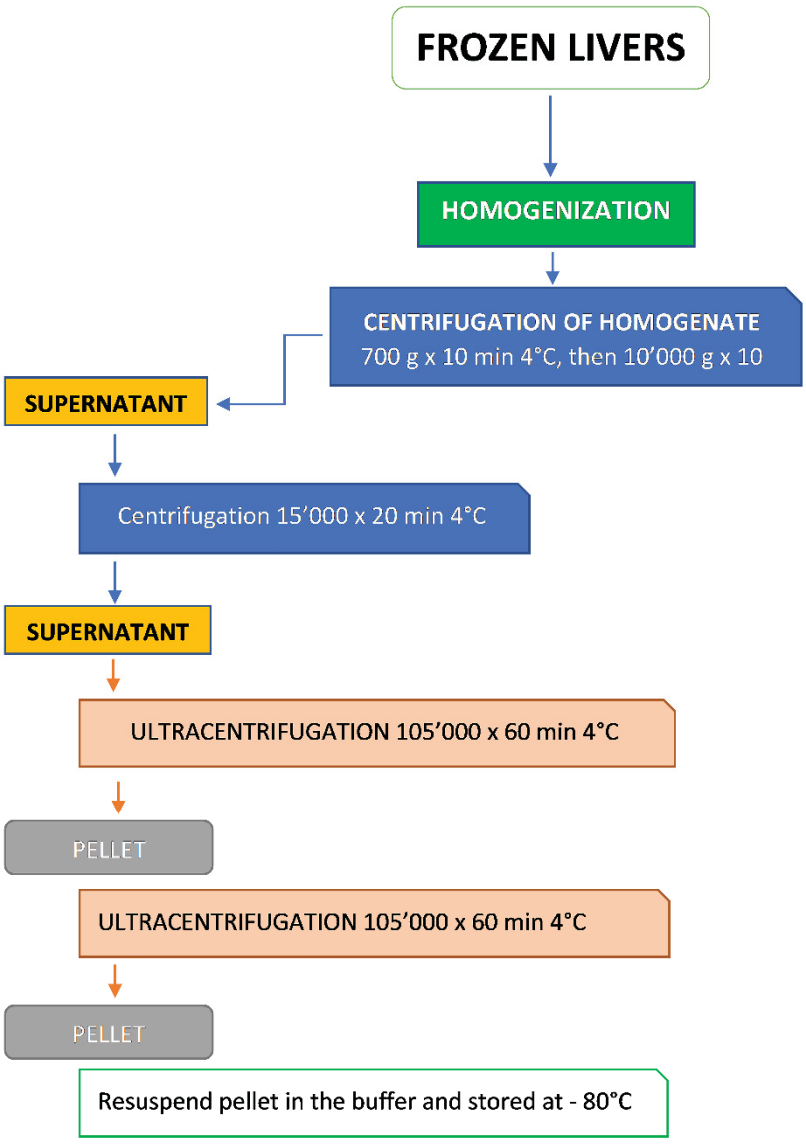

Figure 24. Schematic workflow of microsomes isolation from mouse livers.

3.10.2 Liver microsomes incubation with resveratrol and C17 compounds: investigation of phase I reactions

The extracted liver microsomes were incubated with the test compound and the CYP450 enzymes cofactor (NADPH) to investigate the formation of possible metabolites resulting from phase I reactions over the time through UHPLC. The experimental workflow is reported in figure 25. The test compound was the C17 and the reference compound was resveratrol.

The metabolites of the latter, resulting from the CYP450 enzymes catalytic activity correspond to piceatannol and tetrahydroxystilbene, therefore it was expected that the incubation of resveratrol with microsomes and the activator of CYP450-enzymes resulted in the formation of its metabolites over the time.

As negative controls have been used: the reaction mixture without microsomes, without the NADPH, and without the compound. In the first two negative controls, it was expected to observe a constant level of compound over time.

The experiment consists of compounds dissolution to a stable stock concentration of 500 µM. The reaction mixture is constituted by 86% v/v of 0.1 M potassium phosphate buffer (pH 7.4) pre-warmed to 37°C, 10% v/v of 10 mM NADPH in 0.1 potassium phosphate buffer, and 1% v/v of either the test or reference compound.

After incubation of the reaction mixture at 37°C for 5 minutes, 3% v/v of stock microsomes suspension is added (final concentration is 0.5 mg/mL), and the mixture is incubated at 37°C in a water bath.

Afterwards, at time points of 0', 30', 60', 90' and 120', 200 µL of the mixture was collected and 0.5 volumes of acetonitrile were added to stop the catalytic activity of enzymes. Samples were sonicated for 2 minutes and then a step of centrifugation at 10'000 x g at 4°C was performed. The supernatant was subsequently analysed at the UHPLC.

3.10.3 Liver microsomes incubation with resveratrol and C17 compounds: investigation of phase II reactions

The extracted liver microsomes were incubated with the test compound and the UGT enzymes cofactor (UPDGA) to investigate the formation of possible metabolites resulting from phase II reactions through UHPLC analysis. The experimental workflow is reported in figure 25. The test compound was the C17 and the reference compound was resveratrol. The metabolites of the latter small molecule resulting from the UGT enzymes catalytic activity correspond to 4'-O-monoglucuronide resveratrol and 3-O-monoglucuronide resveratrol, therefore it is expected that the incubation of resveratrol with microsomes activated with alamethicin and the cofactor UPDGA resulted in the formation of these metabolites that increase in their concentration over time. As negative controls, the reaction mixture without microsomes, without the UDPGA, and without the compound were used. In the first two cases, it was expected to observe a constant level of compound over time.

The experiment consists of compounds dissolution to a stable stock concentration of 500 µM. Microsomes are previously diluted to 5 mg/mL in 0.1 M potassium phosphate buffer and activated by a pre-incubation with alamethicin (50 µg/mL) on ice for 30 minutes before use. Alamethicin allows removing the latency of microsomes for use in glucuronidation assay.

The reaction mixture is constituted by 1% v/v of the test or reference compound, 69% v/v of 0.1 M potassium phosphate buffer (pH 7.4), 10% v/v of activated microsomes (final concentration 0.5 mg/mL), and 10% v/v 40 mM magnesium chloride (final concentration 4 mM). After pre-incubation of the reaction mixture at 37°C for 5 minutes, 10% v/v of UDPGA solution (5 mM) is added to the mixture reaction.

Afterwards, at time points of 0', 15', 30', 60', 90' and 120', 200 µL of the mixture was withdrawn and 0.5 volumes of acetonitrile were added to stop the reaction. The samples were sonicated for 2 minutes, vortexed and centrifuged at 10'000 x g at 4°C for 5 minutes. The supernatant was subsequently analysed at the UHPLC.

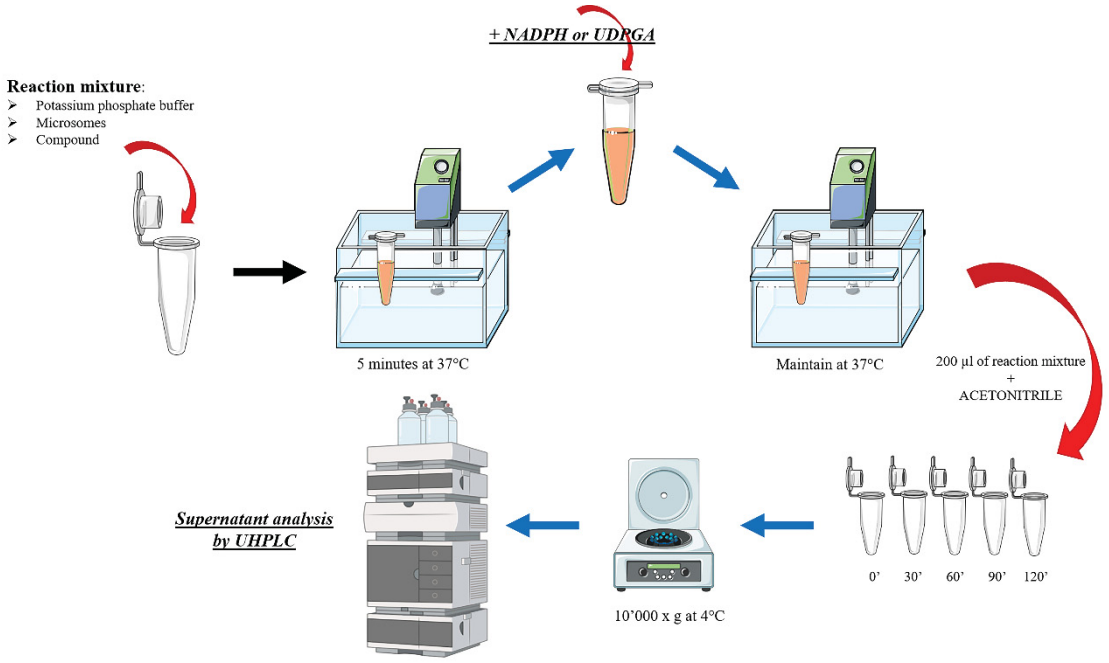

Figure 25. Schematic representation of phase I and phase II metabolism protocols (created with smart.servier.com and Biorender.com).

3.11 UHPLC analysis

UHPLC (ultra-high-performance liquid chromatography) technique bases on a column that contains an apolar stationary "phase" and the mobile phase that is polar and water-based, involving solvents such as acetonitrile. Since most drugs are typically quite hydrophobic, they are repelled by the mobile phase and tend to associate with non-polar stationary phase for a longer time than the more polar metabolites and other cellular material from the experimental incubation. In this way, there will be a chromatographic separation that facilitates an accurate analyte or metabolites quantification.

The UHPLC analysis of samples from both blood stability assay and microsomes incubation with testing compounds have been performed according to the following conditions.

The UHPLC/UV (1290 Infinity LC394 System, Agilent Technologies) exploits a reversed-phase column (Zorbax RRHT Extend C18, 1.8, μm, 50 × 3.0 mm, Agilent Technologies) and a UV diode array detector (190 – 500 nm), at a flow rate of 0.6 mL/min. Applied solvents A and B were water + 0.1% trifluoroacetic acid and acetonitrile, respectively.

The gradient for B was as follows: 10% for 1 min, then from 10 to 100% in 7.0 min, 100% for 0.5 min, then from 100% to 10% in 1.5 min. The injection volume was 5 μL. The eluate was preferentially monitored at 312 nm, corresponding to a maximum of absorbance of both C17 that has a retention time of about 6.6-6.7 minutes and resveratrol, with a retention time of 3.3-3.4 minutes. The temperature of the column was kept at 25°C. Each sample was analyzed at wavelengths of 216, 250, 286, 312, 350 and 400 nm in order to investigate the presence of possible metabolites.

In the blood stability experiments, the mouse blood with the addition of acetonitrile was used as blank solution, while the potassium phosphate was used for the microsomes' experiments.

3.12 Antibodies and chemicals

Rabbit monoclonal anti α-SG (AB189254) and rabbit polyclonal anti β-SG (AB83699) were from Abcam (Cambridge, UK); rabbit polyclonal anti GAPDH (G9545) and rabbit polyclonal anti laminin (L9393) were from Sigma-Aldrich (St. Louis, MO, USA); rabbit polyclonal antibody specific for δ-SG was produced and characterized as previously described (Bianchini et al., 2014).

Western blot secondary antibodies were horseradish peroxidase-conjugated goat anti-rabbit IgG (Sigma-Aldrich, St. Louis, MO, USA) while fluorescent antibodies were Alexa Fluor 488-conjugated goat anti-rabbit IgG (Invitrogen, Carlsbad, CA, USA).

C17 corrector was purchased from Exclusive chemistry (Kaluga region, Obninsk, Russia), Kolliphor-EL and DMSO from Sigma-Aldrich (St. Louis, MO, USA).

3.13 Statistical analysis

Data were expressed as means ± SD. For *in vivo* functional experiments, data were expressed as means ± SEM. Statistical differences among groups were determined by One-way ANOVA test, followed by Tukey's multiple comparisons test. When only two groups were considered, statistical analysis was performed by the unpaired two-tailed Student's t-test. A level of confidence of $P < 0.05$ was used for statistical significance.

4. RESULTS

4.1 Combined CFTR correctors treatment on LGMDR3 myotubes

The results of this part are summarized in the published paper that is attached in the following pages (Carotti et al., 2020).

International Journal of
Molecular Sciences

MDPI

Article

Combined Use of CFTR Correctors in LGMD2D Myotubes Improves Sarcoglycan Complex Recovery

Marcello Carotti [1], Martina Scano [1], Irene Fancello [1], Isabelle Richard [2], Giovanni Risato [1], Mona Bensalah [3], Michela Soardi [1] and Dorianna Sandonà [1,*]

1 Department of Biomedical Sciences, University of Padova, Via U. Bassi 58/b 35131 Padova, Italy; marcello.carotti@unipd.it (M.C.); martina.scano@phd.unipd.it (M.S.); irene.fancello@studenti.unipd.it (I.F.); giovannirisato@gmail.com (G.R.); michelasoardi@gmail.com (M.S.)
2 Généthon INSERM, U951, INTEGRARE Research Unit, Univ Evry, Université Paris-Saclay, 91002 Evry, France; RICHARD@genethon.fr
3 INSERM, Institut de Myologie, U974, Center for Research in Myology, Sorbonne Université, 75013 Paris, France; mona.bensalah@upmc.fr
* Correspondence: dorianna.sandona@unipd.it; Tel.: +39-049-8276028; Fax: +39-049-8276049

Received: 13 February 2020; Accepted: 28 February 2020; Published: 6 March 2020

Abstract: Sarcoglycanopathies are rare limb girdle muscular dystrophies, still incurable, even though symptomatic treatments may slow down the disease progression. Most of the disease-causing defects are missense mutations leading to a folding defective protein, promptly removed by the cell's quality control, even if possibly functional. Recently, we repurposed small molecules screened for cystic fibrosis as potential therapeutics in sarcoglycanopathy. Indeed, cystic fibrosis transmembrane regulator (CFTR) correctors successfully recovered the defective sarcoglycan-complex in vitro. Our aim was to test the combined administration of some CFTR correctors with C17, the most effective on sarcoglycans identified so far, and evaluate the stability of the rescued sarcoglycan-complex. We treated differentiated myogenic cells from both sarcoglycanopathy and healthy donors, evaluating the global rescue and the sarcolemma localization of the mutated protein, by biotinylation assays and western blot analyses. We observed the additive/synergistic action of some compounds, gathering the first ideas on possible mechanism/s of action. Our data also suggest that a defective α-sarcoglycan is competent for assembly into the complex that, if helped in cell traffic, can successfully reach the sarcolemma. In conclusion, our results strengthen the idea that CFTR correctors, acting probably as proteostasis modulators, have the potential to progress as therapeutics for sarcoglycanopathies caused by missense mutations.

Keywords: sarcoglycanopathy; myogenic cells; myotubes; folding-defective proteins; protein folding correctors; CFTR correctors; proteostasis regulators

1. Introduction

LGMD2D (LGMD-R3 according to the new nomenclature [1]) is a rare autosomal recessive disease affecting striated muscle. It belongs to the group of limb girdle muscular dystrophies because of the involvement of the proximal musculature of the shoulders and pelvic girdle [2]. LGMD2D is caused by mutation in the *SGCA* gene coding for α-sarcoglycan (SG) [3–5]. This protein, together with β-, γ- and δ-SG, forms the SG complex, a key component of the dystrophin associated protein complex, significantly contributing in preserving sarcolemma from contraction-induced stress. Moreover, a number of direct or indirect regulative roles have been associated to SG-complex [6,7]. LGMD2D, although heterogeneous, is often characterized by early onset and rapid progression, with people affected becoming wheelchair-bound in the adolescence [8]. Presently, no effective therapy is

available for LGMD2D as well as for the other three forms of sarcoglycanopathy (LGMD2E, 2C and 2F, due to mutations in *SGCB*, *SGCG* and *SGCD* genes, respectively [9]). Most of the gene defects responsible for the onset of sarcoglycanopathy are missense mutations [10–13]. In the last few years, the pathogenic mechanism of the forms of sarcoglycanopathy due to this type of genetic defects has been disclosed. It has been observed that many sarcoglycans with an amino acid substitution are unable to properly fold, are recognized by the quality control system of the cells and delivered to a premature degradation [14–17]. Consequently, the correct assembly, traffic and localization of the SG-complex is impaired, leading to a global reduction in the structural stability of the sarcolemma. An interesting point is the possibility to rescue the defective sarcoglycan as well as the entire SG-complex, by preventing the degradation of the mutant, acting either at the initial [15,16], intermediate [17] or final step [14] of the pathway. On these premises and taking advantage from the tremendous work done on another genetic disease, cystic fibrosis, that shares with sarcoglycanopathy a similar pathogenic mechanism [18], we elaborated a novel strategy of therapeutic intervention [19]. Our approach is based on the use of small molecules known as CFTR correctors, which are effective in rescuing the type II mutants of the cystic fibrosis transmembrane regulator (CFTR) [20,21]. CFTR correctors have been demonstrated effective not only on CFTR mutants but also on structurally correlated [22] as well as structurally uncorrelated defective proteins [23,24]. In our previous paper, incubation of cells, models of sarcoglycanopathy with a number of CFTR correctors, resulted in an increase of the mutated α-SG and the localization at the plasma membrane. Efficacy of one of these small molecules, C17, was subsequently confirmed in myogenic cells from a LGMD2D patient, where we also observed a reduction of the sarcolemma fragility [19]. Here, by using the human pathologic myotubes, we tested the efficacy of additional correctors belonging to the bithiazole family of C17, such as C13 [25], and of the quinoline family, such as C9 and C6 [25,26]. Furthermore, we evaluated two compounds, VX809 and VX661, presently used in combination with the potentiator VX770 for the treatment of CF patients carrying the ΔF508-CFTR mutation [27,28]. The combined administration of C17 with other correctors highlighted the additive and even a potential synergistic activity of such compounds. This foresees the possibility to scale down the dose of the molecules conserving the maximum effect. Moreover, the collected data provided preliminary suggestions concerning the possible mechanism of action. Finally, in the perspective of the development of a cure for sarcoglycanopathy, we also evaluated the ability of the corrected α-SG mutant to interact with the wild type partners as well as the stability at the sarcolemma of the rescued complex.

2. Results

2.1. Rescue of α-SG by CFTR Correctors in LGMD2D Myotubes

In Carotti et al. [19], we checked the ability of a few number of CFTR correctors in rescuing α-SG mutants in cell models. One of them, corrector C17, was in depth analyzed for its efficacy in myogenic cells from a LGMD2D patient, a compound heterozygote for the L31P and V247M mutations on the *SGCA* alleles. Here, we aim to broaden the number of validated compounds, tested in single or combined administration, potentially relevant for the treatment of sarcoglycanopathy. As model systems, we took advantage of the same pathologic myogenic cells as well as of those of healthy subjects. In both cases, seven-day differentiation of myogenic cells resulted in elongated, multinucleated myotubes as already reported [17,19,29]. We evaluated the following correctors: C13, a compound, like C17, belonging to the bithiazole family [25,30]; C9 and C6 derivative of the quinoline structure [25,26] and C17 used as our reference. Myogenic cells differentiated for seven days, were treated the last 72 h with 1‰ DMSO, used as control vehicle, or with the small molecules at the concentrations reported in Figure 1. The phase contrast images of the LGMD2D myotubes, as appearing at the end of treatment (Figure 1A), show no major alterations in the morphology of the elongated syncytia nor signs of cytotoxicity, such as membrane blebbing or cells detaching from the plate, as expected according to [19]. Figure 1B reports the densitometric analysis of western blot experiments in

which the total protein lysates from treated myotubes were probed with specific antibodies for α-SG and β-actin, the latter used to normalize the protein loading. CFTR correctors efficacy was evaluated as the ability to induce an increase of the content of α-SG in comparison to the negative control myotubes (vehicle treated). All the CFTR correctors tested, with the exception of C6, induced approximately 1.5 fold increase of the α-SG content, with C17 being the most effective compound, almost doubling the amount of the protein, in accordance with our previous data [19]. On the contrary, treatments with the same correctors performed on myotubes from a healthy donor elicited no statistically significant effect on the α-SG content (Figure S1). These data confirm what observed in [19], i.e. that CFTR correctors are specifically effective on mutated sarcoglycans.

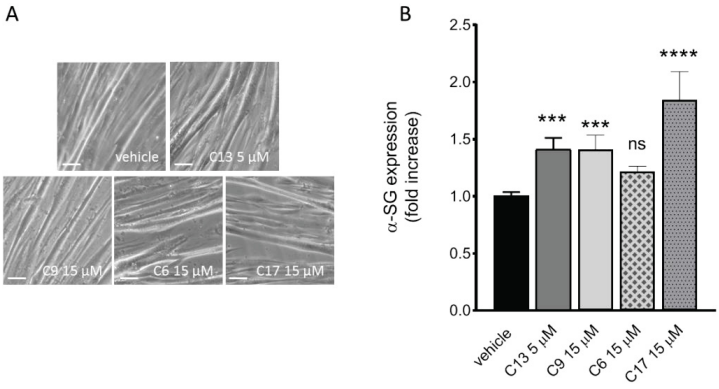

Figure 1. Rescue of α-SG by cystic fibrosis transmembrane regulator (CFTR) correctors in LGMD2D myotubes. Myogenic cells from a patient carrying the L31P/V247M α-SG mutations were differentiated for 7 days and treated for the last 72 h with either 1‰ DMSO (vehicle), C13, C9, C6 or C17 at the indicated concentrations. (**A**) phase contrast images of myotubes at the end of corrector incubation are indistinguishable from the control ones. Scale bar corresponds to 100 μm. (**B**) Densitometric analysis of western blot experiments performed with total protein lysates from LGMD2D myotubes treated as indicated. The α-SG protein was revealed by using specific primary antibody and normalized by the content of β-actin. α-SG content in different samples was expressed as the fold increase (+/− SD) of the amount present in the vehicle treated myotubes, and is the mean value of 3-4 independent experiments (each performed in duplicate). Statistical analysis was performed by One-way ANOVA test followed by multiple comparisons Dunnett's test; n.s., $p > 0.05$; ***, $p \leq 0.001$; ****, $p \leq 0.0001$.

2.2. Additive Effect of C13 in Combination with C17

Subsequently, we evaluated the effect of the combined administration of C17 and C13, both derivatives of the bithiazole moiety [30,31]. We used C17 5 μM, a dose that is ineffective in promoting α-SG rescue in LGMD2D myotubes according to our previous results [19], and C13 5 μM (as in Figure 1), both in single and co-administration. C17 10 and 20 μM was used for comparison. The absence of evident toxic effect elicited by the combined treatment is proved by the phase contrast image of the myotubes, recorded at the end of incubation (Figure 2A). The total α-SG protein content was estimated by western blot and densitometric analysis of myotube lysates. Both C13 and C17 5 μM in single administration promoted a slight increase of the mutated α-SG that was statistically significant for C13 only. On the other hand, the combination C17 + C13 increased the total amount of the mutated α-SG to a level that almost doubled that of the single administrations and is indistinguishable from that elicited by the single administration of C17 10 μM. Finally, as already observed, even a higher increase can be elicited by treating myotubes with C17 15 μM (Figure 2D). To be effective, the rescue must result in the delivery of the recovered protein on the membrane; therefore, we evaluated the fraction of the α-SG mutant present at the sarcolemma by the pull down of biotinylated membrane proteins followed by western blot and densitometric analysis (Figure 2E). It is interesting to note that even if the incubation with C13 5 μM resulted in an increase of the total α-SG mutant content, the fraction able to reach the myotubes surface is considerably lower and not statistically significant. Moreover, in the case

of the single administration of C17 5 μM, we can observe a slight increase, not statistically significant, paralleling what observed in the total extract. However, when the combination C13 5 μM + C17 5 μM is used, a large portion of the protein reached the sarcolemma. A similar result was obtained by C17 10 μM. This suggests that these correctors act on the same way, maybe on the same target, according to their structural similarity, improving escape from degradation and traffic of the mutated sarcoglycan toward the final destination.

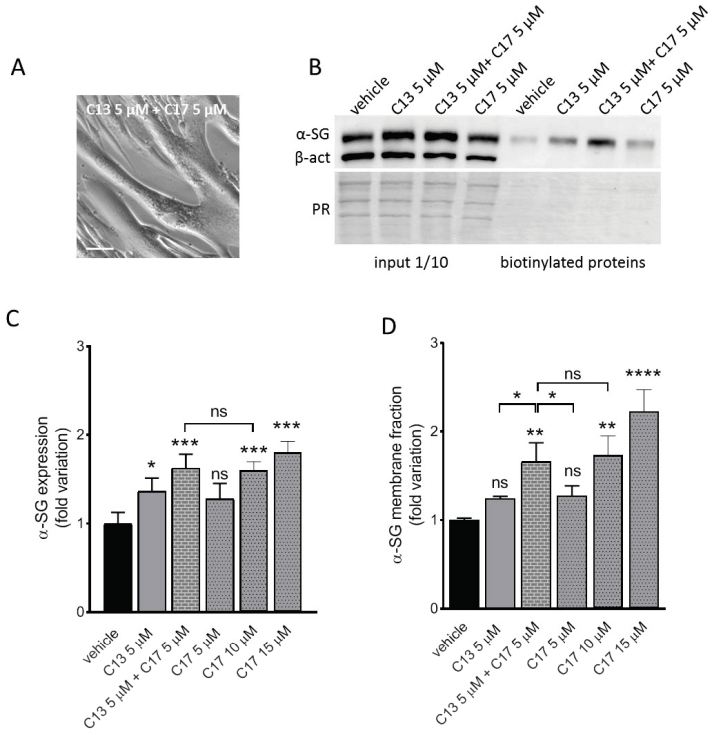

Figure 2. Additive effect of C13 in combination with C17. Myogenic cells from a patient carrying the L31P/V247M α-SG mutations were differentiated for 7 days and treated for the last 72 h with either 1‰ DMSO (vehicle), C13, C17 or C13 + C17 at the indicated concentrations. At the end of incubation, surface proteins were biotinylated. Then, myotubes were lysed and, after quantification, 50 μg of proteins were subjected to pull down assay by streptavidin-conjugated agarose beads. Recovered surface proteins and 1/10 of the starting myotubes lysates (input) were analyzed by SDS-PAGE and western blot with antibodies against α-SG and the cytosolic protein β-actin used as loading control (western blot of input) and to check the absence of biotin internalization (western blot of biotinylated proteins). (**A**) Phase contrast image showing the LGMD2D myotubes at the end of the combined treatment. Scale bar corresponds to 100 μm. (**B**) Representative western blot in which the left part shows the immunodetection of α-SG and β-actin present in the input lysates and the right part the fraction present at the sarcolemma; under the blot, the Ponceau Red staining of the membrane is reported as control of protein loading. Representative western blots of myotubes treated with vehicle, C17 10 μM or 15 μM is reported in Figure S2. (**C**) Quantification of α-SG content by densitometric analysis of the input and **(D)** of the biotinylated fraction of proteins. Values are the mean (+/− SD) of 3–4 independent experiments (each performed in duplicate) and are reported as fold increase of the amount present in the control sample. Statistical analysis was performed by One-way ANOVA test followed by multiple comparisons Tukey's test; n.s., $p > 0.05$; *, $p \leq 0.05$; **, $p \leq 0.01$; ***, $p \leq 0.001$, ****, $p \leq 0.0001$.

2.3. Additive/Synergistic Effects of C6 in Combination with C17

We tested the combination of low doses of C17 with corrector C9 or C6 both belonging to the class of quinoline derivatives [25,32]. As reported in Figure S3A of supplementary data, C9 in either single or co-administration with C17 resulted in a nearly identical increase of α-SG. On the other

hand, this effect did not parallel with an enrichment of the protein at the sarcolemma. Indeed, C9 was ineffective on the traffic of α-SG both when administered alone and in combination with C17 (Figure S3B). Therefore, this corrector was no further investigated.

As reported in Figure 3A the incubation of LGMD2D myotubes with corrector C6 at three different concentrations (5, 10 and 15 μM) as well as with C17 5 μM was almost ineffective at the total protein level. In contrast, the incubation with C17 15 μM resulted in a high increase of the α-SG content, as expected. Interestingly, the dual treatment with C6 + C17 both 5 μM, a concentration that was ineffective when compounds were administered alone, produced a robust increase of the α-SG protein, similar to the one obtained with the highest dose of C17. On the other hand, the dual incubation with C6 5 μM + C17 15 μM elicited an effect almost indistinguishable from the one obtained by the sole C17 15 μM (Figure 3A), suggesting that C17 at this dose and in this condition was, by itself, responsible for the maximum effect. An interesting and potentially promising outcome was observed analyzing the α-SG membrane fraction of these samples (Figure 3B). Indeed, with the exception of the lowest concentration of both correctors, a statistical significant increment of the α-SG membrane level was appreciable in all the other conditions. The membrane localization of α-SG was expected in samples in which C17 induced a substantial rescue of the protein (C17 15 μM), as already observed (see for example Figure 2D). The co-administration of C6 + C17 substantially paralleled what observed at the global level. Conversely, the membrane localization of α-SG in cells treated with C6 10 and 15 μM alone (see Figure 3A) suggests that C6 may foster the traffic towards the membrane of the fraction of α-SG that physiologically skips degradation. Remarkably, the effect of C6 became negligible when it was administered in combination with a high concentration of C17, known to induce a significant rescue of the mutant. All this considered, it is possible to suppose an additive/synergistic activity of C6 and C17.

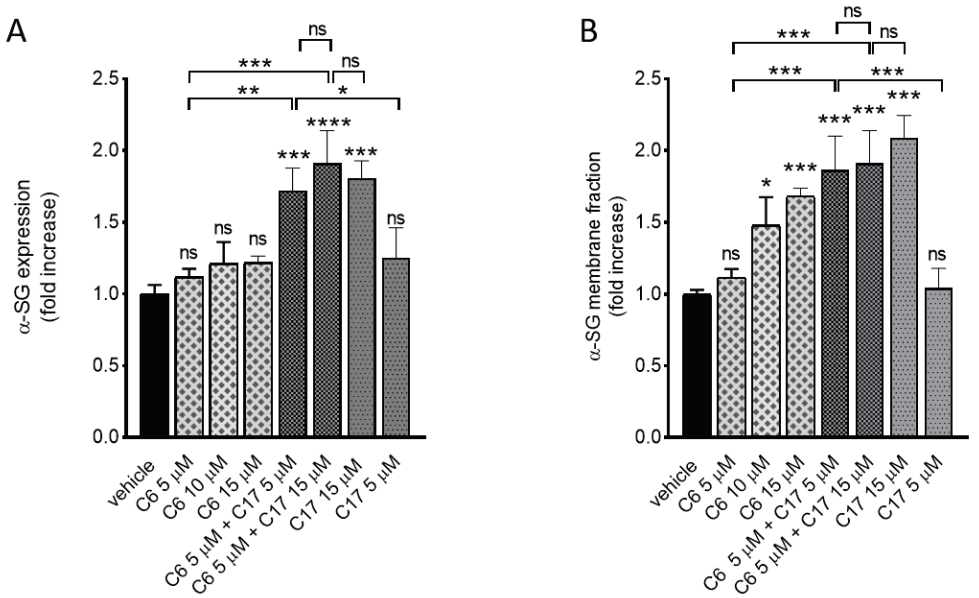

Figure 3. Additive/synergistic effects of C6 in combination with C17. Myogenic cells from a patient carrying the L31P/V247M α-SG mutations were differentiated for 7 days and treated for the last 72 h with either 1‰ DMSO (vehicle), C6, C17 or C6 + C17 at the indicated concentrations. At the end of incubation, myotubes were treated as described in the legend of Figure 2. Representative western blots are reported in Figure S4. (**A**) Quantification of α-SG content by densitometric analysis of the total protein lysates and (**B**) of the biotinylated fraction of proteins. Values are the mean (+/− SD) of 3–4 independent experiments (each performed in duplicate) and are reported as fold increase of the amount present in the control sample. Statistical analysis was performed by One-way ANOVA test followed by multiple comparisons Tukey's test; n.s., $p > 0.05$; *, $p \leq 0.05$; **, $p \leq 0.01$; ***, $p \leq 0.001$, ****, $p \leq 0.0001$.

2.4. CFTR Correctors Are Effective Only on V247M-α-SG Mutant

Considering the genotype of the LGMD2D myotubes used in these experiments, i.e., the presence of different mutations on the two *SGCA* alleles, we cannot exclude that additivity/synergy observed was due to the effect exerted by a single compound on one single mutant. Indeed, our data cannot discriminate if just one or both mutants have been rescued at the sarcolemma. Trying to solve this issue, we treated heterologous cells expressing a single mutant, either V247M-α-SG or L31P-α-SG, with correctors C6 and C17 both in single and co-administration (Figure 4). V247M-α-SG cells are a polyclonal population of HEK293 cells constitutively expressing the mutated form of the human α-SG. As described in [17,19], in these cells, named V-pop, the mutated α-SG moves toward the plasma membrane once recovered by pharmacological treatments. Because of the different sensibility of HEK293 vs myogenic cells towards CFTR correctors, the concentrations here utilized have been selected according to [19]. It is interesting to note that C6 and C17 effectively rescued the mutant and that their activity is presumably synergic. Indeed, the two correctors at a concentration ineffective when use in single administration elicited a strong improvement of α-SG membrane localization when co-administered. The level of V247M-α-SG reached was similar to what obtained by doubling the dose of C17 or C6 and paralleled what observed with LGMD2D myotubes (compare Figures 4A and 3B). A different outcome was obtained when treatments were applied in HEK293 cells transiently transfected with a plasmid expressing the L31P-α-SG mutant. In this case, C6 and C17 were completely ineffective, with no sign of increase of the mutant at the membrane upon either single or combined administration of correctors. As positive control, we evaluated the plasma membrane level of the α-SG protein upon transfection of the wild type form. Altogether these data suggest that the L31P substitution may affect the α-SG structure, making this mutant un-rescuable, at least at these conditions.

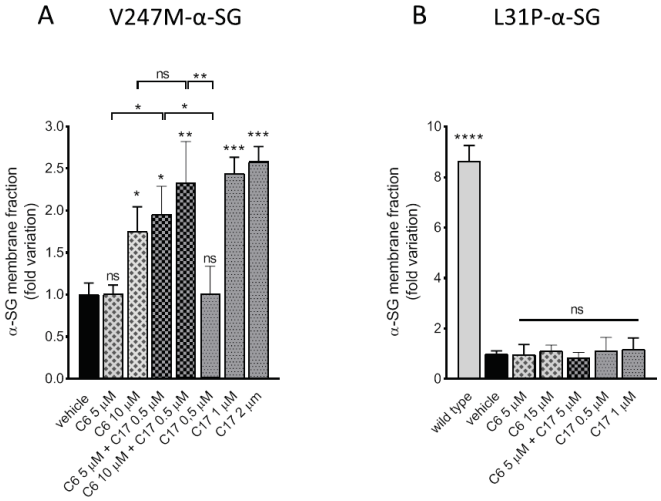

Figure 4. CFTR correctors C6 and C17 are effective on the mutant V247M only. (**A**) HEK293 cells constitutively expressing the V247M mutant of α-SG and (**B**) HEK293 cells transiently expressing the L31P mutant of α-SG were treated for 24 h with either 1‰ DMSO (vehicle), C6, C17 or C6 + C17 at the indicated concentrations. At the end of incubation, cells were lysed and, after quantification, 50 μg of proteins were subjected to pull down assay by streptavidin-conjugated agarose beads. Recovered surface proteins were analyzed by SDS-PAGE and western blot with antibodies against α-SG. Representative western blots are reported in Figure S5. In B, it is reported for comparison the level of a-SG expressed by cells transiently transfected with the wild type form of the protein. Quantification of α-SG content was performed by densitometric analysis. Values are the mean (+/− SD) of 3 independent experiments (each performed in duplicate) and are reported as fold increase of the amount present in the control sample. Statistical analysis was performed by One-way ANOVA test followed by multiple comparisons Tukey's test; n.s., $p > 0.05$; *, $p \leq 0.05$; **, $p \leq 0.01$; ***, $p \leq 0.001$, ****, $p \leq 0.0001$.

2.5. Assembly of the Rescued α-SG into the Sarcoglycan Complex

To analyze in pathologic myotubes the ability of the rescued α-SG mutant to interact with the wild type subunits of the sarcoglycan complex, we performed a co-immunoprecipitation assay by using the antibody against δ-SG or β-SG for immunoprecipitation (IP) and the antibodies specific for α-SG and δ-SG for the western blot analysis. It is known that δ-SG and β-SG form a tight core, to which first binds γ-SG and later interacts α-SG, as the last subunit added during tetramer maturation and traffic towards the plasma membrane [33–35]. Therefore, the identification of α-SG in the immuno-complexes precipitated by either δ-SG or β-SG antibodies means the presence of a complete, fully functional SG-complex. It is interesting to note in Figure 5C, that the immune-complexes contained a fraction of α-SG that paralleled the rate of rescue elicited by C17 alone or by the dual incubation (as reported in Figure 5B). Remarkably, in myotubes treated with C6 15 μM, the amount of α-SG involved in hetero-tetramer assembly was significantly higher in comparison to untreated cells, even if the accumulation of the protein was negligible (compare Figure 5C with Figure 5B). Superimposable results were obtained when immunoprecipitation was carried out with β-SG antibodies (Figure S5). These data support the idea that C6 acts mainly promoting tetramer formation and consequently traffic towards the sarcolemma.

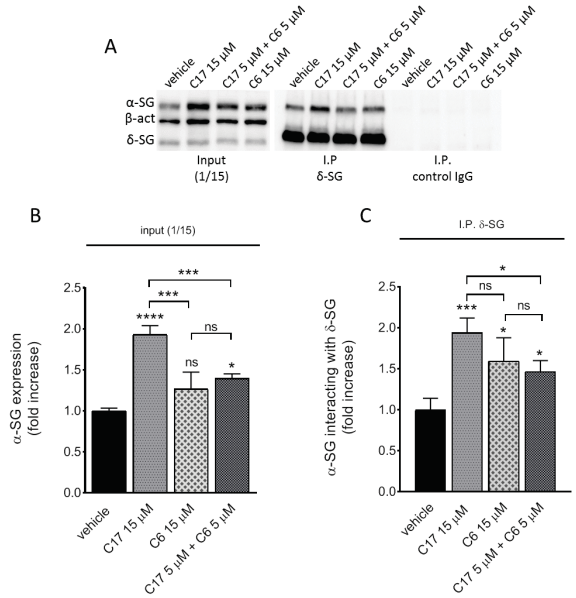

Figure 5. α-SG mutant rescued by correctors C6 and C17 forms a functional SG-complex. Myogenic cells from a patient carrying the L31P/V247M α-SG mutations were differentiated for 7 days and treated for the last 72 h with either 1‰ DMSO (vehicle), C17, C6 or C17 + C6 at the indicated concentrations. At the end of incubation, myotubes were lysed with RIPA buffer without sodium deoxycholate to preserve the sarcoglycans' interactions. After quantification, 100 μg of proteins were subjected to immunoprecipitation with specific δ-SG mouse monoclonal antibody. As negative control, the same amount of protein from each sample was subjected to immunoprecipitation using an IgG antibody of the same isotype as δ-SG antibody. Immunocomplexes were resolved by SDS-PAGE and analyzed by western blot using the antibodies specific for α-SG, δ-SG and β-actin. (**A**) Representative western blot showing total protein lysates (input) (left part); the immunocomplexes recovered by δ-SG antibody (I.P. δ-SG) (central part); the negative control of immunoprecipitation (I.P. control IgG) (right part). (**B**) Quantification of α-SG content by densitometric analysis of the total protein lysates, normalization for protein loading was performed on the signal of β-actin. (**C**) Quantification of α-SG content by densitometric analysis of the immunocomplexes; normalization was performed on the signal of δ-SG. Values are the mean (+/− SD) of 3 independent experiments (each performed in duplicate) and are expressed as fold increase of the control. Statistical analysis was performed by One-way ANOVA test followed by multiple comparisons Tukey's test; n.s., $p > 0.05$; *, $p \leq 0.05$; ***, $p \leq 0.001$, ****, $p \leq 0.0001$.

2.6. The Rescued Protein Is Stable at the Plasma Membrane

An important issue to consider in the development of a new therapy is the duration of the effect elicited by the pharmacological treatment. Starting to dissect this point, we treated LGMD2D myotubes with corrector C17 15 μM or VX661 25 μM for 72 h. Then, after correctors withdrawal, myotubes were analyzed 24 and 48 h later to measure both the total α-SG protein content (Figure S10) and, importantly, the fraction present at the sarcolemma (Figure 6). Firstly, it is seen that the amount of the steady state level of α-SG, in cells treated with vehicle, was constant through to the experiments. Conversely, the amount of sarcolemma-resident α-SG, upon corrector withdrawal, diminished during time, because part of the recovered protein is probably recycled from the membrane. However, the membrane removal of the α-SG rescued by C17 was slow, as 88 and 70% of the initial amount of α-SG was still present at the sarcolemma after 24 and 48 h of corrector withdrawal. Moreover, these differences were statistically irrelevant in comparison to the initial amount of the protein (Figure 6A,B). Conversely, the α-SG rescued by VX661 was faster recycled from the membrane, as the level of the protein became not statistically different from untreated samples after 48 h (Figure 6C,D). No statistically significant differences were observed in the level of the δ-SG present at the sarcolemma nor at the end of correctors incubation, neither at the two time points analyzed upon small molecules withdrawal (Figure S11). On the bases of these data, it is possible to suppose that the corrected α-SG mutant, once at the sarcolemma, is quite stable.

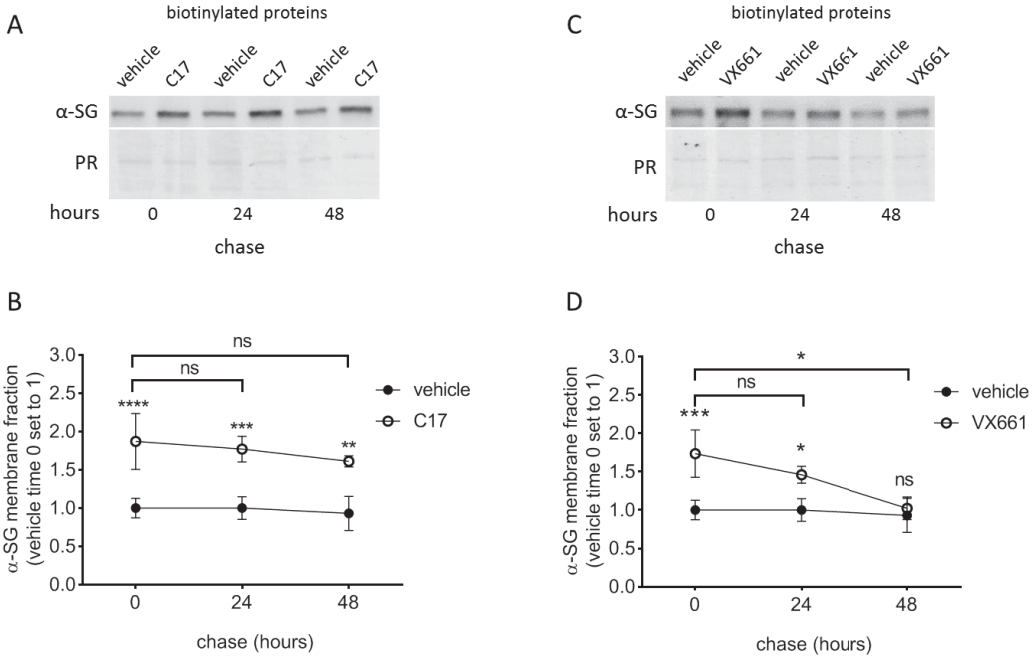

Figure 6. The rescued α-SG protein is stable at the plasma membrane. Myogenic cells from a patient carrying the L31P/V247M α-SG mutations were differentiated for 7 days and treated for the last 78 h with either 1‰ DMSO (vehicle), C17 15 μM or VX661 25 μM. At the end of treatment, corrector-containing medium was removed and replaced with fresh medium. Myotubes were then treated and lysed as described in the legend of Figure 2 at the indicated time points. Representative western blots of the biotinylated membrane fraction from myotubes treated with vehicle or C17 (**A**); with vehicle or VX661 (**C**) probed with antibodies specific for α-SG, Ponceau Red (PR) staining is reported to estimate protein loading. The content of α-SG resident in the sarcolemma of cells pre-treated with C17 (**B**) or VX661 (**D**) was quantified by densitometric analysis of 4 independent experiments. Mean values (+/− SD) are referred to the amount of α-SG present in vehicle-treated cells at time 0. Statistical analysis was performed by One-way ANOVA test followed by multiple comparisons Tukey's test; ns, $p > 0.05$; *, $p \leq 0.05$; **, $p \leq 0.01$; ***, $p \leq 0.001$; ****, $p \leq 0.0001$.

3. Discussion

Sarcoglycans localize at the plasma membrane of striated muscle. Thus, they belong to that part of the cell proteome translocating into the endoplasmic reticulum (ER) for maturation and eventually entering the secretory pathway to reach the cell surface [9]. In this compartment, a stringent quality control system scrutinizes the newly synthetized proteins in order to: (i) allow the properly folded polypeptides to pass forward and (ii) deliver to degradation those folding-defective [36,37]. This ensures protein homeostasis avoiding, at the same time, the accumulation of potentially harmful species. However, the disposal of mutated proteins failing to attain their native conformation, as in CF or sarcoglycanopathy, may result in a loss of function condition [31]. In the last years, many efforts have been devoted to develop pharmacological strategies aiming at restoring proteostasis in these diseases such as protein replacement and pharmacologic chaperone/kinetic stabilizer approaches, as well as readapting the native biology of the cell by proteostasis regulators [38,39]. In this context, the small molecules screened and developed to recover mutants of the CFTR represent the paradigm of how pharmacological chaperons or proteostasis regulators can be successfully used to treat a severe conformational disease like CF [21,38,40]. We recently established the proof of concept that protein-folding correctors belonging to the family of CFTR correctors are effective in rescuing folding-defective α-SG mutants exogenously expressed in cell models. One of such compounds, corrector C17, was then tested in pathologic myogenic cells from a LGMD2D patient showing the recovery of the SG-complex at the sarcolemma with the concomitant reduction of the membrane fragility [19]. Here, we show evidence about the efficacy of other correctors used in single or combined administration, broadening the number of compounds validated *in vitro*, potentially useful in sarcoglycanopathy and highlighting possible additive/synergic effects for some of them. Furthermore, we observed in heterologous cells that the efficacy of such correctors is mutation dependent, as only the V247M mutant is effectively rescued. Finally, by assessing the stability of the SG-complex upon CFTR correctors' incubation, we give a first estimation of the beneficial duration of the treatments.

To evaluate correctors' efficacy, we measured both the global increase of α-SG content but particularly the rise occurring at the sarcolemma, as sign of trafficking rescue of the mutant. CFTR correctors C13, C9 or C17, the latter used as our internal reference, selectively elicited the accumulation of α-SG in pathologic, LGMD2D, myotubes while were ineffective in healthy ones. This supports the idea that these compounds are effective only if a defective sarcoglycan is present, as already observed in [19]. On the other hand, corrector C6 is unable to increase the content of the mutated α-SG in both healthy and LGMD2D myotubes at all the concentrations tested. However, if focusing on the membrane fraction, it is possible to observe that C6 10 or 15 μM increased the localization of α-SG at the sarcolemma (Figure 3B). Membrane localization also occurred with C17 15 μM (Figure 3B), as expected in accordance with [19], on the other hand a strong increase of the total α-SG content was also observed with this concentration of C17. We already evidenced that this corrector is able to increase the amount and stabilize the α-SG mutant expressed by LGMD2D myotubes without affecting its transcription rate [19]. Interestingly, in the case of C6 the significant rise of α-SG at the sarcolemma occurred in the absence of an evident accumulation of the protein. Thus, we may exclude a transcriptional or translational upregulation of α-SG elicited by the corrector. Conversely, this outcome suggests a major role of C6 in promoting the traffic of the portion of mutant that physiologically skips degradation. In support of this view, there are also the IP assays, showing an increased amount of functional hetero-tetramer recoverable from C6-treated myotubes. In this respect, it is important to remind that condition for proper sarcolemma localization is the assembly of the SG-complex [14,41]. The fact that C6 did not improve the membrane localization of α-SG in healthy myotubes may be explained by the saturation of the assembly/transport systems, already working at the maximum rate when the wild type form of each sarcoglycan is present.

As pharmacological chaperons, correctors have been subcategorized in class-I or II depending on the preferential target site on the mutated CFTR protein [42]. Furthermore, there is evidence that the co-administration of CFTR correctors belonging to different classes is beneficial for the

rescue at the plasma membrane of several CFTR mutants, enhancing the folding and stability of the channel, thus improving the release from proteostasis components responsible for retention/delivery to degradation [43–45]. However, sarcoglycans and CFTR are quite different in terms of both structure and function [45,46]; moreover, the examples of CFTR correctors' efficacy on proteins different from the chloride channel are growing [23,24,47]. In consideration of this variety of actions, it is likely that, in the absence of the specific target (CFTR) but in the presence of a protein that being mutated affects the proteostasis network, correctors act mainly modulating the function, composition or concentration of elements of the network itself. Consequently, the perspective that different correctors may act on different targets, offers the opportunity to develop combined treatments also for sarcoglycanopathy. We observed that the protein accumulated by either C13 or C17 alone moved toward the membrane, even though the amount successfully translocated was not statistically significant. Conversely, the combination C17 + C13 resulted in the successful rescue of α-SG at the sarcolemma (Figure 2). All this considered, we might hypothesize an additive effect of the two bithiazole derivatives (C17 and C13), acting on the maturation pathway, probably on the same target. To support this view, there is also the outcome of cells treated by doubling the concentration of C17 (10 μM). Indeed, the amount of α-SG mutant gaining the sarcolemma was superimposable to the one obtained by the co-administration of the two small molecules (each one 5 μM). Conversely, the combination C17+C9 had no additional effect in comparison to the single administration (Figure S2). In this case however, neither the single nor the double administration promoted the membrane translocation. The α-SG mutant accumulated by C9, which is a quinoline derivative, probably acquired a conformation not appropriate for assembly and/or traffic, and not even the presence of corrector C17 can overcome the problem.

A different outcome was observed when C6, another quinoline derivative, was administered concurrently with C17 (each one 5 μM). In this case we measured a robust increase of the α-SG sarcolemma localization, paralleling the accumulation of the mutant (Figure 3). This rescue was not statistically different from the one resulting by the activity of the sole C17 15 μM (three times the dose used in co-administration). Similar results were collected also using heterologous cells expressing the V247M-α-SG. This suggests an additive/synergistic effect of the two small molecules, with C17 promoting folding or reducing degradation of the mutant, and C6 improving assembly/traffic towards the sarcolemma, as suggested by the outcome of the single administration. This is an important hint for drug development, as the co-administration may allow scaling down the concentration of the compounds utilized, thus reducing possible side effects. Remarkably, when administered in combination with a high dose of C17 15 μM, there is no additional effect by the presence of C6. If we suppose C6 is mainly involved in the traffic, it is possible that the amount of α-SG accumulated by the activity of C17 15 μM might saturate the traffic flow of the SG-complex.

Many efforts are presently devoted to the repurposing of available drugs for the treatment of neglected diseases. In this frame, we tested two CFTR correctors, VX661 (Tezacaftor) and VX809 (Lumacaftor) presently on the market in formulation with the potentiator VX770 (Ivacaftor) for CF patients bearing the ΔF508 mutation of CFTR [28,48]. Efficacy of VX661 and VX809 was evaluated in myotubes from both LGMD2D and healthy subjects (Figures S6–S9). Even though modest, the α-SG rescue was evident (Figure S7), especially when VX661 was co-administered with C17 (Figure S9), suggesting possible additive effects of the two small molecules and opening the way for planning novel experiments to identify the useful dose, the timing of incubation, the most effective ratio of the two compounds also aiming to avoid any possible side effect.

Essential issue in drug development is the duration of the effect elicited by the treatment. Our evidence is that, once at the sarcolemma, the SG-complex even if containing a mutated subunit is quite stable. Indeed, 48 h upon C17 corrector withdrawal, the amount of α-SG resident in the sarcolemma was still similar (no statistically different) to that present at the end of the treatment (Figure 6A,B). Even though these experiments need an in vivo validation, this is a first indication that the rescue is effective and durable. By our results with LGMD2D myotubes, we cannot know if just one or both the mutated α-SG polypeptides (carrying either the L31P or the V247M amino acid substitution) have been

rescued by the treatments. Though, data collected with heterologous cells expressing a single mutant suggest that only V247M-α-SG is rescuable. On the other hand, the second mutation introduces a proline in place of a leucine, close (7 aa apart) to the site of cleavage of the α-SG signal peptide [6]. Thus, even though the CLC bio Workbench software used in [16] predicted no modification on the secondary structure, our data suggest that L31P substitution may have an impact on the structure not easily recoverable. Additional experiments will permit an in-depth investigation of this point, also considering a possible action of correctors as pharmacological chaperone, thus able to bind selectively specific mutants. Anyway, this information may be helpful to foresee the outcome of corrector treatments in relation to the type of mutation.

In conclusion, our data support the view that several CFTR correctors, probably acting as proteostasis regulators, could be effective in diseases different from CF. Among the molecules tested, corrector C17 may be classified as the most effective in sarcoglycanopathy. On the other hand, the presence of an additional corrector, such as C6, may guarantee a similar effect, reducing concomitantly the dose of the compounds utilized. This means that these small molecules are probably acting on different steps of the same pathway, in either additive or synergistic way. Finally, the α-SG mutant, especially when "corrected" by C17, is stable once inserted in the complex at the sarcolemma. Although preliminary, these data will be of crucial support in the design of the preclinical experiments in vivo. Finally, even if a deeper investigation on the mechanism of action of CFTR correctors is mandatory, our findings represent a first crucial step towards the development of a remedy for most of the sarcoglycanopathy patients.

4. Material and Methods

4.1. Site Directed Mutagenesis

The full-length cDNA encoding human α-sarcoglycan cloned in the pcDNA3 mammalian expression vector was previously described [49]. The L31P missense mutation was introduced with the GeneArt Site Directed Mutagenesis system (Thermo Fisher Scientific, Waltham, MA, USA) according to manufacturer's instructions, by using the following primer pair: forward 5'-GACCACGCTACACCCACCTGTGGGCCGTGTCTTTG-3', reverse 5'-CAAAGACACGGCCCA CAGGTGGGTGTAGCGTGGTC-3'.

4.2. Chemicals, Cell Culture and Treatments

C6, C9, C13 and C17 were from Exclusive Chemistry (Obninsk, Russia) VX809 and VX661 were from Cayman Chemicals (Ann Arbor, MI, USA). All compounds were dissolved in DMSO at 1000× concentration to have the same content of vehicle (1‰) after the dilution at the final concentration used for treatment.

HEK293 (ATCC, Manassas, VA, USA) and V247M cells (a population of HEK293 cells stably expressing the V247M α-SG, described in [17]) were grown in DMEM (Thermo Fisher Scientific, Waltham, MA, USA) supplemented with 10% FBS (Thermo Fisher Scientific, Waltham, MA, USA). For transient expression, cells were seeded at 50,000 cells/cm^2 on poly-D-Lysine coated plates and transfected the day after seeding with TransIT293 (Mirus Bio, Madison, WI, USA) according to manufacturer's instruction. Twenty-four hours after transfection, medium was replaced with DMEM supplemented with 2% FBS containing the desired concentrations of correctors dissolved in DMSO. After twenty-four hours of treatment, the membrane localization of α-SG mutants was analyzed by the biotinylation assay.

Immortalized human myoblasts (AB678) were from the 'Human cell culture platform' of the Myology Institute in Paris [50]. Primary human myogenic cells from an LGMD2D patient were isolated from a bioptic fragment from the Telethon Genetic Bio-Bank facility (Padova, Italy) [17]. Myogenic cells were grown in Dulbecco's Modified Eagle Medium (DMEM, Sigma-Aldrich, St. Louis, MO, USA) pH 7.2 supplemented with 30% Foetal Bovine Serum (FBS, Thermo Fisher Scientific, Waltham, MA,

USA), insulin 10 μg/mL, Fibroblast Growth Factor (FGF, 25 ng/μL) and Epidermal Growth Factor (EGF, 10 ng/μL) (Sigma-Aldrich, St. Louis, MO, USA). To start differentiation, myoblasts, grown at confluence, were incubated with DMEM supplemented with 2% Horse Serum (Euroclone, Milano, Italy), 10 μg/mL human recombinant insulin (Sigma, St. Louis, MO, USA), 100 μg/mL human transferrin (Sigma-Aldrich, St. Louis, MO, USA). Differentiation was carried out for seven days. CFTR correctors dissolved in DMSO were added 72 h before myotubes lysis or biotinylation. After treatments, cells were washed twice with ice cold PBS and lysed with RIPA buffer (Tris-HCl 50 mM pH 7.5, NaCl 150 mM, NP-40 1% *v/v*, sodium deoxycholate 0.5% *w/v*, SDS 0.1% *w/v*) supplemented with complete protease inhibitor (Sigma-Aldrich, St. Louis, MO, USA).

4.3. Biotinylation of Surface Proteins

For the biotinylation reaction, at the end of the experiments, myotubes were incubated at 4 °C for at least 10 min and all the procedures were performed at this temperature to slow down cellular processes and to prevent the internalization of biotin by endocytosis. Cells were then washed three times with ice cold PBS supplemented with calcium and magnesium and incubated under gentle agitation with a solution of 0.5 mg/mL biotin (EZ-Link Sulfo-NHS-LC-Biotin, Thermo Fisher Scientific, Waltham, MA, USA) in PBS for 20 min at 4 °C. The biotinylation reaction was stopped washing the cells twice with 100 mM glycine in PBS (each wash 5 min), and twice with PBS. Cells were lysed with RIPA buffer, and lysates were centrifuged 30′ at 20,000× *g* at 4 °C. The supernatants were quantified by BCA assay, and 50 μg of proteins were incubated with streptavidin agarose resin (Thermo Fisher Scientific, Waltham, MA, USA) (30 μL of resin for each sample) over night at 4 °C. The streptavidin-resin, after the incubation under gentle rotation with myotubes lysates, was washed three times with RIPA buffer. Bound proteins were eluted with Laemmli sample buffer and analyzed by western blot. As negative control, lysate of non-biotinylated cells was incubated with the streptavidin resin and analyzed by western blot to exclude nonspecific binding to the streptavidin resin. The absence of biotin internalization was assessed probing the western blot membranes with an antibody specific for the cytosolic protein β-actin.

4.4. Co-Immunoprecipitation

After 72 h treatment, AB678 or 6813 cells were lysed with RIPA buffer without sodium deoxycholate to preserve the interaction between the sarcoglycans and then lysates were centrifuged at 20,000× *g* for 30′ at 4 °C. Protein concentration was determined by BCA assay, and 100 μg of protein was incubated under gentle rotation with 1 μg of anti-delta-SG mouse monoclonal antibody (Leica Biosystem, Wetzlar Germany) or with 1 μg of mouse IgG (Sigma-Aldrich, St. Louis, MO, USA) as negative control, for 2 h at 4°C. Finally, 40 μL of Pure Proteome Protein G magnetic beads (Merck-Millipore, Darmstadt, Germany) were added and after 1 h at 4 °C under gentle rotation, magnetic beads were collected with a magnetic stand and washed three times with RIPA buffer without sodium deoxycholate. Bound proteins were eluted with Laemmli buffer and analyzed by western blot.

4.5. Western Blot Analysis

Proteins were resolved by SDS-PAGE, blotted onto a nitrocellulose membrane and probed with selected antibodies (see below). Secondary antibodies were horseradish peroxidase-conjugated, and blots were developed with ECL chemiluminescent substrate (Euroclone, Milano, Italy), and chemiluminescent signals were digitally acquired with Alliance Mini HD9 Imaging System (Uvitec, Cambridge, UK). Densitometry was performed with the ImageJ software. The intensities of sarcoglycan bands were normalized for the intensity of the total protein loading, evaluated by Ponceau Red staining of the membranes or β-actin.

4.6. Antibodies

Rabbit monoclonal anti α-SG (AB189254) was from Abcam (Cambridge, UK); mouse monoclonal antibodies specific for β-SG, δ-SG and γ-SG were from Leica Biosystem (Wetzlar Germany) mouse

monoclonal anti β-actin was from Sigma-Aldrich (St. Louis, MO, USA). Rabbit polyclonal antibody specific for α- and δ-SG were produced as previously described [17]. Secondary antibodies were horseradish peroxidase-conjugated goat anti-mouse or anti-rabbit IgG (Sigma-Aldrich, St. Louis, MO, USA).

4.7. Statistical Analysis

Values are expressed as means ± SD. Before performing the statistical analysis, data were checked for normal distribution with the Kolmogorov–Smirnov normality test (GraphPad Software, San Diego, CA). Statistical differences among groups were then determined by One-way ANOVA test, followed by either Dunnett's test for simultaneous multiple comparisons with control, or Tukey's test for simultaneous comparisons of all possible contrasts (pairs). A level of confidence of $p < 0.05$ was used for statistical significance.

Supplementary Materials: Supplementary materials can be found at http://www.mdpi.com/1422-0067/21/5/1813/s1.

Author Contributions: D.S. and I.R. conceived the experiments; M.C. and D.S. designed the experiments; M.B. provided the healthy donor myogenic cells; M.C., M.S. (Martina Scano), I.F., M.S. (Michela Soardi) and G.R. performed the experiments; M.C, M.S. (Martina Scano), M.S. (Michela Soardi) and D.S. analyzed the data; D.S. wrote the paper. All authors have read and agreed to the published version of the manuscript.

Funding: This work was supported by Association Françoise contre les Myopathies (18620 to D.S. and I.R.), Italian Telethon Foundation (GEP120581 and GGP15140 to D.S.), and Muscular Dystrophy Association (MDA 577888 to D.S.)

Acknowledgments: Vincent Mouly and the "Human cell culture platform" of the Myology Institute Université Pierre et Marie Curie, Paris 6, are gratefully thanked for providing immortalized human myoblasts derived from healthy subjects. Elena Pegoraro and the Telethon Genetic Bio-Bank facility, University of Padova, are gratefully thanked for providing the skeletal muscle biopsy of a LGMD2D patient. A special acknowledgment is reserved to the Cystic Fibrosis Foundation for providing the first stock of CFTR correctors.

Conflicts of Interest: The authors declare no conflict of interest. The funders had no role in the design of the study; in the collection, analyses, or interpretation of data; in the writing of the manuscript, or in the decision to publish the results.

References

1. Straub, V.; Murphy, A.; Udd, B. Group lws: 229th ENMC international workshop: Limb girdle muscular dystrophies—Nomenclature and reformed classification Naarden, the Netherlands, 17–19 March 2017. *Neuromuscul. Disord.* **2018**, *28*, 702–710. [CrossRef] [PubMed]
2. Bushby, K.; Norwood, F.; Straub, V. The limb-girdle muscular dystrophies—Diagnostic strategies. *Bba Mol. Basis Dis.* **2007**, *1772*, 238–242. [CrossRef]
3. Romero, N.B.; Tome, F.M.S.; Leturcq, F.; Elkerch, F.; Azibi, K.; Bachner, L.; Anderson, R.D.; Roberds, S.L.; Campbell, K.P.; Fardeau, M.; et al. Genetic-heterogeneity of severe childhood autosomal recessive muscular-dystrophy with adhalin (50 Kda dystrophy-associated glycoprotein) deficiency. *Comptes Rendus Acad. Sci. Ser. III Sci. Vie* **1994**, *317*, 70–76.
4. Allamand, V.; Leturcq, F.; Piccolo, F.; Jeanpierre, M.; Azibi, K.; Roberds, S.L.; Lim, L.E.; Campbell, K.P.; Beckmann, J.S.; Kaplan, J.C. Adhalin gene polymorphism. *Hum. Mol. Genet.* **1994**, *3*, 2269. [CrossRef] [PubMed]
5. Nigro, V.; Savarese, M. Genetic basis of limb-girdle muscular dystrophies: the 2014 update. *Acta Myol.* **2014**, *33*, 1–12.
6. Sandona, D.; Betto, R. Sarcoglycanopathies: Molecular pathogenesis and therapeutic prospects. *Expert Rev. Mol. Med.* **2009**, *11*, e28. [CrossRef]
7. Tarakci, H.; Berger, J. The sarcoglycan complex in skeletal muscle. *Front. Biosci.* **2016**, *21*, 744–756.
8. Kirschner, J.; Lochmuller, H. Sarcoglycanopathies. *Handb. Clin. Neurol.* **2011**, *101*, 41–46.
9. Carotti, M.; Fecchio, C.; Sandona, D. Emerging therapeutic strategies for sarcoglycanopathy. *Expert Opin. Orphan Drugs* **2017**, *5*, 381–396. [CrossRef]

10. Ginjaar, H.B.; van der Kooi, A.J.; Ceelie, H.; Kneppers, A.L.; van Meegen, M.; Barth, P.G.; Busch, H.F.; Wokke, J.H.; Anderson, L.V.; Bonnemann, C.G.; et al. Sarcoglycanopathies in Dutch patients with autosomal recessive limb girdle muscular dystrophy. *J. Neurol.* **2000**, *247*, 524–529. [CrossRef]
11. Vainzof, M.; Passos-Bueno, M.R.; Pavanello, R.C.; Marie, S.K.; Oliveira, A.S.; Zatz, M. Sarcoglycanopathies are responsible for 68% of severe autosomal recessive limb-girdle muscular dystrophy in the Brazilian population. *J. Neurol. Sci.* **1999**, *164*, 44–49. [CrossRef]
12. Duggan, D.J.; Gorospe, J.R.; Fanin, M.; Hoffman, E.P.; Angelini, C.; Pegoraro, E.; Noguchi, S.; Ozawa, E.; Pendlebury, W.; Waclawik, A.J.; et al. Mutations in the sarcoglycan genes in patients with myopathy. *N. Engl. J. Med.* **1997**, *336*, 618–624. [CrossRef] [PubMed]
13. Xie, Z.; Hou, Y.; Yu, M.; Liu, Y.; Fan, Y.; Zhang, W.; Wang, Z.; Xiong, H.; Yuan, Y. Clinical and genetic spectrum of sarcoglycanopathies in a large cohort of Chinese patients. *Orphanet J. Rare Dis.* **2019**, *14*, 43. [CrossRef] [PubMed]
14. Gastaldello, S.; D'Angelo, S.; Franzoso, S.; Fanin, M.; Angelini, C.; Betto, R.; Sandona, D. Inhibition of proteasome activity promotes the correct localization of disease-causing alpha-sarcoglycan mutants in HEK-293 cells constitutively expressing beta-, gamma-, and delta-sarcoglycan. *Am. J. Pathol.* **2008**, *173*, 170–181. [CrossRef]
15. Bartoli, M.; Gicquel, E.; Barrault, L.; Soheili, T.; Malissen, M.; Malissen, B.; Vincent-Lacaze, N.; Perez, N.; Udd, B.; Danos, O.; et al. Mannosidase I inhibition rescues the human alpha-sarcoglycan R77C recurrent mutation. *Hum. Mol. Genet.* **2008**, *17*, 1214–1221. [CrossRef]
16. Soheili, T.; Gicquel, E.; Poupiot, J.; N'Guyen, L.; Le Roy, F.; Bartoli, M.; Richard, I. Rescue of sarcoglycan mutations by inhibition of endoplasmic reticulum quality control is associated with minimal structural modifications. *Hum. Mutat.* **2012**, *33*, 429–439. [CrossRef]
17. Bianchini, E.; Fanin, M.; Mamchaoui, K.; Betto, R.; Sandona, D. Unveiling the degradative route of the V247M alpha-sarcoglycan mutant responsible for LGMD-2D. *Hum. Mol. Genet.* **2014**, *23*, 3746–3758. [CrossRef]
18. Gelman, M.S.; Kannegaard, E.S.; Kopito, R.R. A principal role for the proteasome in endoplasmic reticulum-associated degradation of misfolded intracellular cystic fibrosis transmembrane conductance regulator. *J. Biol. Chem.* **2002**, *277*, 11709–11714. [CrossRef]
19. Carotti, M.; Marsolier, J.; Soardi, M.; Bianchini, E.; Gomiero, C.; Fecchio, C.; Henriques, S.F.; Betto, R.; Sacchetto, R.; Richard, I.; et al. Repairing folding-defective alpha-sarcoglycan mutants by CFTR correctors, a potential therapy for limb-girdle muscular dystrophy 2D. *Hum. Mol. Genet.* **2018**, *27*, 969–984. [CrossRef]
20. Rogan, M.P.; Stoltz, D.A.; Hornick, D.B. Cystic fibrosis transmembrane conductance regulator intracellular processing, trafficking, and opportunities for mutation-specific treatment. *Chest* **2011**, *139*, 1480–1490. [CrossRef]
21. Birault, V.; Solari, R.; Hanrahan, J.; Thomas, D.Y. Correctors of the basic trafficking defect of the mutant F508del-CFTR that causes cystic fibrosis. *Curr. Opin. Chem. Biol.* **2013**, *17*, 353–360. [CrossRef] [PubMed]
22. Sabirzhanova, I.; Pacheco, M.L.; Rapino, D.; Grover, R.; Handa, J.T.; Guggino, W.B.; Cebotaru, L. Rescuing trafficking mutants of the ATP-binding cassette protein, ABCA4, with small molecule correctors as a treatment for stargardt eye disease. *J. Biol. Chem.* **2015**, *290*, 19743–19755. [CrossRef] [PubMed]
23. Sampson, H.M.; Lam, H.; Chen, P.C.; Zhang, D.L.; Mottillo, C.; Mirza, M.; Qasim, K.; Shrier, A.; Shyng, S.L.; Hanrahan, J.W.; et al. Compounds that correct F508del-CFTR trafficking can also correct other protein trafficking diseases: An In Vitro study using cell lines. *Orphanet J. Rare Dis.* **2013**, *8*, 11. [CrossRef] [PubMed]
24. Van Der Woerd, W.L.; Wichers, C.G.K.; Vestergaard, A.L.; Andersen, J.P.; Paulusma, C.C.; Houwen, R.H.J.; van de Graaf, S.F.J. Rescue of defective ATP8B1 trafficking by CFTR correctors as a therapeutic strategy for familial intrahepatic cholestasis. *J. Hepatol.* **2016**, *64*, 1339–1347. [CrossRef] [PubMed]
25. Pedemonte, N.; Lukacs, G.L.; Du, K.; Caci, E.; Zegarra-Moran, O.; Galietta, L.J.; Verkman, A.S. Small-molecule correctors of defective DeltaF508-CFTR cellular processing identified by high-throughput screening. *J. Clin. Investig.* **2005**, *115*, 2564–2571. [CrossRef] [PubMed]
26. Robert, R.; Carlile, G.W.; Pavel, C.; Liu, N.; Anjos, S.M.; Liao, J.; Luo, Y.; Zhang, D.L.; Thomas, D.Y.; Hanrahan, J.W. Structural analog of sildenafil identified as a novel corrector of the F508del-CFTR trafficking defect. *Mol. Pharmacol.* **2008**, *73*, 478–489. [CrossRef]
27. Connett, G.J. Lumacaftor-ivacaftor in the treatment of cystic fibrosis: Design, development and place in therapy. *Drug Des. Dev. Ther.* **2019**, *13*, 2405–2412. [CrossRef]

28. Taylor-Cousar, J.L.; Munck, A.; McKone, E.F.; van der Ent, C.K.; Moeller, A.; Simard, C.; Wang, L.T.; Ingenito, E.P.; Mckee, C.; Lu, Y.M.; et al. Tezacaftor-ivacaftor in patients with cystic fibrosis homozygous for Phe508del. *N. Engl. J. Med.* **2017**, *377*, 2013–2023. [CrossRef]
29. Thorley, M.; Duguez, S.; Mazza, E.M.C.; Valsoni, S.; Bigot, A.; Mamchaoui, K.; Harmon, B.; Voit, T.; Mouly, V.; Duddy, W. Skeletal muscle characteristics are preserved in hTERT/cdk4 human myogenic cell lines. *Skelet. Muscle* **2016**, *6*, 43. [CrossRef]
30. Yoo, C.L.; Yu, G.J.; Yang, B.; Robins, L.I.; Verkman, A.S.; Kurth, M.J. 4′-methyl-4,5′-bithiazole-based correctors of defective Delta F508-CFTR cellular processing. *Bioorg. Med. Chem. Lett.* **2008**, *18*, 2610–2614. [CrossRef]
31. Noack, J.; Pisoni, G.B.; Molinari, M. Proteostasis: Bad news and good news from the endoplasmic reticulum. *Swiss Med. Wkly.* **2014**, *144*, w14001. [CrossRef] [PubMed]
32. Rowe, S.M.; Verkman, A.S. Cystic fibrosis transmembrane regulator correctors and potentiators. *Cold Spring Harb. Perspect. Med.* **2013**, *3*, a009761. [CrossRef] [PubMed]
33. Shi, W.; Chen, Z.; Schottenfeld, J.; Stahl, R.C.; Kunkel, L.M.; Chan, Y.M. Specific assembly pathway of sarcoglycans is dependent on beta- and delta-sarcoglycan. *Muscle Nerve* **2004**, *29*, 409–419. [CrossRef] [PubMed]
34. Draviam, R.A.; Shand, S.H.; Watkins, S.C. The beta-delta-core of sarcoglycan is essential for deposition at the plasma membrane. *Muscle Nerve* **2006**, *34*, 691–701. [CrossRef] [PubMed]
35. Allikian, M.J.; McNally, E.M. Processing and assembly of the dystrophin glycoprotein complex. *Traffic* **2007**, *8*, 177–183. [CrossRef]
36. Sicari, D.; Igbaria, A.; Chevet, E. Control of protein homeostasis in the early secretory pathway: Current status and challenges. *Cells* **2019**, *8*, 1347. [CrossRef]
37. Adams, B.M.; Oster, M.E.; Hebert, D.N. Protein quality control in the endoplasmic reticulum. *Protein J.* **2019**, *38*, 317–329. [CrossRef]
38. Balch, W.E.; Roth, D.M.; Hutt, D.M. Emergent properties of proteostasis in managing cystic fibrosis. *Cold Spring Harb. Perspect. Biol.* **2011**, *3*, a004499. [CrossRef]
39. Hutt, D.M.; Powers, E.T.; Balch, W.E. The proteostasis boundary in misfolding diseases of membrane traffic. *FEBS Lett.* **2009**, *583*, 2639–2646. [CrossRef]
40. Mijnders, M.; Kleizen, B.; Braakman, I. Correcting CFT folding defects by small-molecule correctors to cure cystic fibrosis. *Curr. Opin. Pharmacol.* **2017**, *34*, 83–90. [CrossRef]
41. Noguchi, S.; Wakabayashi, E.; Imamura, M.; Yoshida, M.; Ozawa, E. Formation of sarcoglycan complex with differentiation in cultured myocytes. *Eur. J. Biochem.* **2000**, *267*, 640–648. [CrossRef] [PubMed]
42. Okiyoneda, T.; Veit, G.; Dekkers, J.F.; Bagdany, M.; Soya, N.; Xu, H.J.; Roldan, A.; Verkman, A.S.; Kurth, M.; Simon, A.; et al. Mechanism-based corrector combination restores Delta F508-CFTR folding and function. *Nat. Chem. Biol.* **2013**, *9*, 444–469. [CrossRef] [PubMed]
43. Lopes-Pacheco, M.; Sabirzhanova, I.; Rapino, D.; Morales, M.M.; Guggino, W.B.; Cebotaru, L. Correctors rescue CFTR mutations in nucleotide-binding domain 1 (NBD1) by modulating proteostasis. *Chembiochem* **2016**, *17*, 493–505. [CrossRef] [PubMed]
44. Lopes-Pacheco, M.; Boinot, C.; Sabirzhanova, I.; Rapino, D.; Cebotaru, L. Combination of correctors rescues CFTR transmembrane-domain mutants by mitigating their interactions with proteostasis. *Cell Physiol. Biochem.* **2017**, *41*, 2194–2210. [CrossRef]
45. Cant, N.; Pollock, N.; Ford, R.C. CFTR structure and cystic fibrosis. *Int. J. Biochem. Cell Biol.* **2014**, *52*, 15–25. [CrossRef]
46. Dickens, N.J.; Beatson, S.; Ponting, C.P. Cadherin-like domains in alpha-dystroglycan, alpha/epsilon-sarcoglycan and yeast and bacterial proteins. *Curr. Biol.* **2002**, *12*, R197–R199. [CrossRef]
47. Cebotaru, L.; Liu, Q.N.; Sabirzhanova, I.; Bergbower, E.; Yanda, M.; Guggino, W. The CFTR corrector, VX-809 (Lumacaftor) and Hsp27 rescues ABCA4 trafficking mutants: A potential treatment for Stargardt disease. *Investig. Ophthalmol. Vis. Sci.* **2018**, *59*, 218.
48. Wainwright, C.E.; Elborn, J.S.; Ramsey, B.W.; Marigowda, G.; Huang, X.; Cipolli, M.; Colombo, C.; Davies, J.C.; De Boeck, K.; Flume, P.A.; et al. Lumacaftor-ivacaftor in patients with cystic fibrosis homozygous for Phe508del CFTR. *N. Engl. J. Med.* **2015**, *373*, 220–231. [CrossRef]

49. Sandona, D.; Gastaldello, S.; Martinello, T.; Betto, R. Characterization of the ATP-hydrolysing activity of alpha-sarcoglycan. *Biochem. J.* **2004**, *381 Pt 1*, 105–112. [CrossRef]
50. Zhu, C.H.; Mouly, V.; Cooper, R.N.; Mamchaoui, K.; Bigot, A.; Shay, J.W.; Di Santo, J.P.; Butler-Browne, G.S.; Wright, W.E. Cellular senescence in human myoblasts is overcome by human telomerase reverse transcriptase and cyclin-dependent kinase 4: consequences in aging muscle and therapeutic strategies for muscular dystrophies. *Aging Cell* **2007**, *6*, 515–523. [CrossRef]

4.2 Efficacy of C17 corrector treatment on LGMDR4 myotubes

The effects of the C17 CFTR corrector, as the most prominisg in our hands, were assessed on primary cells deriving from the biopsy of a LGMDR4 subject, carrying the missense mutation I92P on the β-SG gene. The protocol consists in the treatment of 7 days differentiated myotubes with CFTR correctors for the last 48 hours. As reported on the left in figure 26 A, CFTR corrector treatment increased the total β-SG protein level in comparison to vehicle treated myotubes. However, to be effective, the rescue must result in the delivery of the recovered protein on the membrane. To verify this aspect, the protein membrane fraction was purified by biotinylation and the expression of β-SG was evaluated by western blot, followed by densitometric analysis. It is interesting to note, on the the right of figure 26 A, that also the fraction of β-SG able to reach the myotubes surface is statistically significant higher if compared to vehicle-treated myotubes. Furthermore, the correct localization of the β-SG protein on myotubes sarcolemma was evaluated by immunofluorescence of intact cells. As shown in figure 26 B, it is clear that the fraction of the protein immunolabeled with the β-SG antibody on the sarcolemma of C17 treated myotubes is strongly higher than control.

The absence of evident toxic effect, like membrane blebbing or cells detaching from the plate, elicited by the treatment is proved by the phase contrast image of the myotubes, recorded at the end of incubation (figure 26 C).

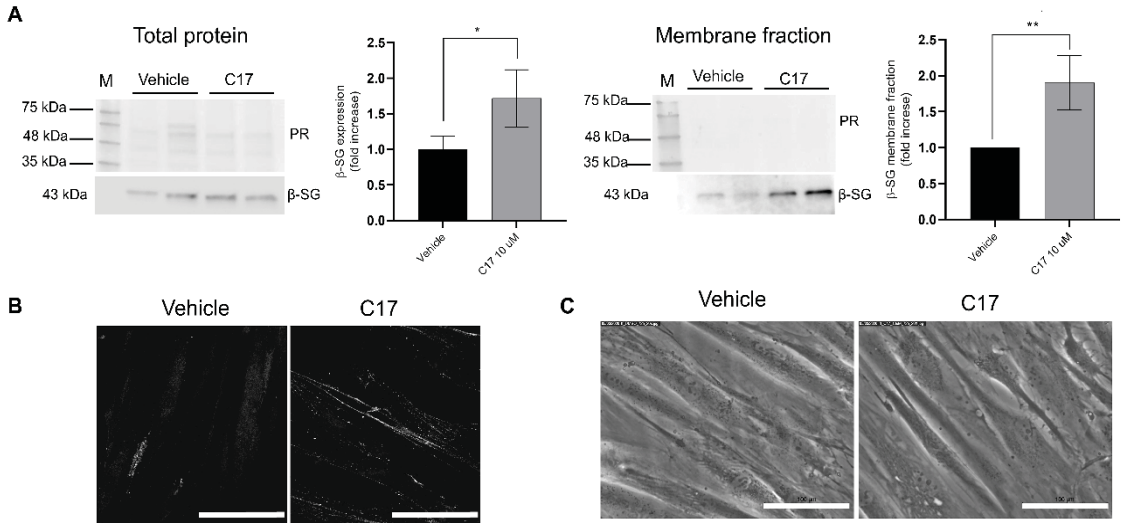

Figure 26. C17 corrector treatment induced β-SG protein recovery at the sarcolemma of LGMDR4 myotubes.

(A) Five-day old LGMDR4 myotubes were treated for 48 hours with either corrector C17 (10 μM) or 1‰ DMSO (vehicle). At the end of treatments, β-SG expression was evaluated by western blot analysis (representative WBs are reported) of total protein lysates (on the left) and of the membrane fractions, purified by biotinylation (on the right). The graphs show the average values (± SD) of β-SG expression determined by densitometric analysis of at least three independent experiments and indicated as fold increase of control (vehicle). Statistical analysis was performed using Student t test *, P≤ 0.05; **P≤ 0.01.
(B) Five-day old LGMDR4 myotubes, grown on glass coverslips, were treated for 48 hours with C17 (10 μM) or 1‰ DMSO (vehicle). At the end of treatments, intact myotubes (unpermeabilized) were decorated with β-SG specific primary antibodies and visualized by a goat anti-rabbit Alexa-fluor 488 secondary antibody. Images were recorded, at the same magnification and setting condition, with a Leica SP5 laser scanning confocal microscope. Bars corresponds to 100 μm
(C) Phase contrast images showing the myotubes at the end of the treatment. Scale bar corresponds to 100 μm.

These promising results are in accordance with previous ones obtained on LGMDR3 myotubes (Carotti et al., 2018, Carotti et al., 2020) and sustain the evidence that CFTR correctors are effective in sarcoglycanopathy caused by a missense mutation, independently on the *SGC* gene involved.

Obvious and essential further step is, at this point, the assessment of C17 efficacy and safety *in vivo*. As already mentioned in the introduction chapter, the availabe KO and KI mouse models are respectively unsuitable and unusable to test the efficacy of the C17 corrector aiming at recovering folding defective SGs. Thus, the generation of appropriate *in vivo* murine models, carring a missense mutation in the α-SG gene and their treatment with the molecule are reported in the following chapters.

4.3 Generation of a new mouse model of LGMDR3 by hind limbs humanization

The generation of a novel murine model of LGMDR3 mirroring the human condition caused by a missense mutation in the *SGCA* gene is an important step to test the efficacy of the C17 molecule. To this intent we expressed the human α-SG sequence in the background of the *sgca*-null mouse by using the AAV1 that is known to have a good muscle tropism (Hauck & Xiao, 2003, Pacak, Conlon et al., 2008, Zincarelli et al., 2008). The virus was engineered to express the human α-SG carrying the WT, as a positive control of transduction, and either the V247M or the R98H mutation. The choice of the mutations to be expressed in humanized mice was driven by several consideration. The amino acid substitution R77C was not considered, despite being the most frequently reported mutation in LGMDR3, as the corresponding Knock In (KI) mice failed to develop a dystrophic phenotype (Bartoli et al., 2008, Kobuke et al., 2008). The focus on the V247M mutation was dictated by the fact that it is one of the two variants carried by the myogenic cells used to test CFTR correctors *in vitro.* Furthermore, it is among the most frequently reported missense mutations in LGMDR3 (Bianchini et al., 2014, Carotti et al., 2017, Carotti et al., 2020). Finally, the R98H mutation was selected as it is associated with a mild/severe phenotype and was classified, like V247M, as a rescuable mutant by in vitro experiments (Carotti et al., 2018, Gastaldello et al., 2008, Soheili et al., 2012). The tMCK (truncated muscle creatine kinase) tissue specific promoter was used to confine the expression of the human protein in the striated muscle, in the case of the virus spillover from the site of injection. Figure 27 reports the map of the recombinant AAV1 carrying the *SGCA* sequence.

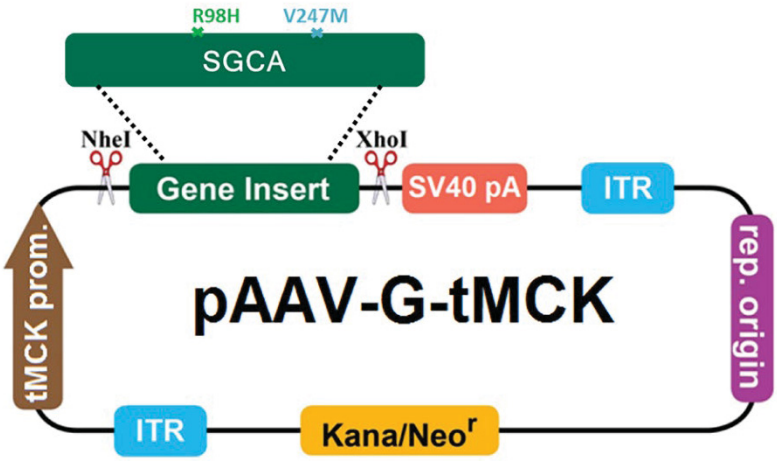

Figure 27. Map of the plasmid for recombinant adeno associated virus serotype 1 (rAAV-1) generation.

The human α-SG sequence, either WT or carrying the R98H or the V247M missense mutations (mapping as indicated) was cloned under the control of the muscle specific promoter tMCK using the NheI and XhoI restriction sites. The SV40 polyadenylation sequence is present to assure the proper maturation of the mRNAs. The inverted terminal repeats (ITRs) of AAV1 are the only viral sequences included in this vector to assure both viral DNA replication and packaging of the rAAV vector genome. The Kanamycin/Neomycin resistant cassette and the replication origin allow for prokaryote/eukaryote cell selection and vector amplification.

Animals were transduced by intramuscular injection of $9x10^9$ vg (viral genome) of AAV1 in one hind limb of 1-2-day-old *sgca*-null mouse pups, the contralateral leg was used as negative control. This early transduction is expected to induce tolerance toward the human sequence and assures the skeletal muscle development in the presence of the exogenous protein. In this manner the human α-SG should follow the proper biosynthetic and maturation process, leading to the development of either healthy or dystrophic hind limbs depending on the sequence of the protein. In addition, this results in the development of "humanized hind limbs" expressing either the endogenous β-, γ- and δ-SGs and the exogenous human α-SG carried by the viral vector. Ten weeks upon transduction, mice were sacrificed and the tibialis anterior (TA) muscle of the humanized hind limbs were snap-frozen for further histological and molecular analyses (figure 28 reports the adopted strategy).

Figure 28. Scheme of the experimental workflow (created with BioRender.com).

1-2-day-old *sgca*-null mouse pups were injected in one hind limb with $9x10^9$ vg of AAV1 carrying the human α-SG sequence. In the contralateral leg, physiological solution was injected as control. Ten weeks upon transduction, mice were sacrificed and the TA muscles explanted for further analyses.

Eight µm thin cryo-sections of TA muscles were stained with hematoxylin and eosin (H&E), or immunolabelled with antibodies specifically recognizing either α-, β- or δ-SG. Representative pictures of the different TA samples from humanized mice are reported in figure 29, together with WT and *sgca*-null samples as reference muscles.

Sgca-null mouse cryo-sections are characterized by muscle fibers of heterogeneous diameter, internal nuclei, with some fibers undergoing necrosis or regeneration and by the presence of mononuclear cell infiltrate. These signs of myopathy are clearly evident in comparison to the healthy, WT samples that conversely are characterized by homogeneous fiber size with peripherally located nuclei. Antibodies against the three SGs strongly mark the sarcolemma of the fibers in the C57BL6 mice. Conversely, the signal is absent (for α-SG) or very reduced and mainly localized in the internal part of the fibers in *sgca*-null mouse cryo-sections for δ- and β-SG, with β-SG being the most preserved subunit at the sarcolemma.

The transduction of the human α-SG wild-type sequence resulted, as expected, in strong improvement of the dystrophic phenotype at the histological level, representing our positive control of transduction. Importantly, the human α-SG localized at the sarcolemma, together with the endogenous β- and δ SG, as proven by the IF staining. This means that the human sequence was tolerated by the mice, forming a functional SG complex with the murine subunits.

By contrast, transduction with the mutated human α-SG sequences had different outcome. Indeed, the presence of the V247M mutation did not result in the development of myopathic features because a whole SG-complex localized at the sarcolemma. The histological recovery was the consequence of the localization of the SG complex at the sarcolemma, as assessed by IF staining. Even though unexpected on the bases of the *in vitro* experiments, the lack of phenotype in SG-KI animals teaches that some difference may be envisaged between human and mouse in the quality control system and/or endoplasmic reticulum associated degradation (ERAD). As a consequence, it is not easy to predict the final outcome of a well described human SG mutation when expressed in mouse.

On the contrary the transduction with the R98H-α-SG mutant led to the development of a dystrophic phenotype, with a clear variability in fiber size, nuclei internally located and inflammation. The α-SG immunoreactivity at the sarcolemma was extremely low, while traces were visible intracellularly in certain fibers. The surface localization of WT δ- and β-SG subunits was also reduced, with much of the signal coming from within the fibers.

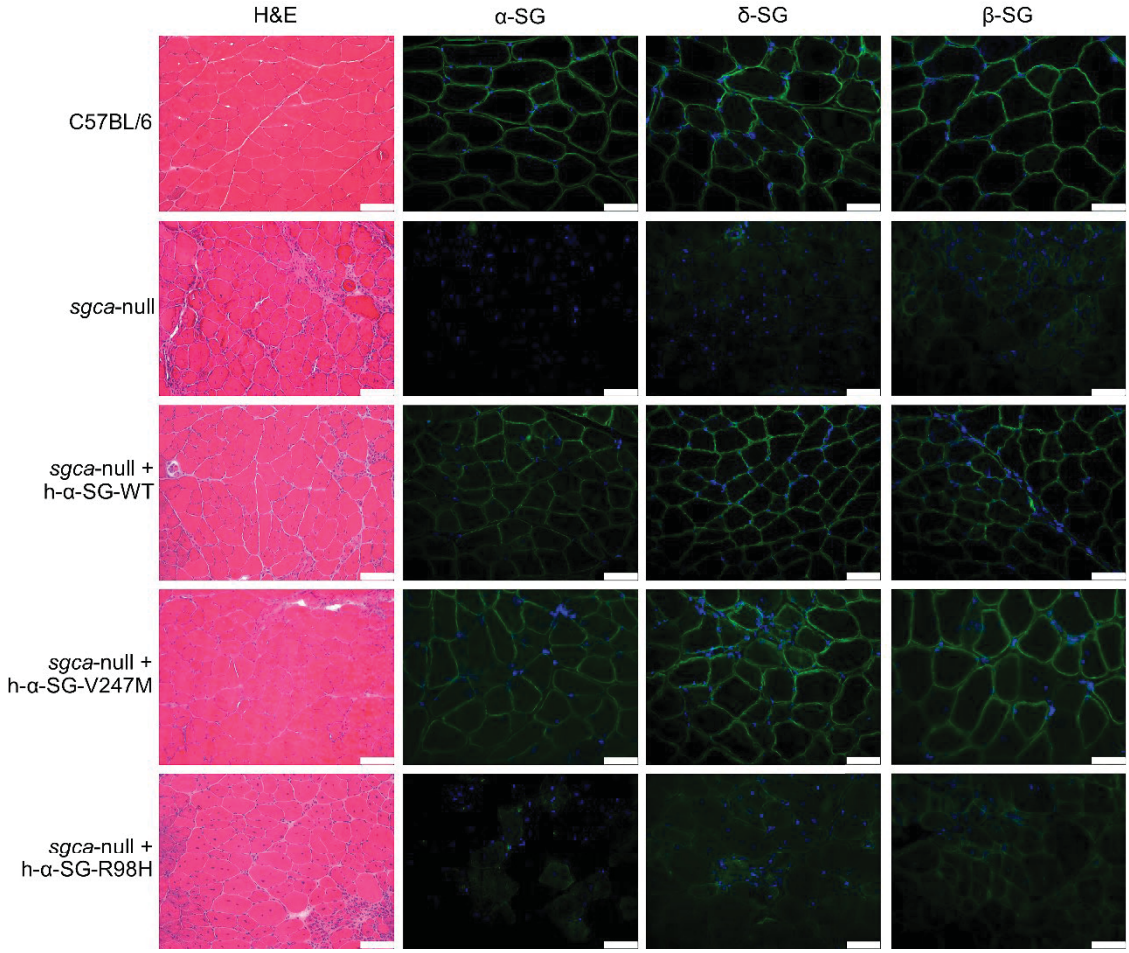

Figure 29. Histological (H&E) and IF analyses of TA muscles cryo-sections from C57BL/6 and *sgca*-null mice, *sgca*-null humanized with either the WT α-SG sequence (*sgca*-null+h-α-SG-WT), the V247M-α-SG sequence (sgca-null+h-α-SG-V247M) or the R98H-α-SG sequence (*sgca*-null+h-α-SG-R98H).

Primary antibodies specific for α-, δ- and β-SG, as indicated, were revealed by Alexa-Fluor488-conjugated secondary antibodies. IF images were captured at the same setting conditions. Bars correspond to 100 µm and 50 µm in H&E and IF images, respectively.

These findings were confirmed by western blot (WB) analysis (figure 30) of total protein lysates from TA muscle of the different mice. Indeed, α-SG was found in almost equal amount in muscles transduced with either the WT or V247M human α-SG sequence, while a very low amount of R98H-α-SG was detected. Indeed, to appreciate its signal the WB membrane had to be exposed for a longer period. This suggests that α-SG carrying this mutation was efficiently recognized by the QC system and underwent fast degradation, confirming what observed *in vitro* (Bianchini et al., 2014, Gastaldello et al., 2008).

This humanized mouse, is characterized by transient SG expression, even if different works reports the expression of the protein for up to one year in the absence of any toxicity signs (Pacak et al., 2008, Rodino-Klapac et al., 2008). Once the model has been generated, mice with *mutated R98H humanized hind limbs* were used to test *in vivo* the efficacy of corrector C17, to confirm the previous *in vitro* data.

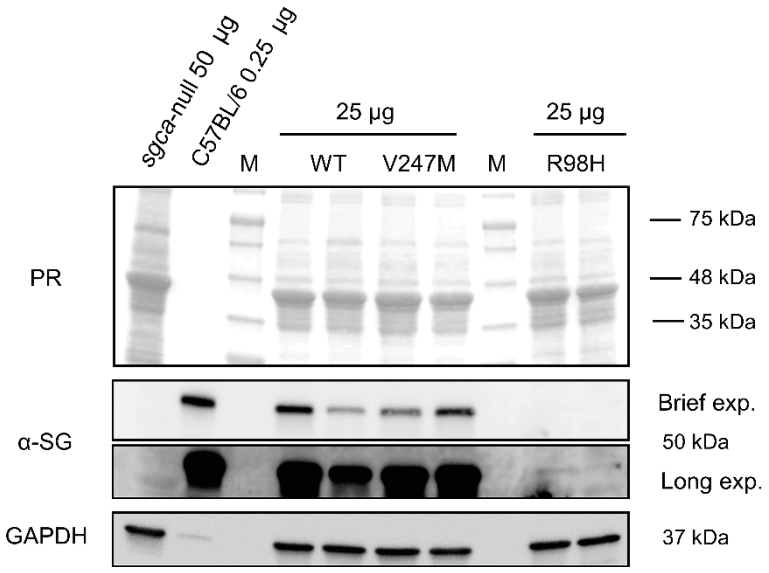

Figure 30. WB analysis of total protein lysates of representative TA muscle samples from *sgca*-null and C57BL/6 mice and mice humanized with the different α-SG sequences, as indicated.

The membrane was probed with primary antibodies against α-SG and GAPDH, used as loading control, together with Ponceau Red (PR) protein staining. Protein bands were revealed by the HRP-conjugated secondary antibodies. Two exposition-times of the α-SG-probed membrane are reported to appreciate the expression of the R98H mutant.

4.4 C17 chronic treatment of humanized mice expressing the R98H α-SG mutant

As mice transduced with the human R98H-α-SG seem to mimic with high fidelity the human pathological condition, experiments aiming at validating the efficacy of corrector C17 *in vivo* were carried out in this humanized animal model. S*gca*-null mouse pups were transduced as above described in both hind limbs. Seven weeks upon transduction, mice were treated systemically by daily intraperitoneal injection (IP) of either corrector C17 or its vehicle. Corrector C17 is a bithiazole derivative (figure 31), already used to successfully rescue mutants of the ABC transporter family, as well as structurally uncorrelated proteins (Loo, Bartlett et al., 2012, van der Woerd et al., 2016, Yoo, Yu et al., 2008). C17 was the most promising CFTR corrector tested in LGMDR3 cellular models, rerouting the SG-complex to the sarcolemma that resulted strengthened (Carotti et al., 2018, Carotti et al., 2020).

Being hydrophobic, C17 was prepared in a vehicle comprising 5% DMSO and 5% of the emulsifier Kolliphor® EL, already used for the formulation of many other hydrophobic compounds, such as diazepam, propofol, vitamin K (Aronson, 2016). To exclude the possibility of any interference on the spectroscopic properties of the molecule due to the formulation, we analyzed the UV/visible spectrum of C17 dissolved in this new formulation or in the canonical DMSO solvent (figure 31).

The C17 dose of 25mg/kg was chosen according to (Davison, Taylor et al., 2011) that is the sole paper describing the administration and distribution of a fluorescent derivative of the compound in mouse.

The IP route of administration was adopted because it is minimally stressful in chronic treatments of small rodents and commonly used for proof-of-concept studies (Al Shoyaib, Archie et al., 2019).

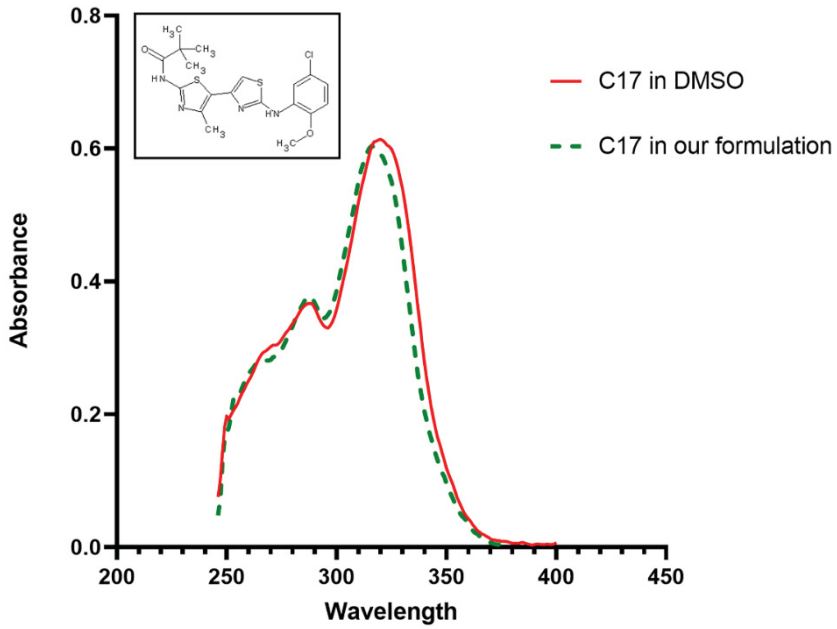

Figure 31. C17 UV-visible spectra.

The chemical structure of corrector C17 is reported in the inset.
Five mg of C17 were dissolved in either 1 ml of DMSO or 50 µl DMSO, 50 µl of Kolliphor EL and 900 µl of physiological solution (this is the concentration used to inject the animals, corresponding to 25 mg per Kg of mouse weight). Spectra were recorded at 22°C, upon dilution at 50 µg/ml. The two spectra are superimposable, indicating no interference on the spectroscopic properties of the small molecule by the vehicle used.

4.4.1 Three weeks C17 treatment induced myopathic phenotype amelioration

Mice expressing the human R98H α-SG mutant in both hind limbs were treated IP and daily for 3 weeks with the C17 molecule, according to the scheme in figure 32.

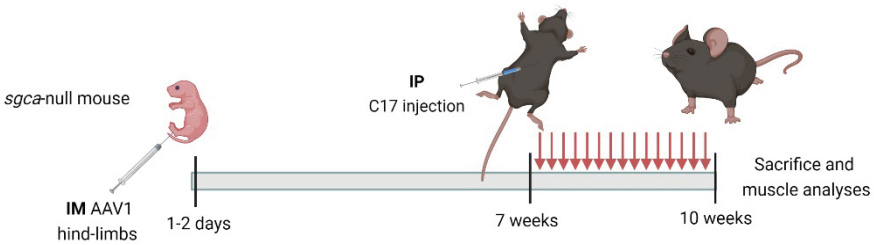

Figure 32. Scheme of the experimental workflow (created with BioRender.com).

1-2-day-old *sgca*-null mouse pups were injected in both hind limbs with $9x10^9$ vg of AAV1. Seven weeks upon transduction, mice were treated systemically for 3 weeks by daily IP injection of either corrector C17 or its vehicle. At the end of the treatment, mice were sacrificed and the TA muscles explanted for further analyses.

IF analysis of TA muscle cryosections (figure 33) shows that C17 administration induced a strong α-SG localization at the sarcolemma; conversely the signal was very low and partially confined intracellularly in vehicle treated samples. Notably, there was an impressive rerouting at the sarcolemma of the δ-SG protein in treated samples, if compared to vehicle treated ones. The superimposable pattern of α- and δ-SG staining was the proof that the whole SG-complex localized at the sarcolemma upon C17 administration (Allikian & McNally, 2007, Draviam et al., 2006, Shi, Chen et al., 2004). Of note, the SG-complex recovery ameliorated the histological phenotype of C17 treated samples as evaluated by histological analysis reported in figure 33.

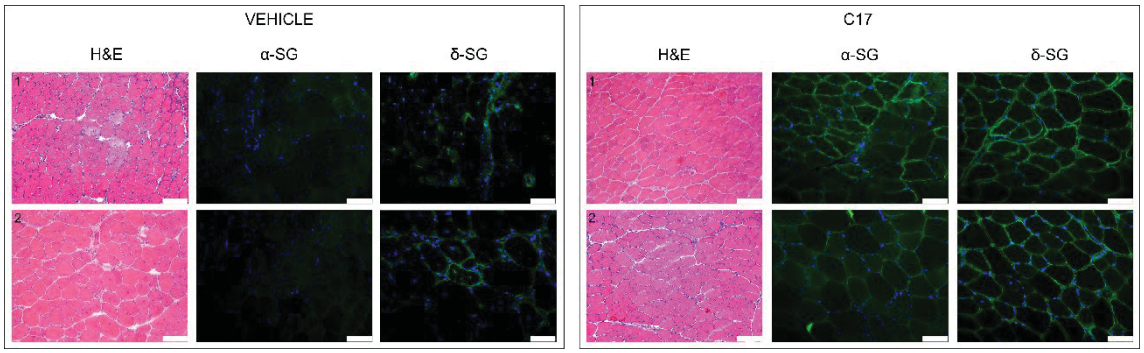

Figure 33. H&E staining and IF analysis of representative TA muscle cryo-sections of humanized R98H-α-SG mice treated for 3 weeks with either vehicle or corrector C17.

Primary antibodies against α- and δ-SG, as indicated, were revealed by Alexa-Fluor-488-conjugated secondary antibodies. Images were captured at the same setting conditions; bars correspond to 100 μm and 50 μm in H&E and IF images, respectively.

Furthermore, as fiber size is a critical factor correlated to the health and function of the muscle, a more in-depth analysis of muscle histopathology was performed (Pozsgai, Griffin et al., 2017). It revealed a slight reduction in the number of small fibers size accompanied by an increase in mean fiber cross sectional area (CSA) in TA muscles from C17 treated animals in comparison to the vehicle treated ones (figure 34).

Total protein lysates were resolved by SDS PAGE and the level of the α-SG protein was evaluated by WB. In figure 35 the analysis of samples from humanized mice treated with either the vehicle or corrector C17 is reported.

It is interesting to note that, despite the natural variability of living animals, the densitometric analysis, reported in figure 35 B, evidenced a slight increase in the average amount of the R98H mutant in C17 vs. vehicle treated samples that however is not statistically significant.

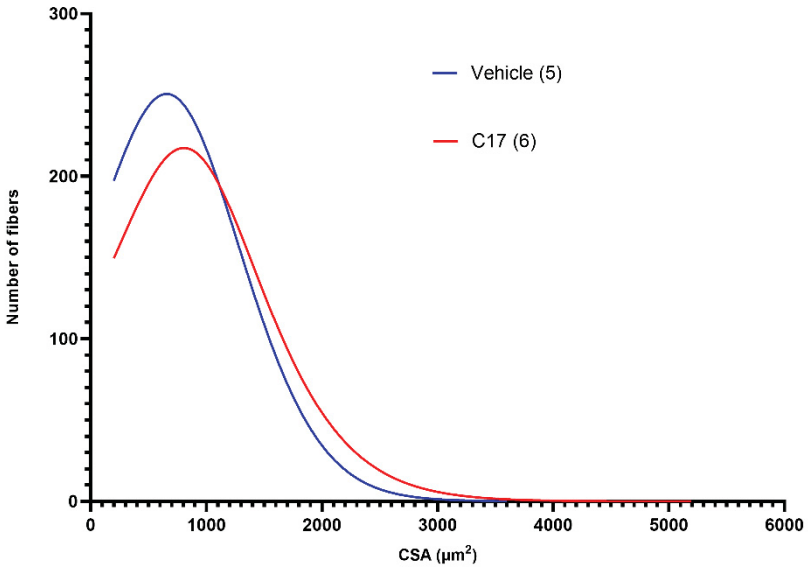

Figure 34. Fibers cross-sectional area (CSA).

Graph reporting the distribution of CSA of TA muscles from humanized R98H-α-SG mice treated for 3 weeks with either vehicle (5 samples) or corrector C17 (6 samples). The CSA of an average of 1500 fibers for muscle was measured.

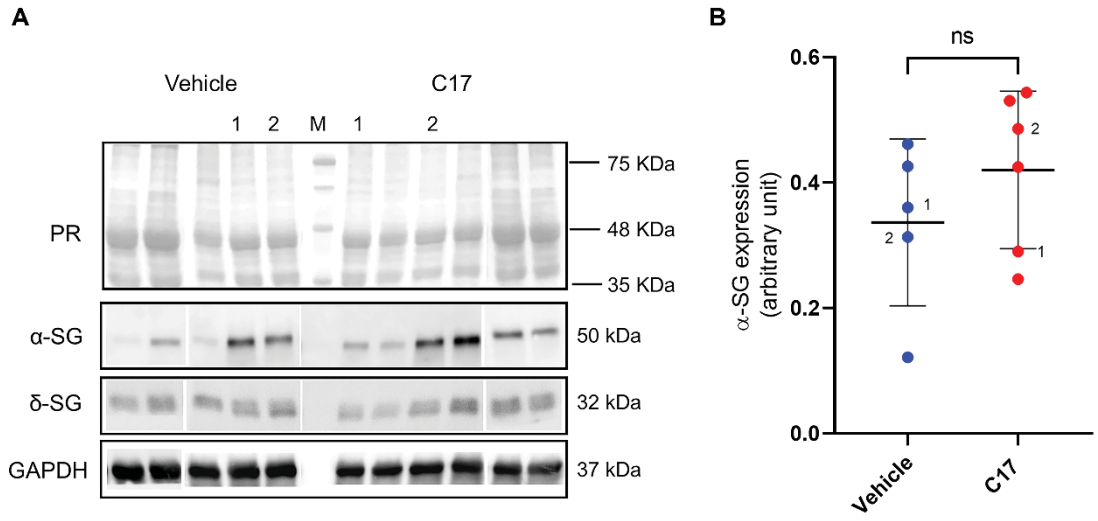

Figure 35. Western blots of TA muscle lysates from humanized mice treated with either vehicle or C17.

(A) Representative western blot of total protein lysates (25 µg each) of TA muscle samples from humanized mice expressing the R98H α-SG, treated for 3 weeks with either vehicle or corrector C17 (25 mg/Kg), as indicated. The numbers in the figure refer to the sample analyzed in figure 33. Membranes were probed with the primary antibodies specific for α-SG, δ-SG and GAPDH, used as loading control together with Ponceau Red (PR) total protein staining.
(B) Densitometric analysis of WB experiments reporting the α-SG expression, normalized for the expression of the housekeeping protein GAPDH, of vehicle or C17 treated samples. Numbers close to symbols indicate the samples analyzed figure 33. The graph also reports the mean values ± SD; statistical analysis was performed by unpaired two-tailed Student's t-test; ns, P> 0.05.

4.4.2 Five weeks C17 treatment induced muscle force recovery

Mice expressing the human R98H α-SG mutant in both hind limbs were used to perform a longer C17 treatment, ending with the assessment of the TA muscle force *in vivo*. Animals were IP injected daily for 5 weeks with either the vehicle or C17 formulation, according to the scheme in figure 36.

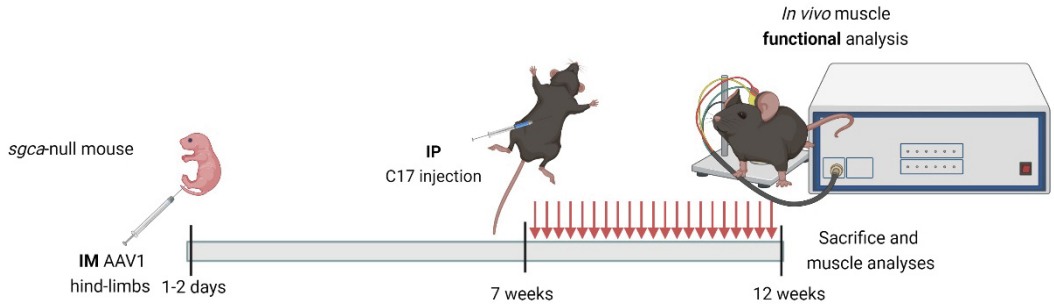

Figure 36. Scheme of the experimental workflow (created with BioRender.com).

1-2-day-old *sgca*-null mouse pups were injected in both hind limbs with $9x10^9$ vg of AAV1. Seven weeks upon transduction, mice were treated systemically for 5 weeks by daily IP injection of either corrector C17 or its vehicle. At the end of the treatment, *in vivo* TA muscle force was evaluated, mice were then sacrificed and the TA muscles explanted for further analyses.

As expected, the systemic administration of C17 promoted the proper localization of the SG complex and the amelioration of the myopathic phenotype.

IF and histological analyses of representative control and treated samples are reported in figure 37 where it is possible to observe that in cryo-sections from vehicle treated samples only traces of α-SG were recognizable and the signal coming from δ-SG was mainly localized in the fibers' cytosol.

Conversely, a reduction of centrally nucleated fibers and inflammatory infiltrate was evident in samples treated with C17, whose sarcolemma was immunodecorated by both α- and δ-SG specific antibodies.

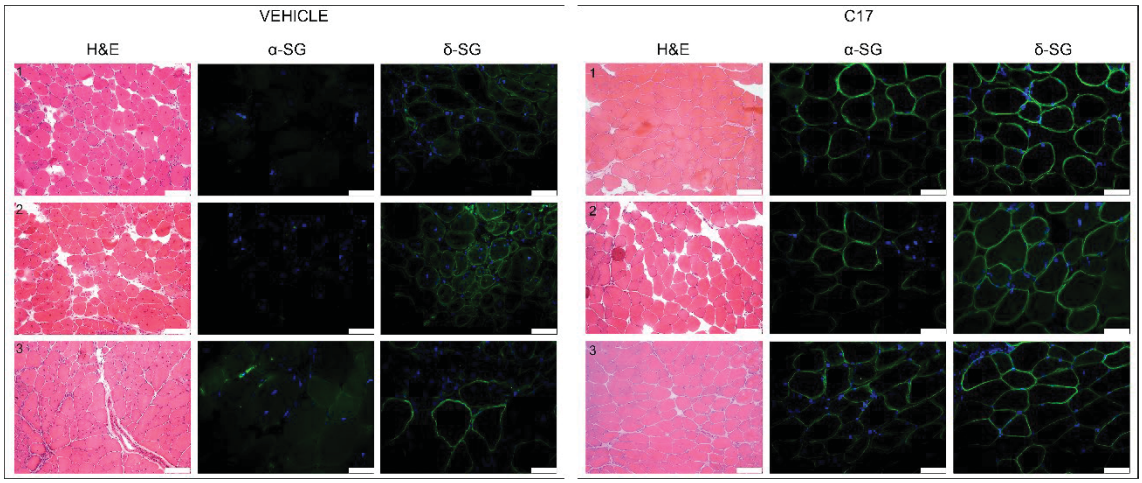

Figure 37. H&E staining and IF analysis of representative TA muscle cryo-sections of humanized mice expressing the R98H-α-SG treated for 5 weeks with either vehicle or corrector C17.

Primary antibodies specific for α- and δ-SG, as indicated, were revealed by Alexa-Fluor-488-conjugated secondary antibodies. Images were captured at the same setting conditions; bars correspond to 100 µm and 50 µm in H&E and IF images, respectively.

Surprisingly, the WB experiment showed no statistical difference in the α-SG protein content between C17 and vehicle treated samples. Indeed, some samples treated with the vehicle are characterized by a high α-SG protein expression, as the sample number 3 in the representative WB (figure 38). Of note, the amount of re-routed SG complex at the sarcolemma, which is the fraction properly folded, is increased only in the case of C17 treatment.

A first possible explanation for this WB outcome is that this expression could be the result of a higher transduction rate, thus we performed an absolute quantitative Real Time PCR to verify the amount of transduced α-SG cDNA in all samples. The analysis evidenced no statistical difference in the amount of human α-SG cDNA present in C17 and vehicle treated muscles excluding an effect on h-α-SG expression due to viral transduction level (figure 39). Furthermore, analyzing in depth the results, it is possible to observe that vehicle-treated sample number 3, which protein level was clearly measurable, presented a low gene copy number. Conversely sample number 2, that presented a very faint signal of the protein in WB, had a higher gene copy number. It is therefore possible to suppose that the α-SG expression might be affected by the conditions/physiology of the specific animal.

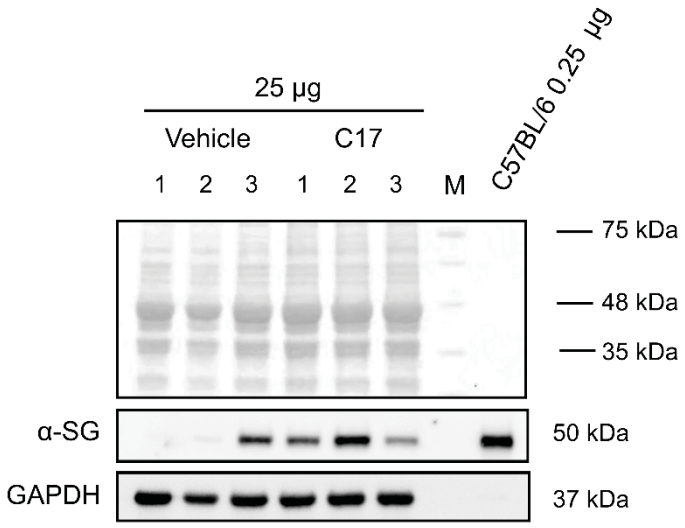

Figure 38. Representative WB of total protein lysates from TA muscle of humanized mice treated for 5 weeks with either vehicle or C17.

The membrane was probed with primary antibodies to α-SG and GAPDH, used as loading control, together with Ponceau Red (PR) protein staining. Protein bands were revealed by the HRP-conjugated secondary antibodies.

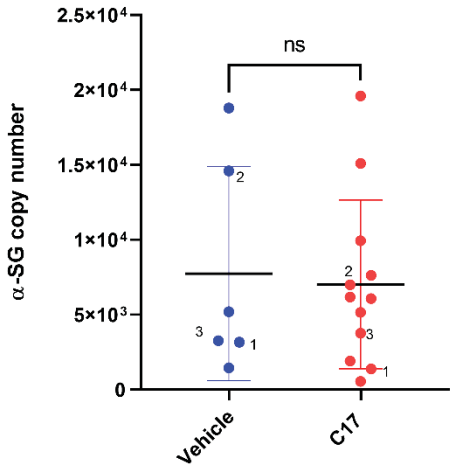

Figure 39. Human α-SG cDNA copy number, evaluated by q-PCR, present in transduced TA muscles at the end of the experiment.

The numbers close to symbols indicate the samples analyzed in figure 37. The graph also reports the mean values ± SD; statistical analysis was performed by unpaired two-tailed Student's t-test; ns, P≥ 0.05.

To investigate muscle function upon 5 weeks of C17 treatment the activity of TA muscles was evaluated by assessing force production *in vivo* (Blaauw, Agatea et al., 2010, Rossi, Flaibani et al., 2011).

Notably, the SG-complex rescue had positive functional effects. The activity of TA muscles was evaluated by assessing force production *in vivo* in response to nerve stimulation at different frequencies, ranging from single twitch to a completely fused tetanus (150 Hz). Figure 40 A reports the comparison of the normalized-force/frequency curves of TA muscles from wild-type, *sgca*-null and vehicle or C17 treated humanized mice.

It is interesting to note that at the maximum level of stimulation (150 Hz), the TA muscle force of C17 treated humanized mice (red line) was significantly higher than the one of the *sgca*-null mice (light blue line); it was improved in comparison to the vehicle control mice (blue line) and it was nearly indistinguishable from the force of the wild-type animals. The improvement of muscle force of the C17 treated humanized animals was evident since the first stimulation and observed at all the frequencies tested (figure 40 B). It is interesting to note that there was no difference in terms of force generated between the TA muscles of wild-type and C17-treated humanized mice, even though the amount of α-SG is remarkably lower, of about one hundred times, in these latter sample (see the WB analysis reported in figure 38). Although being not statistically significant, a slight increase of the force generated by vehicle treated muscles was evident in comparison to the *sgca*-null TA muscles. This was probably the consequence of the fact that in humanized mice a minimal amount of the expressed R98H α-SG skips from degradation with some localization at the sarcolemma together with the wild-type partners. This small amount, difficult to be appreciated in IF, is however sufficient for a partial rescue of the force.

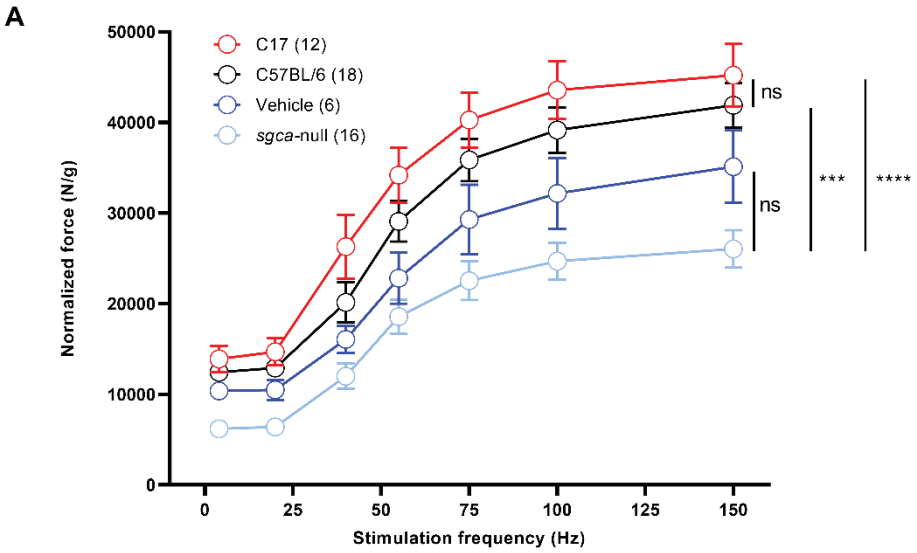
A
C17 (12)
C57BL/6 (18)
Vehicle (6)
sgca-null (16)
Normalized force (N/g)
Stimulation frequency (Hz)
ns
ns
***
****

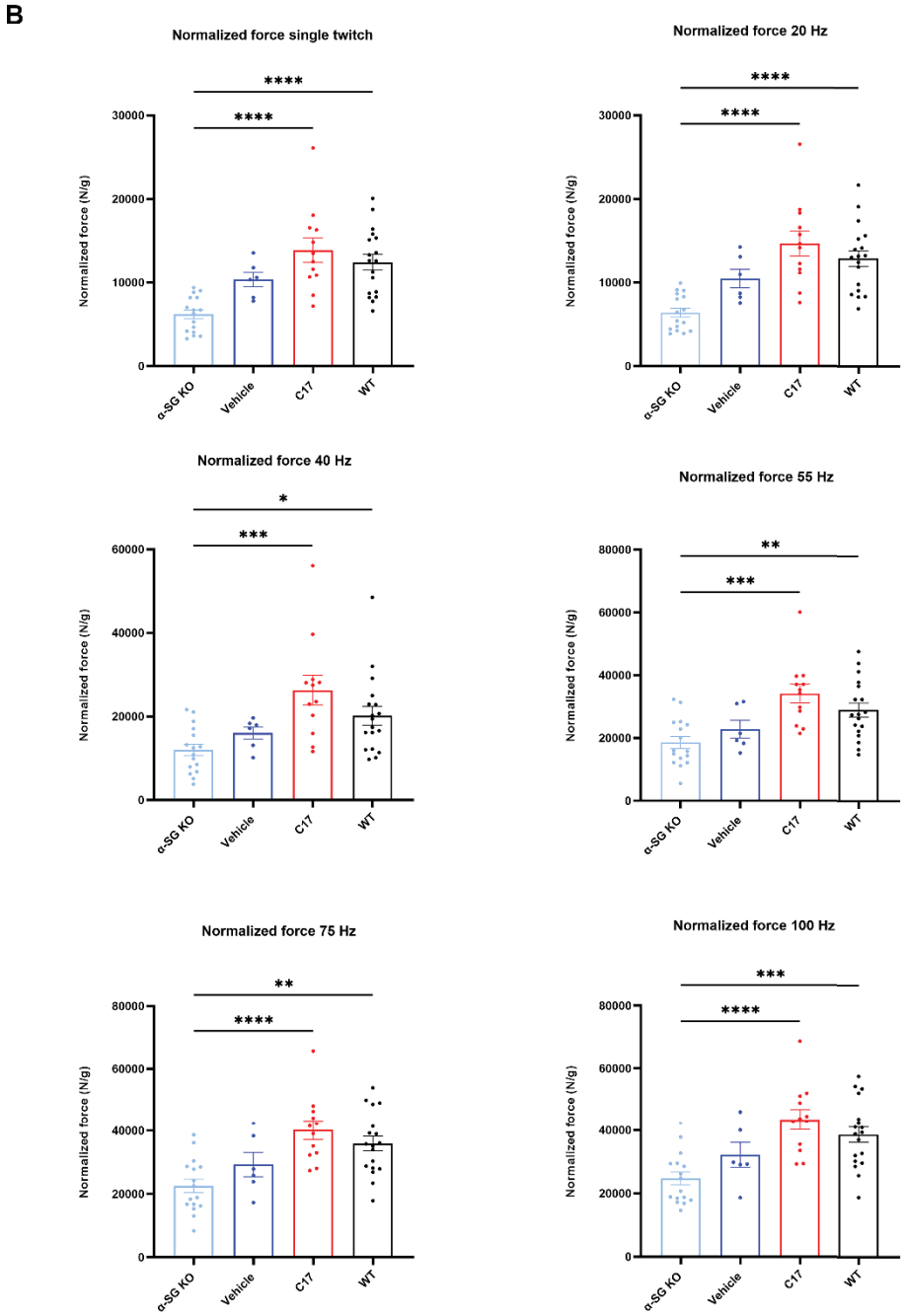
B
Normalized force single twitch
Normalized force 20 Hz
Normalized force 40 Hz
Normalized force 55 Hz
Normalized force 75 Hz
Normalized force 100 Hz
Normalized force (N/g)
α-SG KO
Vehicle
C17
WT

Figure 40. Force-frequency curves of TA muscle.

(A) Force-frequency curves of TA muscle (normalized for muscle weight) elicited by electrical stimulation at the indicated frequencies of WT (positive control), *sgca*-null mice (negative control), and humanized mice treated for 5 weeks with either vehicle or C17 25mg/kg. Statistical analysis was performed by One-way ANOVA test followed by multiple comparisons Tukey's test; for clarity statistic symbols are reported for the 150Hz frequency only. Data are reported as mean values ± SEM. ***, P ≤ 0.001; ****, ≤ P 0.0001; ns, P ≥ 0.05.
(B) TA muscle force (normalized for muscle weight) of living animals was recorded at different frequencies of stimulation as indicated. Each graph reports the normalized force distribution of *sgca*-null (n=14) C57BL/6 (n=18) and humanized R98H treated with either vehicle (n=6) or C17 (n=12). The mean values ± SEM are also indicated. Statistical analysis was performed by One-way ANOVA test followed by multiple comparisons Tukey's test; *, ≤ 0.05; **, ≤ 0,01; ***, P ≤ 0.001; ****, ≤ P 0.0001.

4.5 C17 chronic treatment did not cause major toxic effect in humanized mice upon five weeks of C17 administration

No acute sign of toxicity was revealed during the experimentation, all C17 injected animals ended the treatment, showing neither behavioral difference nor sign of distress in comparison to vehicle treated mice. They grew at similar rate reaching an average final weight of 23.63 ± 2.74 gr (C17 treated) and 23.90 ± 2.275 gr (vehicle treated) as reported in figure 41 A.

Evaluation of liver and kidney biopsy for adverse drug reaction is one of the most challenging problems in pathology. Drug-induced nephrotoxicity accounts for up to 25% of the reported serious adverse effects and drug-related injury can mimic all the patterns observed in primary liver disease (John & Herzenberg, 2009, Kleiner, 2018, Ramachandran & Kakar, 2009).

Moreover, if we consider that liver and kidney are the primary organs involved in metabolism and excretion of pharmacological compounds and that chronic toxicity may alter cell morphology and organ architecture, the analysis of liver and kidney biopsies is important for a preliminary assessment of C17 possible toxicological profile.

The histological analysis of kidneys and livers of humanized mice showed no major difference between vehicle and C17 animals treated for 5 weeks (figure 41 B).

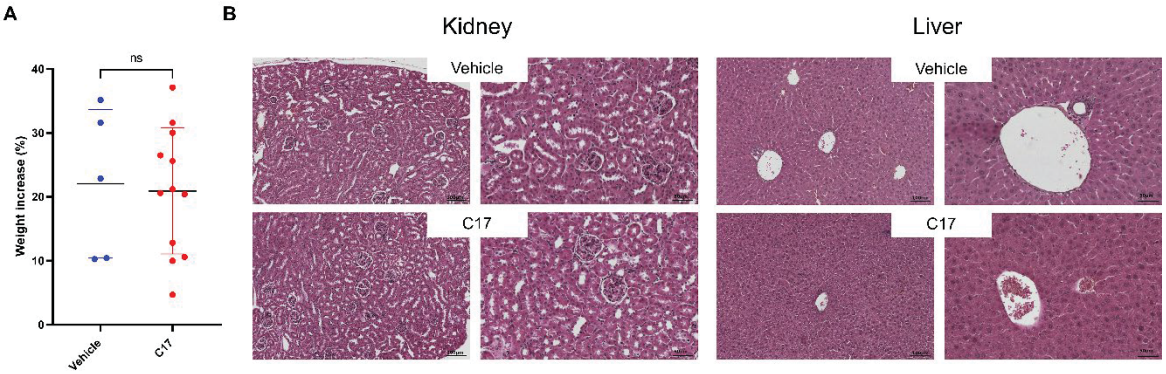

Figure 41. No major toxic effect was observed in humanized mice upon 5 weeks of C17 administration.

(A) The graph reports the distribution of the body-weight increase of mice at the end of 5 weeks treatment. Mean values ± SD are also indicated. Statistical analysis was performed by unpaired two-tailed Student's t-test; ns, P> 0.05.
(B) H&E staining of fixed kidney (cortex) and liver sections from humanized mice treated with either vehicle or C17. Each field is from a different mouse, two magnifications are reported to better appreciate cell-tissue organization.

The results reported until now are also summarized in our recently published paper (Scano, Benetollo et al., 2021)

4.6 Preliminary C17 pharmacokinetic characterization

The C17 molecule seems to be really promising in recovering folding defective sarcoglycans both *in vitro* and *in vivo.* Thus, to define the optimal concentration to achieve a therapeutic effect we started a pharmacokinetic study of the small molecule. To this intent, its blood stability and its possible liver metabolism were investigated.

4.6.1 C17 blood stability

Inside the body, a drug molecule has to be sufficiently stable in order to exert its pharmacological effect over a satisfactory time period. Thus, the molecule stability in the blood is a fundamental factor to be investigated. The first step in this experiment consists of the collection of blood from WT mice and its incubation at 37°C with different concentrations of C17 compound. At different time points (0', 30', 120' and 240') the blood containing C17 was collected and samples were analysed at the UHPLC. As reference control, the blood without the compound was used.

Chromatograms at the wavelength of 312 nm, the wavelength at which C17 has the maximum of absorbance, as already shown in figure 31, were used to quantify the C17 recovered in each sample by determining the Area Under the Curve (AUC) through the integral function. The chromatogram analysis consists of the AUC evaluation in correspondence to the peak of the C17 molecule, that has a retention time (rt) of about 6.60-6.65 min, as reported in figure 42 A. It was assumed that the concentration calculated at the time point 0' corresponds to the 100% of C17. Thus, the obtained integral values corresponding to a specific C17 concentration have been plotted against the time.

The graph in figure 42 B shows that 25 μM C17 incubated with blood underwent to a reduction during the first 30 minutes to remain then stable until 240 minutes. The percentage of remaining C17 molecule was higher than 80% at the end of the experiment. This trend suggests that C17 is stable in the blood until 4 hours after an initial decline that can be accountable to the binding to plasma proteins or to physical instability resulting in the interaction of the compound with the surface of the reaction mixture container. However, no metabolic or by-products have been recognized. Indeed, the chromatograms analysed at different wavelengths (216, 250, 286, 312, 350 and 400 nm) did not show any peaks that could correspond to C17 metabolites.

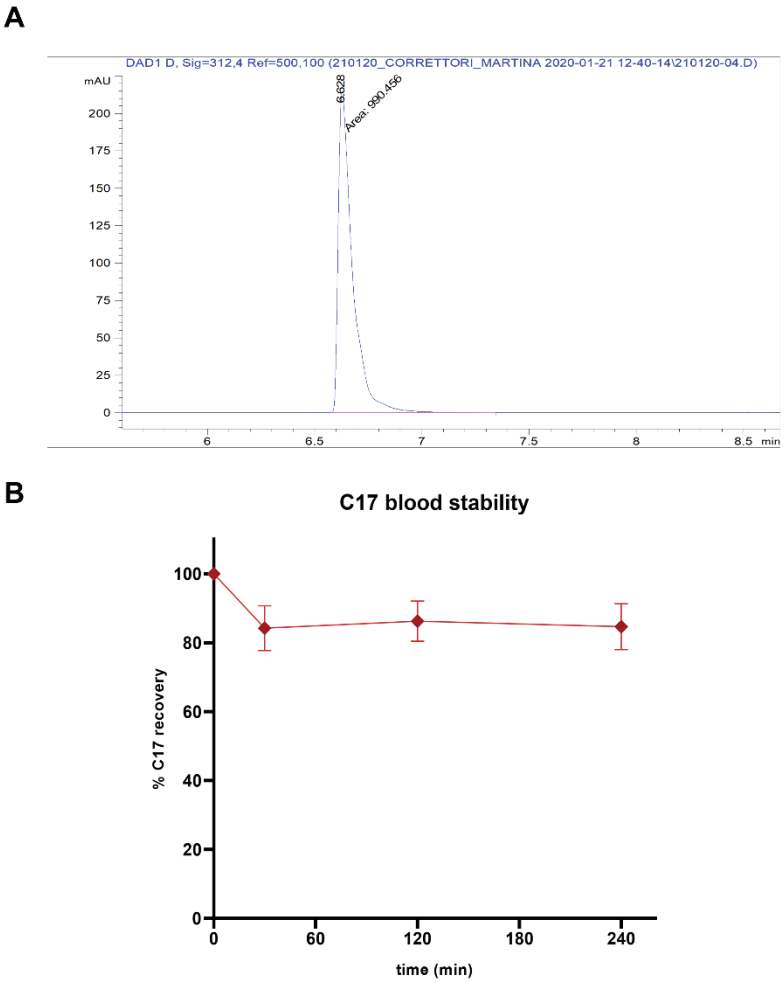

Figure 42. C17 blood stability.

(A) Chromatogram at wavelength 312 nm corresponding to the elution of C17, that has a retention time (rt) of about 6.60-6.65 min.
(B) Graph showing the percentage of recovered C17 at different time points, as indicated, after UHPLC analysis at 312 nm. Average of 3 independent experiments.

4.6.2 C17 biotransformation studies

4.6.2.1 Liver microsomes extraction

Microsomes were obtained from mouse livers and stored at -80°C, according to the protocol described in M&M. Starting from 8 mouse livers for a total of 14 grams, microsomes at a concentration of 16 mg/ml have been obtained. According to the literature, this concentration is optimal since it is in the range of 10-20 mg/ml that is the typical yield obtained through liver microsomes isolation (Pelkonen et al., 1974).

Microsomes are cell fractions enriched in ER-associated proteins, such as CYP350 and UGT enzymes. To verify the presence of CYPs and UGTs in microsomes we performed a WB experiment. Liver lysates were loaded as positive control. The left part of figure 43 showed that

CYP450 1A2 enzyme, marked with the anti CYP450 1A2 antibody, is correctly detectable, confirming the correct isolation of the liver microsomes.

Since microsomes are enriched in ER-proteins, the CYP450 enzymes are present in higher amount in microsomes than in liver lysates, and according to this, also the level of calnexin, used as an ER protein marker, is higher. The presence of UGTs enzymes was also confirmed by a western blot in which microsomes and liver lysates were marked with the anti-UGT 1A1 antibody (Figure 43, right), suggesting that the protocol allowed to proper isolate the microsomal fraction, including the different metabolic enzymes, which will be fundamental for the following experiments.

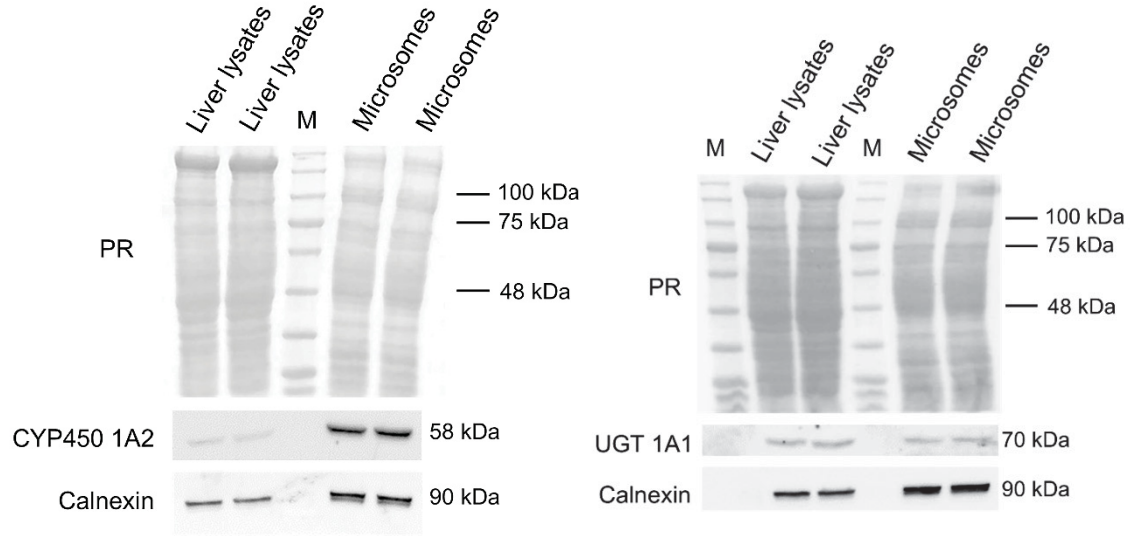

Figure 43. CYP450 1A2 and UGT 1A1 enzymes content evaluated by WB.

Analysis of 40 µg of liver lysates and microsomes isolated from mouse livers. The membrane was probed with primary antibodies to CYP450 1A2 (on the left), UGT 1A1 (on the right) and calnexin, together with Ponceau Red (PR) protein staining used as loading control. Protein bands were revealed by the HRP-conjugated secondary antibodies.

4.6.2.2 Phase I metabolism

Once the presence of CYP enzymes has been assessed, their effective functionality was also investigated in order to study C17 corrector metabolism. As a positive control, the molecule resveratrol has been used (Springer & Moco, 2019). The metabolism of this molecule is already known; indeed, during the phase I reactions mediated by CYP enzymes, it is metabolised by CYP450 1A2 into piceatannol and tetrahydroxystilbene.

The UHPLC method has been applied for the determination of resveratrol phase I metabolic products in mice liver microsomes. Resveratrol was added to microsomes at a concentration of 5 µM, following the incubation of resveratrol at 37°C in microsomes with a NADPH generating system, a reduction in the peak corresponding to the resveratrol molecule during time was determined. The AUC of each peak, with a retention time equal to 3.33-3.34, was integrated, and

the obtained values were plotted as a function of time. The trend of the phase I metabolism of resveratrol resulting from the CYP450s activity led, as expected, to a reduction of about 30% of the reference compound.

As negative controls, two mixtures lacking respectively microsome and NAPDH have been tested and analyzed at the UHPLC to assess the absence of molecule alterations due to the experimental settings. In the first case, metabolism cannot occur without microsomes, and in the latter case, the absence of the CYPs cofactor NADPH do not permit microsomes to perform their metabolic activity. Once the metabolic activity of the isolated microsomes has been validated, the metabolism of the C17 corrector 5 µM, mediated by phase I reaction of CYP450 enzymes, was determined. C17 seems to be not metabolized by these enzymes as its level is preserved during the microsomes incubation until 120 minutes. Both resveratrol and C17 graphs showing the percentage of molecules recovery after phase metabolism are reported in figure 44.

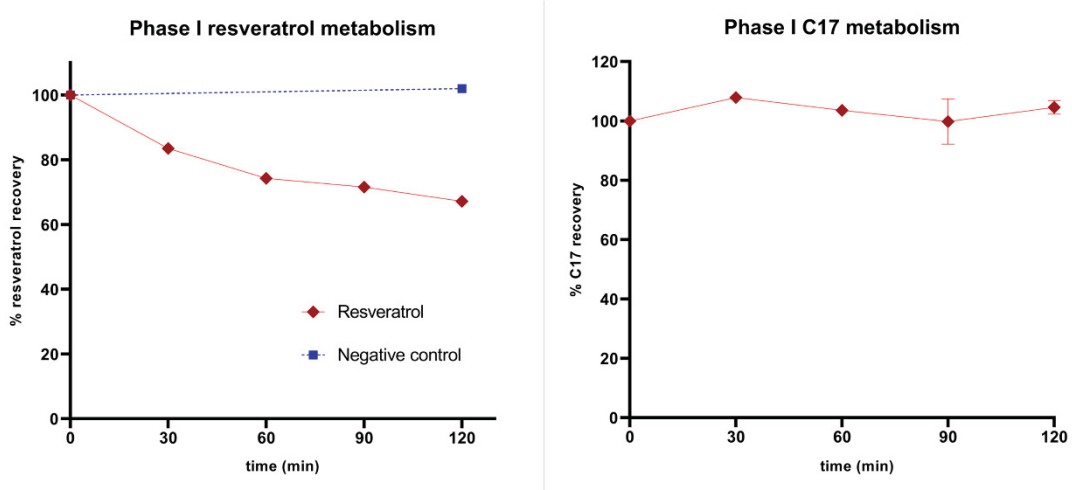

Figure 44. Phase I metabolism of resveratrol and C17.

Graphs showing the percentage of recovered molecules after CYP enzymes incubation at different time points, as indicated, and analysed with UHPL at 312 nm. On the left, graph showing the percentage of recovered resveratrol in the presence of the complete reaction mixture (red line) and in the absence of the NADPH co-factor (blue line); on the right, graph showing the percentage of recovered C17 in the presence of the complete reaction mixture. Average of 2 independent experiments.

4.6.2.3 Phase II metabolism

The effective functionality of uridine-glucuronosyltransferase (UGTs) was firstly assessed by incubating alamethicin-activated liver microsomes with resveratrol, the reference compound. After a brief incubation at 37°C, the UDPGA, the cofactor of UGTs enzymes, was added to the reaction mixture, allowing the phase II reactions to start.

From the reaction mixture, 200 µL of samples were collected at time points 0, 15, 30, 60, 90 and 120 minutes and analysed at the UHPLC. As expected, resveratrol is metabolized by UGTs and its metabolites can be already observed at the first experimental time point (figure 45 A). After 30 minutes the peak of resveratrol is already undetectable, meaning that all compound was

metabolized (figure 45 B). Indeed starting from 30 minutes, peaks corresponding to metabolites remains stable over time. Metabolites have a retention time lower than the reference compound, 2.5 and 2.7 minutes, and both of them are glucuronidated.

Resveratrol is therefore completely metabolized in 15-30 minutes after the addition of the UPDGA, as reported in the graph in figure 45 C. The negative controls consisting of the reaction mixture in absence of UDPGA or microsomes evidenced that the reaction conditions are optimal for the performance of the experiment, indeed no metabolites were detected even after 120 min of incubation. These results allowed us to proceed investigating the C17 metabolism mediated by phase II reactions.

The C17 compound was incubated with microsomes and with the addition of the UGTs cofactor UDPGA that initiate the reaction. In this case, no other peaks corresponding to possible metabolites were identified by UHPLC analysis. On the other hand, the peak corresponding to the tested molecule remained constant over time (figure 46 A-B) and the percentage of recovery, as shown in the graph (Figure 46 C), remains stable at 100% for the duration of the entire experiment. These data suggest that UGT enzymes are unable to modify corrector C17.

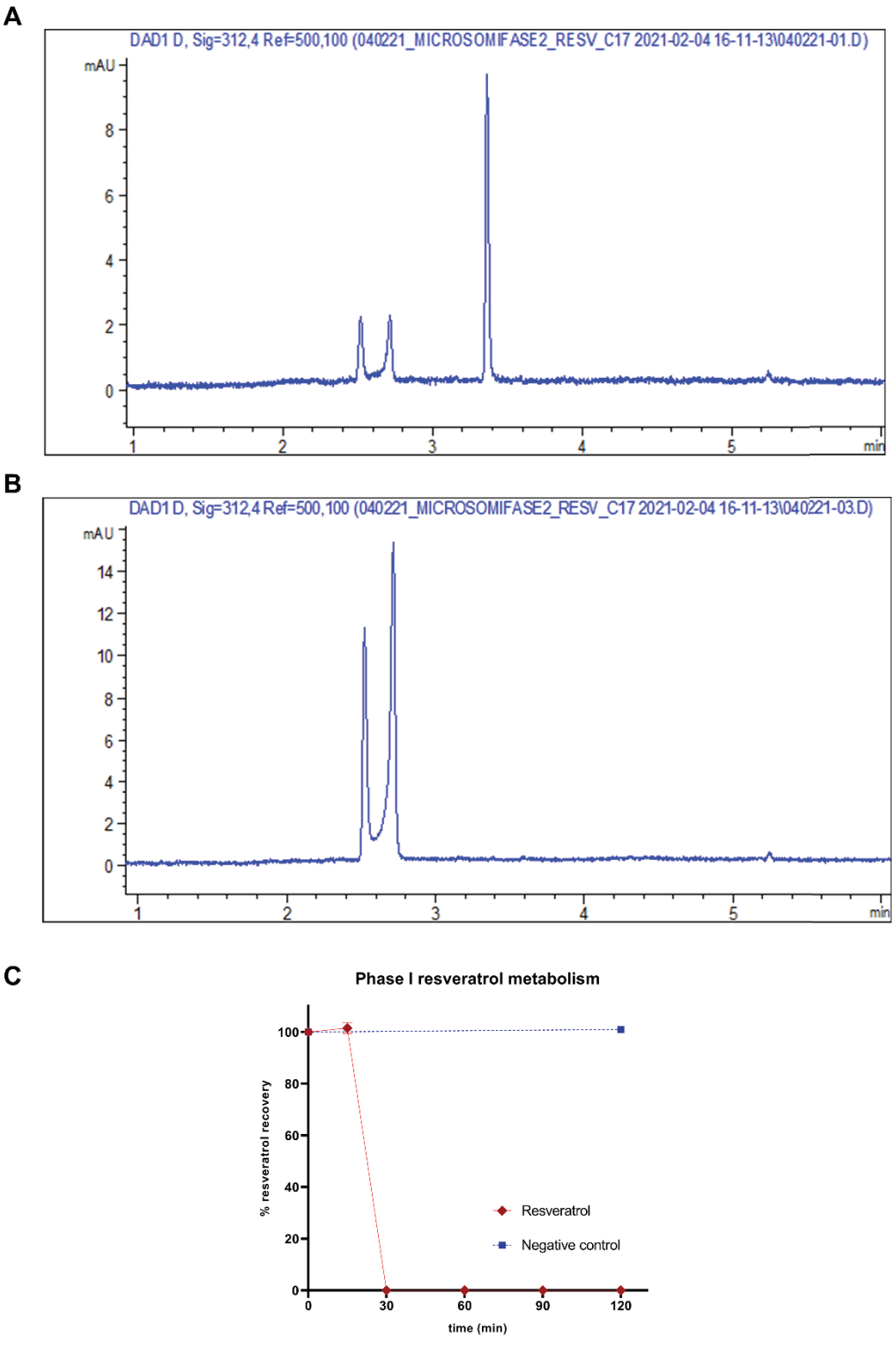

Figure 45. Phase II metabolism of resveratrol, the reference compound, performed by UGT enzymes.

Chromatograms correspond to the wavelength of 312 nm.
(A) Chromatogram of the time point 0, in which resveratrol metabolites are already detectable.
(B) Chromatograms of the time point 30 minutes, in which the resveratrol is undetectable.
(C) Graph showing the percentage of recovered resveratrol at different time points, as indicated, after UHPLC analysis, in the presence of the complete reaction mixture (red line) and in the absence of the UDPGA co-factor (blue line). Average of 2 independent experiments.

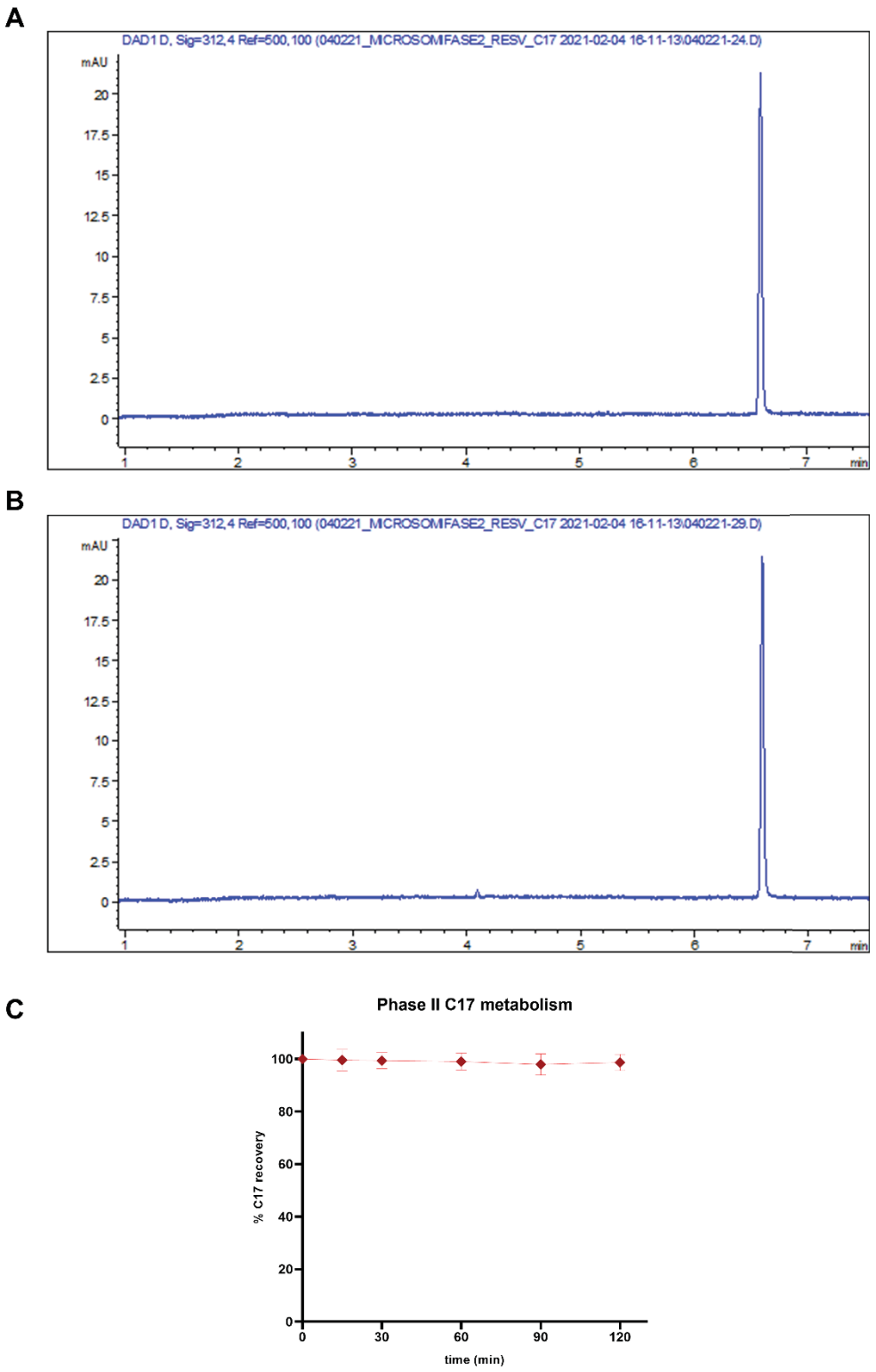

Figure 46. Phase II metabolism of C17, performed by UGTs enzymes.

Chromatograms correspond to the wavelength of 312 nm.
(A) Chromatogram of the time point 0, in which the C17 is detectable.
(B) Chromatogram of the time point 120 minutes, completely superimposable to the chromatogram in A.
(C) Graph showing the percentage of recovered C17 in the presence of the complete reaction mixture at different time points, as indicated, after UHPLC analysis. Average of 2 independent experiments.

5. CONCLUSIONS

Sarcoglycanopathies, also known as limb-girdle muscular dystrophy (LGMDR3-6), are a group of autosomal recessive muscle wasting diseases that mainly affect the proximal musculature of the scapular and pelvic girdles. Sarcoglycanopathies are due to mutations in the genes coding for α-, β-, γ-, δ- sarcoglycans (SGs).

Sarcoglycanopathies are heterogeneous disorders for both age of onset and phenotype severity. However, they are invariably characterized by a progressive degeneration of the skeletal muscle tissue, with increase of serum CK due to sarcolemma fragility, often ending in loss of ambulation. Additional features are calf hypertrophy, scapular winging, contractures, and scoliosis. Patients can suffer of restrictive ventilatory syndrome with the need for respiratory support, and/or dilated cardiomyopathy that requires a concomitant cardiac therapy. Respiratory and/or cardiac complications can be fatal if not continuously monitored (Angelini & Fanin, 2016, Vainzof, Souza et al., 2021).

Although supportive interventions aim at ameliorate the quality of life of patients, the sole available pharmacological approach is the symptomatic treatment with corticosteroids to decrease inflammation (Carotti et al., 2017). Even though cell and gene therapy-based approaches are currently under investigation, they are challenging and the collected results are not completely satisfactory (Biressi et al., 2020, Mendell et al., 2019, Negroni et al., 2016). Thus, no causative therapeutic approach for sarcoglycanopathy has still reached clinical application.

SGs are four transmembrane glycoproteins of striated muscle that form a tetrameric complex at the sarcolemma. SG-complex is closely linked to the major dystrophin associated protein complex (DAPC) and plays a fundamental role in assuring the membrane integrity during the muscle contraction cycles (Mohassel & Bönnemann, 2015).

Mutations in any SG gene (*SGCA, SGCB, SGCG, SGCD*) result in the strong reduction or total loss of the affected protein as well as of the WT partners. The disruption of this key membrane complex is responsible for the alteration of the DAPC structural properties that results in an increased membrane fragility. This leads to progressive muscle wasting and the onset of a progressive form of severe dystrophy (Sandona & Betto, 2009).

SG mutations reported until now are either nonsense, out of-frame, in-frame small deletions/insertion or missense mutations. The latter, producing a full-length protein with a single amino acid substitution, are the most frequently reported (on the whole, they represent more than 65% of all known SG genetic defects).

In the last few years, it has been observed that a single amino acid substitution results in a possible functional but folding defective protein which is recognized and rapidly degraded by the QC machinery of the cell.

Therefore, the QC system allows the maturation and correct localization of native proteins only to avoid the possible accumulation of folding defective proteins that could elicit toxic effects.

Thanks to this knowledge, two novel possible therapeutic approaches have been hypothesized for the forms of sarcoglycanopathy characterized by the presence of missense mutations. Both strategies aim at recovering a functional SG-complex at the proper cellular site, by using small molecules able either to avoid the degradation or to "repair" the folding defective SG (Bartoli et al., 2008, Bianchini et al., 2014, Carotti et al., 2018, Carotti et al., 2020, Gastaldello et al., 2008, Soheili et al., 2012).

Concerning the first approach, it was reported that, by targeting different steps of the degradative pathway, most of the SG missense mutants are recovered at the sarcolemma, thus strengthening the concept that these mutants are still functional even if folding defective (Bianchini et al., 2014, Gastaldello et al., 2008). However, as this strategy is not specific for SGs, a safer approach is represented by the use of small molecules aiming to help the folding process of SG missense mutants.

These molecules, known as correctors of the cystic fibrosis transmembrane regulator channel (CFTR) were screened for their ability to assist the folding of the conformational mutants of the chloride channel responsible for the development of cystic fibrosis (Bell et al., 2015).

Indeed, many mutations occurring in cystic fibrosis, classified as type II mutants are missense mutations leading to defects in the folding and trafficking of an otherwise functional CFTR protein, a mechanism that is in common with sarcoglycanopathies (Veit et al., 2016).

On these premises, CFTR correctors were successfully tested *in vitro* in sarcoglycanopathy models and the proof of concept of this therapeutic approach was first described in Carotti et al., 2018. Data from both cell models and notably, primary myotubes from a patient suffering of α-sarcoglycanopathy, strongly suggest the feasibility of the "protein repair strategy" to treat LGMDR3. Indeed, upon CFTR correctors treatment, the total amount and the cell membrane fraction of the mutated α-SG increased thanks to protein stabilization, without any effect on gene transcription. The accumulation of α-SG mutants is expected to be therapeutically effective as followed by SG-complex assembly and localization at the sarcolemma. The SG complex, although containing a mutated subunit, is functional as its presence strengthened the sarcolemma, reducing the release of the cytosolic CK protein under stressful condition. The same approach is supposed to be effective also with the other sarcoglycanopathy forms linked to missense mutations, since all of them share a similar pathogenic mechanism (Carotti et al., 2017, Soheili et al., 2012).

To translate the discovery of a new drug into a treatment, an animal model mimicking the pathologic phenotype is essential. In our case, there is the need of vertebrate animals carrying

missense mutations in the SG genes that cause the loss or strong reduction of the tetrameric complex, in order to reproduce the human condition.

This model will be suitable to test the efficacy, the pharmacodynamics and the pharmacokinetics of the drug. The presently available murine models, as described in the previous chapters, are unusable. Indeed, the KO mouse for SGs, even though reproducing the dystrophic phenotype, do not produce the protein and hence they are not suitable to test the therapeutic approaches aiming at rescuing a defective protein (Coral-Vazquez et al., 1999, Duclos et al., 1998, Durbeej et al., 2000, Hack et al., 1998). On the other hand, the α-SG$^{H77C/H77C}$ and β-SG$^{T153R/T153R}$ mice do not recapitulate the disease, as the mutated protein and the entire complex properly localize at the sarcolemma and mice do not develop a dystrophic phenotype (Bartoli et al., 2008, Henriques et al., 2018, Kobuke et al., 2008).

Thus, this PhD thesis project focuses on the generation and characterization of novel mouse models of sarcoglycanopathy and on the study of CFTR correctors as possible therapeutic strategy for this disease, at present incurable. As our laboratory recently established the proof of concept that protein-folding correctors are effective in rescuing folding-defective α-SG (Carotti et al., 2018) here we reported evidence about the efficacy of other correctors used in single or combined administration. Indeed, it is generally known that a combination of two or more CFTR modulators (both correctors and potentiators) will be required to achieve a significant clinical benefit, enhancing the folding and stability of the channel and thus avoiding the retention/delivery to degradation and thus improving the CFTR mutant activity (Clancy et al., 2012, de Wilde et al., 2019, Okiyoneda et al., 2013).

To evaluate correctors' efficacy in sarcoglycanopathy, we measured both the total increase of α-SG content but particularly the sarcolemma fraction, as sign of trafficking rescue of the mutant. CFTR correctors C13, C9 or C17, the latter used as our internal reference, selectively elicited the accumulation of α-SG in LGMDR3 myotubes while they were ineffective in healthy ones, supporting the idea that these compounds are effective only if a defective SG is present. On the other hand, corrector C6 is unable to increase the content of the mutated α-SG in both healthy and LGMDR3 myotubes at all the concentrations tested. However, if focusing on the membrane fraction, it is possible to observe that C6 increased the localization of α-SG at the sarcolemma, suggesting a major role of C6 in promoting the traffic of the portion of mutant that physiologically skips degradation.

Altogether these results evidenced the possibility to broaden the number of compounds validated *in vitro*, potentially useful in sarcoglycanopathy and highlighted the possible additive or even synergic effect for some of them. These data have been summarized in a recently published paper (Carotti et al., 2020).

As the proof of concept of the strategy has been already established for LGMDR3 (Carotti et al., 2018, Carotti et al., 2020) it would be important to verify the feasibility of the approach in another type of sarcoglycanopathy (i.e. due to mutations on a different SG gene). For this purpose, the effect of the most promising corrector in our hand, C17, has been assessed on LGMDR4 patient's myotubes, carrying a missense mutation on the *SGCB* allele. LGMDR4 primary cells were incubated for seven days in an appropriate medium supplemented with adenovirus carrying the MyoD ORF. By this strategy, cells are induced to differentiate into myotubes, multinucleated cells expressing markers of the skeletal muscle lineage (Kabadi, Thakore et al., 2015). C17 molecule were applied for 48 hours before cell lysis. The total and membrane fractions of β-SG protein were evaluated by western blot, while the correct localization of the protein at the cell membrane was evaluated by immunofluorescence. The western blot revealed the increased expression of the mutated β-SG protein, upon corrector treatment, if compared to myotubes incubated with the vehicle (DMSO). In particular, C17 induced a two-fold increase in the β- SG membrane fraction in comparison to the DMSO treated cells. The immunofluorescence analysis confirmed this result, as the treatment restored the β-SG protein at the myotubes surface. Even if these are only the first results obtained with LGMDR4 patient myotubes, they are in accordance with the previous ones obtained with a LGMDR3 patient myotubes, confirming the hypothesis that the use of CFTR correctors could be applied to sarcoglycanopathies cases linked to missense mutations, regardless of the *SGC* gene mutated.

To translate the promising results collected *in vitro* into a therapy for sarcoglycanopathy we generated an ad hoc novel mouse model useful to validate the most promising CFTR corrector C17. We adopted an alternative approach to generate a valuable model of LGMDR3. In the background of the *sgca*-null mouse, we induced the expression of the human α-SG carrying either the WT and the mutated, V247M and R98H missense mutation by exploiting the transduction via AAV1 (Zincarelli et al., 2008). The injection was performed in newborn mice of 1-2 days, and this ensured tolerance toward the human protein and the development and growth of the muscle in the presence of the human SG, avoiding adverse immune responses mediated by the presence of a non-self-protein. As expected according to (Allamand, Donahue et al., 2000), the injection of the WT sequence resulted in humanized hind limbs with a phenotype close to the one of the healthy mice, with the SG-complex residing at the sarcolemma. This means that mouse tolerated the human protein that assembled into a functional SG-complex with the murine subunits and that it was sufficient one hundredth of the normal amount of α-SG (as assessed by WB) to guarantee the development of a nearly normal phenotype. As already mentioned, the focus on the α-SG V247M mutation was driven by the fact that it is one of the two variants carried by the myogenic cells used to test CFTR correctors *in vitro* and it is among the most frequently reported missense mutations in LGMDR3 (Carotti et al., 2017). In addition, the R98H mutation was selected as it is associated with a mild/severe phenotype and is classified, like V247M, as a rescuable mutant by

in vitro experiments (Bianchini et al., 2014, Carotti et al., 2018, Gastaldello et al., 2008, Soheili et al., 2012). Conversely, the R77C amino acid substitution was not considered, despite being the most frequently reported mutation in LGMDR3, as the corresponding KI mice failed to develop a dystrophic phenotype (Bartoli et al., 2008, Kobuke et al., 2008). Notably, the outcome of the transduction with the human V247M-α-SG was the presence of the SG-complex at the sarcolemma and the lack of an evident dystrophic phenotype at histological level of the TA muscle. Even though unexpected on the bases of the *in vitro* experiments (Bianchini et al., 2014, Carotti et al., 2018, Gastaldello et al., 2008), this result is in line with the lack of phenotype of SG-KI animals (Bartoli et al., 2008, Henriques et al., 2018, Kobuke et al., 2008). In addition, it contributes to strengthen the hypothesis that some difference in the QC system may occur between human and mouse and that some mechanisms are still unclear (Qi, Tsai et al., 2017). Furthermore, it is in accordance with the recent genotype-phenotype correlation analysis reporting that LGMDR3 subjects with V247M-α-SG developed a milder disease phenotype with a residual amount of the SG at the sarcolemma higher than 30% (Alonso-Perez et al., 2020).

By contrast, when the human R98H-α-SG was transduced, clear myopathic features were present in the TA muscle, well mimicking the pathology, with only traces of the mutated protein and a strong reduction of the wild-type subunits, β-, γ- and δ-SG at the sarcolemma. This suggests that the QC system efficiently recognized α-SG carrying this mutation that underwent fast degradation, confirming what already observed *in vitro* (Bianchini et al., 2014, Carotti et al., 2018, Gastaldello et al., 2008).

This humanized mouse, novel model of sarcoglycanopathy, is characterized by transient SG expression restricted to the hind limbs. This means that to generate this model, the animal must be transduced with the sequence every time. At the same time this system is versatile, in principle allowing testing any possible mutations in any SG-KO mouse. In addition, different works suggested that the use of AAV1 and the tMCK promoter assure efficient delivery and controlled skeletal muscle expression of the human α-SG protein, evidencing a long persistence, up to one year, of the transgenic protein in the absence of toxicity, allowing the possibility of long-term studies in this humanized animals (Pacak et al., 2008, Pacak, Walter et al., 2007, Rodino-Klapac et al., 2008).

As the transduction with the human R98H-α-SG sequence resulted in humanized muscles well mirroring the LGMDR3 condition, we utilized this model for assessing *in vivo* the efficacy and safety of corrector C17. It is well known that *sgca*-null mice develop a progressive muscular dystrophy starting 1 week upon birth and becoming highly severe at 2 months of age (Duclos et al., 1998, Liu & Engvall, 1999). However, it is conceivable a slower progression of the disease in mice bearing a missense mutation in comparison to mice lacking the protein (*sgca*-null), as in humans.

Thus, as we wanted animals in which the disease was established but was still recoverable, we chosen a time interval of 7-12 weeks upon AAV1 injection to analyze the outcome of corrector treatments.

The daily systemic administration of C17, performed for three or five weeks, in mice with humanized hind limbs resulted in a clear amelioration of the myopathic features at the histological level and the rerouting of the SG-complex at the sarcolemma, as evidenced by immunofluorescence. In addition, we observed also a slight increase in mean fiber cross sectional area (CSA), suggesting the improvement of the dystrophic phenotype pattern. Indeed, even though skeletal muscle fiber size is highly variable, the "*optimal fiber size hypothesis"* proposes that large fiber size in healthy skeletal muscle is beneficial in supporting the metabolic cost of maintaining membrane potential (Jimenez, Dillaman et al., 2013).

However, the key finding was the recovery of the muscular function after the five weeks treatment, as assessed *in vivo*. The normalized force produced by TA muscles from C17 treated humanized mice was strongly improved in comparison to the *sgca*-null mice and is almost indistinguishable from that of the WT, healthy animals, proving the efficacy of the corrector in a model of LGMDR3. Of note, WT mice and C17 treated model animals elicited nearly identical muscle force, even though the total amount of α-SG was about one hundred times lower in humanized samples, as assessed by WB analysis. This suggests that a small amount of protein at the proper location is the prerequisite for providing sarcolemma protection from damages and preserving muscle functionality.

It is also interesting to consider that the muscle force generated by vehicle treated humanized animals was slightly higher, although not statistically significant, if compared to *sgca*-null mice. This could be the consequence of a minimal escape from degradation of the R98H-α-SG protein that can localize at the sarcolemma together with WT partners. Even though the amount is borderline for detection by IF, it is conceivably enough to assure a partial rescue of muscle force in humanized animals, which however is not statistically significant. This further suggests that α-SG missense mutants are potentially active and their preservation from degradation is indispensable for therapeutic purposes. Remarkably, when the whole process is improved (i.e. by the C17 corrector) the fraction of re-routed mutant/SG-complex is sufficient to guarantee full functional recovery.

Another essential point is that animals treated for 5 weeks with C17 showed neither behavioral difference nor sign of distress in comparison to vehicle treated mice and they grew at similar rate, reaching the experimental endpoint. Furthermore, the histological analysis of kidneys and livers shows no major difference between vehicle and C17 treated animals, suggesting that the molecule is safe in mouse, at the regimen and dose adopted. However, further experiments are needed to definitely exclude toxicity and to establish the minimal effective dose and the best route of administration.

Analyzing data coming from the blood stability experiments performed *ex vivo* and the biotransformation assays we can assume that C17 is a quite stable molecule. Indeed, when incubated with blood, after an initial decline of about 20% the C17 concentration remained stable for at least 4 hours. The initial fast decline could be due to physical instability related to changes in compound physical state, being hydrophobic can aggregate and precipitate or interact with the container walls, or to the binding with plasma proteins.

This is not a real instability due to enzymatic modification, however, plasma protein binding can substantially affect pharmacokinetics and pharmacodynamics of drugs, becoming a fundamental parameter to evaluate in molecule/drug metabolism. More lipophilic is a compound, more significant will be the plasma protein binding (Shakya, Al-Najjar et al., 2018). For a lipophilic compound as C17, we expect significant plasma protein binding that must be further investigated.

As for any other drug/molecule, C17 metabolism could lead to the formation of toxic metabolites. For this reason, and considering that the hepatic metabolism represents the major elimination route for most drugs we evaluated the activity of phase I and phase II reaction by using mouse liver microsomes, activated by the addition of cofactor suitable for the activation of CYP450 and UGTs enzymes respectively. The lack of C17 metabolite formation upon incubation with microsome could suggest that the compound is extremely stable or that we did not apply the optimal assay conditions. Such a hypothesis, C17 could be modified first by phase II enzymes and then by CYP450s. Indeed, CYP450 enzymes have principally an oxidase activity and due to the chemical characteristic of the C17 bithiazole compound it seems possible that the molecule is first modified (e.g. by UGT enzymes that typically act on small hydrophobic molecules) and then oxidized by cytochrome enzymes. To overcome this issue, the simultaneous activation of the different enzymes present in a liver fraction, could be useful to better mimic the *in vivo* aspects of drug metabolism. Furthermore, it would be useful to consider the use of microsomes from different species, including humans, as well as the use of different liver fractions instead of microsomes (i.e. fractions corresponding to the cytosol, etc.).

Another issue that we intend to investigate will be the C17 molecule duration of effect on the humanized mouse muscle. To this intent, the regimen of administration of the small molecule will be modified. In the last experiments, the treatment was performed daily and the effect on the humanized muscle was assessed 24 hours after the last injection. We plan to apply alternating administration (one week on, one week off), the prolongation of the elapsing time between the last injection and the assessment of the effect in the muscle, etc. Certainly, this can give important hints for the definition of a potential drug regimen in subsequent clinical trials.

In conclusion, our *in vivo* collected findings, together with data coming from the treatment of pathological human cells, are the proof that a CFTR corrector, specifically C17, is effective in LGMDR3, opening new venues of therapeutic intervention for this still neglected disease.

Considering the *in vitro* evidence suggesting that all forms of sarcoglycanopathy due to missense mutations share a similar pathogenic mechanism (Soheili et al., 2012) and our data with myogenic cells from a LGMDR4 subject, it is possible to predict a beneficial effect of CFTR correctors in LGMDR4-6 too.

It is clear that the forms of sarcoglycanopathy linked to large deletions/insertions or null/out of frame mutations are not treatable with this approach. However, except for LGMDR5, the sarcoglycanopathy subjects who are homozygotes for such defects represent a minority of all reported cases. Furthermore, compound heterozygosis is frequently reported (Alonso-Perez et al., 2020, Carotti et al., 2017, Guglieri, Magri et al., 2008). Thus, considering that a residual amount of SGs at sarcolemma higher than 30% seems linked to a mild disease phenotype (Alonso-Perez et al., 2020), it is conceivable that the recovery of some quantity of protein, even coded by one allele only, should be sufficient to assure phenotype amelioration. This enlarges the cohort of sarcoglycanopathy patients who could benefit from this pharmacological approach.

In conclusion, our data on sarcoglycans together with studies performed with proteins other than CFTR (structurally uncorrelated proteins) (Loo et al., 2012, van der Woerd et al., 2016) prove that the activity of a CFTR corrector is not limited to cystic fibrosis, but can be extended to sarcoglycanopathies and, theoretically, to other diseases characterized by the presence of a folding-defective, but potentially functional mutant.

REFERENCES

Al Shoyaib A, Archie SR, Karamyan VT (2019) Intraperitoneal Route of Drug Administration: Should it Be Used in Experimental Animal Studies? *Pharm Res* 37: 12

Allamand V, Donahue KM, Straub V, Davisson RL, Davidson BL, Campbell KP (2000) Early adenovirus-mediated gene transfer effectively prevents muscular dystrophy in alpha-sarcoglycan-deficient mice. *Gene Ther* 7: 1385-91

Allikian MJ, McNally EM (2007) Processing and assembly of the dystrophin glycoprotein complex. *Traffic* 8: 177-83

Alonso-Perez J, Gonzalez-Quereda L, Bello L, Guglieri M, Straub V, Gallano P, Semplicini C, Pegoraro E, Zangaro V, Nascimento A, Ortez C, Comi GP, Dam LT, De Visser M, van der Kooi AJ, Garrido C, Santos M, Schara U, Gangfuss A, Lokken N et al. (2020) New genotype-phenotype correlations in a large European cohort of patients with sarcoglycanopathy. *Brain* 143: 2696-2708

Amm I, Sommer T, Wolf DH (2014) Protein quality control and elimination of protein waste: the role of the ubiquitin-proteasome system. *Biochim Biophys Acta* 1843: 182-96

Angelini C, Fanin M (2016) Pathogenesis, clinical features and diagnosis of sarcoglycanopathies. *Expert Opin Orphan D* 4: 1239-1251

Angelini C, Fanin M, Freda MP, Duggan DJ, Siciliano G, Hoffman EP (1999) The clinical spectrum of sarcoglycanopathies. *Neurology* 52: 176-9

Angelini C, Fanin M, Menegazzo E, Freda MP, Duggan DJ, Hoffman EP (1998) Homozygous alpha-sarcoglycan mutation in two siblings: one asymptomatic and one steroid-responsive mild limb-girdle muscular dystrophy patient. *Muscle Nerve* 21: 769-75

Araishi K, Sasaoka T, Imamura M, Noguchi S, Hama H, Wakabayashi E, Yoshida M, Hori T, Ozawa E (1999) Loss of the sarcoglycan complex and sarcospan leads to muscular dystrophy in beta-sarcoglycan-deficient mice. *Hum Mol Genet* 8: 1589-98

Aronson JK (2016) Polyoxyl castor oil. In *Meyler's Side Effects of Drugs*, pp 866-867.

Asha S, Vidyavathi M (2009) Cunninghamella--a microbial model for drug metabolism studies--a review. *Biotechnol Adv* 27: 16-29

Barresi R, Confalonieri V, Lanfossi M, Di Blasi C, Torchiana E, Mantegazza R, Jarre L, Nardocci N, Boffi P, Tezzon F, Pini A, Cornelio F, Mora M, Morandi L (1997) Concomitant deficiency of beta- and gamma-sarcoglycans in 20 alpha-sarcoglycan (adhalin)-deficient patients: immunohistochemical analysis and clinical aspects. *Acta Neuropathol* 94: 28-35

Bartoli M, Gicquel E, Barrault L, Soheili T, Malissen M, Malissen B, Vincent-Lacaze N, Perez N, Udd B, Danos O, Richard I (2008) Mannosidase I inhibition rescues the human alpha-sarcoglycan R77C recurrent mutation. *Hum Mol Genet* 17: 1214-21

Bell SC, De Boeck K, Amaral MD (2015) New pharmacological approaches for cystic fibrosis: promises, progress, pitfalls. *Pharmacol Ther* 145: 19-34

Betto R, Senter L, Ceoldo S, Tarricone E, Biral D, Salviati G (1999) Ecto-ATPase activity of alpha-sarcoglycan (adhalin). *J Biol Chem* 274: 7907-12

Bianchini E, Fanin M, Mamchaoui K, Betto R, Sandona D (2014) Unveiling the degradative route of the V247M alpha-sarcoglycan mutant responsible for LGMD-2D. *Hum Mol Genet* 23: 3746-58

Biressi S, Filareto A, Rando TA (2020) Stem cell therapy for muscular dystrophies. *J Clin Invest* 130: 5652-5664

Blaauw B, Agatea L, Toniolo L, Canato M, Quarta M, Dyar KA, Danieli-Betto D, Betto R, Schiaffino S, Reggiani C (2010) Eccentric contractions lead to myofibrillar dysfunction in muscular dystrophy. *J Appl Physiol (1985)* 108: 105-11

Bonnemann CG, Modi R, Noguchi S, Mizuno Y, Yoshida M, Gussoni E, McNally EM, Duggan DJ, Angelini C, Hoffman EP (1995) Beta-sarcoglycan (A3b) mutations cause autosomal recessive muscular dystrophy with loss of the sarcoglycan complex. *Nat Genet* 11: 266-73

Brancaccio A (2019) A molecular overview of the primary dystroglycanopathies. *J Cell Mol Med* 23: 3058-3062

Brandon EF, Raap CD, Meijerman I, Beijnen JH, Schellens JH (2003) An update on in vitro test methods in human hepatic drug biotransformation research: pros and cons. *Toxicol Appl Pharmacol* 189: 233-46

Bushby K, Finkel R, Birnkrant DJ, Case LE, Clemens PR, Cripe L, Kaul A, Kinnett K, McDonald C, Pandya S, Poysky J, Shapiro F, Tomezsko J, Constantin C, Group DMDCCW (2010) Diagnosis and management of Duchenne muscular dystrophy, part 1: diagnosis, and pharmacological and psychosocial management. *Lancet Neurol* 9: 77-93

Bushby KMD (1999) Making sense of the limb-girdle muscular dystrophies. *Brain* 122: 1403-1420

Carotti M, Fecchio C, Sandona D (2017) Emerging therapeutic strategies for sarcoglycanopathy. *Expert Opin Orphan D* 5: 381-396

Carotti M, Marsolier J, Soardi M, Bianchini E, Gomiero C, Fecchio C, Henriques SF, Betto R, Sacchetto R, Richard I, Sandona D (2018) Repairing folding-defective alpha-sarcoglycan mutants

by CFTR correctors, a potential therapy for limb-girdle muscular dystrophy 2D. *Hum Mol Genet* 27: 969-984

Carotti M, Scano M, Fancello I, Richard I, Risato G, Bensalah M, Soardi M, Sandona D (2020) Combined Use of CFTR Correctors in LGMD2D Myotubes Improves Sarcoglycan Complex Recovery. *Int J Mol Sci* 21

Carrie A, Piccolo F, Leturcq F, de Toma C, Azibi K, Beldjord C, Vallat JM, Merlini L, Voit T, Sewry C, Urtizberea JA, Romero N, Tome FM, Fardeau M, Sunada Y, Campbell KP, Kaplan JC, Jeanpierre M (1997) Mutational diversity and hot spots in the alpha-sarcoglycan gene in autosomal recessive muscular dystrophy (LGMD2D). *J Med Genet* 34: 470-5

Chan YM, Bonnemann CG, Lidov HG, Kunkel LM (1998) Molecular organization of sarcoglycan complex in mouse myotubes in culture. *J Cell Biol* 143: 2033-44

Chaudhuri TK, Paul S (2006) Protein-misfolding diseases and chaperone-based therapeutic approaches. *FEBS J* 273: 1331-49

Chen JW, Shi WX, Zhang YG, Sokol R, Cai H, Lun MY, Moore BF, Farber MJ, Stepanchick JS, Bonnemann CG, Chan YMM (2006) Identification of functional domains in sarcoglycans essential for their interaction and plasma membrane targeting. *Exp Cell Res* 312: 1610-1625

Clancy JP, Rowe SM, Accurso FJ, Aitken ML, Amin RS, Ashlock MA, Ballmann M, Boyle MP, Bronsveld I, Campbell PW, De Boeck K, Donaldson SH, Dorkin HL, Dunitz JM, Durie PR, Jain M, Leonard A, McCoy KS, Moss RB, Pilewski JM et al. (2012) Results of a phase IIa study of VX-809, an investigational CFTR corrector compound, in subjects with cystic fibrosis homozygous for the F508del-CFTR mutation. *Thorax* 67: 12-8

Coral-Vazquez R, Cohn RD, Moore SA, Hill JA, Weiss RM, Davisson RL, Straub V, Barresi R, Bansal D, Hrstka RF, Williamson R, Campbell KP (1999) Disruption of the sarcoglycan-sarcospan complex in vascular smooth muscle: a novel mechanism for cardiomyopathy and muscular dystrophy. *Cell* 98: 465-74

Cui X, Shi Y, Zhao L, Gu S, Wei C, Yang Y, Wen S, Chen H, Ge J (2018) Application of Real-Time Quantitative PCR to Detect Mink Circovirus in Naturally and Experimentally Infected Minks. *Front Microbiol* 9: 937

Davison HR, Taylor S, Drake C, Phuan PW, Derichs N, Yao C, Jones EF, Sutcliffe J, Verkman AS, Kurth MJ (2011) Functional fluorescently labeled bithiazole DeltaF508-CFTR corrector imaged in whole body slices in mice. *Bioconjug Chem* 22: 2593-9

de Wilde G, Gees M, Musch S, Verdonck K, Jans M, Wesse AS, Singh AK, Hwang TC, Christophe T, Pizzonero M, Van der Plas S, Desroy N, Cowart M, Stouten P, Nelles L, Conrath

K (2019) Identification of GLPG/ABBV-2737, a Novel Class of Corrector, Which Exerts Functional Synergy With Other CFTR Modulators. *Front Pharmacol* 10: 514

Dickens NJ, Beatson S, Ponting CP (2002) Cadherin-like domains in alpha-dystroglycan, alpha/epsilon-sarcoglycan and yeast and bacterial proteins. *Curr Biol* 12: R197-9

Dincer P, Bonnemann CG, Erdir Aker O, Akcoren Z, Nigro V, Kunkel LM, Topalolu H (2000) A homozygous nonsense mutation in delta-sarcoglycan exon 3 in a case of LGMD2F. *Neuromuscul Disord* 10: 247-50

Dombernowsky NW, Olmestig JNE, Witting N, Kruuse C (2018) Role of neuronal nitric oxide synthase (nNOS) in Duchenne and Becker muscular dystrophies - Still a possible treatment modality? *Neuromuscul Disord* 28: 914-926

Draviam RA, Shand SH, Watkins SC (2006) The beta-delta-core of sarcoglycan is essential for deposition at the plasma membrane. *Muscle Nerve* 34: 691-701

Duclos F, Straub V, Moore SA, Venzke DP, Hrstka RF, Crosbie RH, Durbeej M, Lebakken CS, Ettinger AJ, van der Meulen J, Holt KH, Lim LE, Sanes JR, Davidson BL, Faulkner JA, Williamson R, Campbell KP (1998) Progressive muscular dystrophy in alpha-sarcoglycan-deficient mice. *J Cell Biol* 142: 1461-71

Dudda A, Kuerzel GU (2013) Metabolism Studies In Vitro and In Vivo. In *Drug Discovery and Evaluation: Safety and Pharmacokinetic Assays*, pp 1053-1094.

Duggan DJ, Gorospe JR, Fanin M, Hoffman EP, Angelini C (1997) Mutations in the sarcoglycan genes in patients with myopathy. *N Engl J Med* 336: 618-24

Durbeej M, Cohn RD, Hrstka RF, Moore SA, Allamand V, Davidson BL, Williamson RA, Campbell KP (2000) Disruption of the beta-sarcoglycan gene reveals pathogenetic complexity of limb-girdle muscular dystrophy type 2E. *Mol Cell* 5: 141-51

Ehmsen J, Poon E, Davies K (2002) The dystrophin-associated protein complex. *J Cell Sci* 115: 2801-3

Ettinger AJ, Feng G, Sanes JR (1997) epsilon-Sarcoglycan, a broadly expressed homologue of the gene mutated in limb-girdle muscular dystrophy 2D. *J Biol Chem* 272: 32534-8

Eymard B, Romero NB, Leturcq F, Piccolo F, Carrie A, Jeanpierre M, Collin H, Deburgrave N, Azibi K, Chaouch M, Merlini L, Themar-Noel C, Penisson I, Mayer M, Tanguy O, Campbell KP, Kaplan JC, Tome FM, Fardeau M (1997) Primary adhalinopathy (alpha-sarcoglycanopathy): clinical, pathologic, and genetic correlation in 20 patients with autosomal recessive muscular dystrophy. *Neurology* 48: 1227-34

Fanin M, Tasca E, Nascimbeni AC, Angelini C (2009) Sarcolemmal neuronal nitric oxide synthase defect in limb-girdle muscular dystrophy: an adverse modulating factor in the disease course? *J Neuropathol Exp Neurol* 68: 383-90

Gastaldello S, D'Angelo S, Franzoso S, Fanin M, Angelini C, Betto R, Sandona D (2008) Inhibition of proteasome activity promotes the correct localization of disease-causing alpha-sarcoglycan mutants in HEK-293 cells constitutively expressing beta-, gamma-, and delta-sarcoglycan. *Am J Pathol* 173: 170-81

Gonzalez-Quereda L, Gallardo E, Topf A, Alonso-Jimenez A, Straub V, Rodriguez MJ, Lleixa C, Illa I, Gallano P, Diaz-Manera J (2018) A new mutation of the SCGA gene is the cause of a late onset mild phenotype limb girdle muscular dystrophy type 2D with axial involvement. *Neuromuscul Disord* 28: 633-638

Guglieri M, Magri F, D'Angelo MG, Prelle A, Morandi L, Rodolico C, Cagliani R, Mora M, Fortunato F, Bordoni A, Del Bo R, Ghezzi S, Pagliarani S, Lucchiari S, Salani S, Zecca C, Lamperti C, Ronchi D, Aguennouz M, Ciscato P et al. (2008) Clinical, molecular, and protein correlations in a large sample of genetically diagnosed Italian limb girdle muscular dystrophy patients. *Hum Mutat* 29: 258-66

Hack AA, Ly CT, Jiang F, Clendenin CJ, Sigrist KS, Wollmann RL, McNally EM (1998) Gamma-sarcoglycan deficiency leads to muscle membrane defects and apoptosis independent of dystrophin. *J Cell Biol* 142: 1279-87

Hauck B, Xiao W (2003) Characterization of tissue tropism determinants of adeno-associated virus type 1. *J Virol* 77: 2768-74

Henriques SF, Patissier C, Bourg N, Fecchio C, Sandona D, Marsolier J, Richard I (2018) Different outcome of sarcoglycan missense mutation between human and mouse. *PLoS One* 13: e0191274

Higuchi I, Kawai H, Umaki Y, Kawajiri M, Adachi K, Fukunaga H, Nakagawa M, Arimura K, Osame M (1998) Different manners of sarcoglycan expression in genetically proven alpha-sarcoglycan deficiency and gamma-sarcoglycan deficiency. *Acta Neuropathol* 96: 202-6

Holt KH, Campbell KP (1998) Assembly of the sarcoglycan complex. Insights for muscular dystrophy. *J Biol Chem* 273: 34667-70

Homburger F, Baker JR, Nixon CW, Wilgram G (1962) New hereditary disease of Syrian hamsters. Primary, generalized polymyopathy and cardiac necrosis. *Arch Intern Med* 110: 660-2

Imamura M, Mochizuki Y, Engvall E, Takeda S (2005) Epsilon-sarcoglycan compensates for lack of alpha-sarcoglycan in a mouse model of limb-girdle muscular dystrophy. *Hum Mol Genet* 14: 775-83

Jimenez AG, Dillaman RM, Kinsey ST (2013) Large fibre size in skeletal muscle is metabolically advantageous. *Nat Commun* 4

John R, Herzenberg AM (2009) Renal toxicity of therapeutic drugs. *J Clin Pathol* 62: 505-15

Jumper J, Evans R, Pritzel A, Green T, Figurnov M, Ronneberger O, Tunyasuvunakool K, Bates R, Zidek A, Potapenko A, Bridgland A, Meyer C, Kohl SAA, Ballard AJ, Cowie A, Romera-Paredes B, Nikolov S, Jain R, Adler J, Back T et al. (2021) Highly accurate protein structure prediction with AlphaFold. *Nature*

Jung D, Duclos F, Apostol B, Straub V, Lee JC, Allamand V, Venzke DP, Sunada Y, Moomaw CR, Leveille CJ, Slaughter CA, Crawford TO, McPherson JD, Campbell KP (1996) Characterization of delta-sarcoglycan, a novel component of the oligomeric sarcoglycan complex involved in limb-girdle muscular dystrophy. *J Biol Chem* 271: 32321-9

Kabadi AM, Thakore PI, Vockley CM, Ousterout DG, Gibson TM, Guilak F, Reddy TE, Gersbach CA (2015) Enhanced MyoD-induced transdifferentiation to a myogenic lineage by fusion to a potent transactivation domain. *ACS Synth Biol* 4: 689-99

Kleiner DE (2018) Recent Advances in the Histopathology of Drug-Induced Liver Injury. *Surg Pathol Clin* 11: 297-311

Knights KM, Stresser DM, Miners JO, Crespi CL (2016) In Vitro Drug Metabolism Using Liver Microsomes. *Curr Protoc Pharmacol* 74: 7 8 1-7 8 24

Kobuke K, Piccolo F, Garringer KW, Moore SA, Sweezer E, Yang B, Campbell KP (2008) A common disease-associated missense mutation in alpha-sarcoglycan fails to cause muscular dystrophy in mice. *Hum Mol Genet* 17: 1201-13

Lim LE, Duclos F, Broux O, Bourg N, Sunada Y, Allamand V, Meyer J, Richard I, Moomaw C, Slaughter C, et al. (1995) Beta-sarcoglycan: characterization and role in limb-girdle muscular dystrophy linked to 4q12. *Nat Genet* 11: 257-65

Liu F, Zhang Z, Csanady L, Gadsby DC, Chen J (2017) Molecular Structure of the Human CFTR Ion Channel. *Cell* 169: 85-95 e8

Liu LA, Engvall E (1999) Sarcoglycan isoforms in skeletal muscle. *J Biol Chem* 274: 38171-6

Loo TW, Bartlett MC, Clarke DM (2013) Bithiazole correctors rescue CFTR mutants by two different mechanisms. *Biochemistry* 52: 5161-3

Loo TW, Bartlett MC, Shi L, Clarke DM (2012) Corrector-mediated rescue of misprocessed CFTR mutants can be reduced by the P-glycoprotein drug pump. *Biochem Pharmacol* 83: 345-54

Lopes-Pacheco M (2019) CFTR Modulators: The Changing Face of Cystic Fibrosis in the Era of Precision Medicine. *Front Pharmacol* 10: 1662

Matsumura K, Campbell KP (1993) Deficiency of dystrophin-associated proteins: a common mechanism leading to muscle cell necrosis in severe childhood muscular dystrophies. *Neuromuscul Disord* 3: 109-18

McNally EM, Passos-Bueno MR, Bonnemann CG, Vainzof M, de Sa Moreira E, Lidov HG, Othmane KB, Denton PH, Vance JM, Zatz M, Kunkel LM (1996) Mild and severe muscular dystrophy caused by a single gamma-sarcoglycan mutation. *Am J Hum Genet* 59: 1040-7

McNally EM, Yoshida M, Mizuno Y, Ozawa E, Kunkel LM (1994) Human adhalin is alternatively spliced and the gene is located on chromosome 17q21. *Proc Natl Acad Sci U S A* 91: 9690-4

Mendell JR, Chicoine LG, Al-Zaidy SA, Sahenk Z, Lehman K, Lowes L, Miller N, Alfano L, Galliers B, Lewis S, Murrey D, Peterson E, Griffin DA, Church K, Cheatham S, Cheatham J, Hogan MJ, Rodino-Klapac LR (2019) Gene Delivery for Limb-Girdle Muscular Dystrophy Type 2D by Isolated Limb Infusion. *Hum Gene Ther* 30: 794-801

Mercuri E, Bonnemann CG, Muntoni F (2019) Muscular dystrophies. *Lancet* 394: 2025-2038

Mohassel P, Bönnemann CG (2015) Limb-girdle Muscular Dystrophies. In *Neuromuscular Disorders of Infancy, Childhood, and Adolescence*, pp 635-666.

Morandi L, Barresi R, Di Blasi C, Jung D, Sunada Y, Confalonieri V, Dworzak F, Mantegazza R, Antozzi C, Jarre L, Pini A, Gobbi G, Bianchi C, Cornelio F, Campbell KP, Mora M (1996) Clinical heterogeneity of adhalin deficiency. *Ann Neurol* 39: 196-202

Moreira ES, Vainzof M, Suzuki OT, Pavanello RC, Zatz M, Passos-Bueno MR (2003) Genotype-phenotype correlations in 35 Brazilian families with sarcoglycanopathies including the description of three novel mutations. *J Med Genet* 40: E12

Mouisel E, Vignaud A, Hourde C, Butler-Browne G, Ferry A (2010) Muscle weakness and atrophy are associated with decreased regenerative capacity and changes in mTOR signaling in skeletal muscles of venerable (18-24-month-old) dystrophic mdx mice. *Muscle Nerve* 41: 809-18

Naso MF, Tomkowicz B, Perry WL, 3rd, Strohl WR (2017) Adeno-Associated Virus (AAV) as a Vector for Gene Therapy. *BioDrugs* 31: 317-334

Negroni E, Bigot A, Butler-Browne GS, Trollet C, Mouly V (2016) Cellular Therapies for Muscular Dystrophies: Frustrations and Clinical Successes. *Hum Gene Ther* 27: 117-26

Nigro V, Piluso G, Belsito A, Politano L, Puca AA, Papparella S, Rossi E, Viglietto G, Esposito MG, Abbondanza C, Medici N, Molinari AM, Nigro G, Puca GA (1996) Identification of a novel

sarcoglycan gene at 5q33 encoding a sarcolemmal 35 kDa glycoprotein. *Hum Mol Genet* 5: 1179-86

Noguchi S, Wakabayashi E, Imamura M, Yoshida M, Ozawa E (2000) Formation of sarcoglycan complex with differentiation in cultured myocytes. *Eur J Biochem* 267: 640-8

Okiyoneda T, Veit G, Dekkers JF, Bagdany M, Soya N, Xu H, Roldan A, Verkman AS, Kurth M, Simon A, Hegedus T, Beekman JM, Lukacs GL (2013) Mechanism-based corrector combination restores DeltaF508-CFTR folding and function. *Nat Chem Biol* 9: 444-54

Oliveira Santos M, Coelho P, Roque R, Conceicao I (2020) Very late-onset limb-girdle muscular dystrophy type 2D: A milder form with a normal muscle biopsy. *J Clin Neurosci* 72: 471-473

Pacak CA, Conlon T, Mah CS, Byrne BJ (2008) Relative persistence of AAV serotype 1 vector genomes in dystrophic muscle. *Genet Vaccines Ther* 6: 14

Pacak CA, Walter GA, Gaidosh G, Bryant N, Lewis MA, Germain S, Mah CS, Campbell KP, Byrne BJ (2007) Long-term skeletal muscle protection after gene transfer in a mouse model of LGMD-2D. *Mol Ther* 15: 1775-81

Pedemonte N, Lukacs GL, Du K, Caci E, Zegarra-Moran O, Galietta LJ, Verkman AS (2005) Small-molecule correctors of defective DeltaF508-CFTR cellular processing identified by high-throughput screening. *J Clin Invest* 115: 2564-71

Pelkonen O, Kaltiala EH, Larmi TK, Karki NT (1974) Cytochrome P-450-linked monooxygenase system and drug-induced spectral interactions in human liver microsomes. *Chem Biol Interact* 9: 205-16

Pogue RE, Cavalcanti DP, Shanker S, Andrade RV, Aguiar LR, de Carvalho JL, Costa FF (2018) Rare genetic diseases: update on diagnosis, treatment and online resources. *Drug Discov Today* 23: 187-195

Powers ET, Morimoto RI, Dillin A, Kelly JW, Balch WE (2009) Biological and chemical approaches to diseases of proteostasis deficiency. *Annu Rev Biochem* 78: 959-91

Pozsgai ER, Griffin DA, Heller KN, Mendell JR, Rodino-Klapac LR (2017) Systemic AAV-Mediated beta-Sarcoglycan Delivery Targeting Cardiac and Skeletal Muscle Ameliorates Histological and Functional Deficits in LGMD2E Mice. *Mol Ther* 25: 855-869

Qi L, Tsai B, Arvan P (2017) New Insights into the Physiological Role of Endoplasmic Reticulum-Associated Degradation. *Trends Cell Biol* 27: 430-440

Ramachandran R, Kakar S (2009) Histological patterns in drug-induced liver disease. *J Clin Pathol* 62: 481-92

Rando TA (2001) The dystrophin-glycoprotein complex, cellular signaling, and the regulation of cell survival in the muscular dystrophies. *Muscle Nerve* 24: 1575-94

Reed GA (2016) Stability of Drugs, Drug Candidates, and Metabolites in Blood and Plasma. *Curr Protoc Pharmacol* 75: 7 6 1-7 6 12

Roberds SL, Anderson RD, Ibraghimov-Beskrovnaya O, Campbell KP (1993) Primary structure and muscle-specific expression of the 50-kDa dystrophin-associated glycoprotein (adhalin). *J Biol Chem* 268: 23739-42

Roberds SL, Leturcq F, Allamand V, Piccolo F, Jeanpierre M, Anderson RD, Lim LE, Lee JC, Tome FM, Romero NB, et al. (1994) Missense mutations in the adhalin gene linked to autosomal recessive muscular dystrophy. *Cell* 78: 625-33

Rodino-Klapac LR, Lee JS, Mulligan RC, Clark KR, Mendell JR (2008) Lack of toxicity of alpha-sarcoglycan overexpression supports clinical gene transfer trial in LGMD2D. *Neurology* 71: 240-7

Rossi CA, Flaibani M, Blaauw B, Pozzobon M, Figallo E, Reggiani C, Vitiello L, Elvassore N, De Coppi P (2011) In vivo tissue engineering of functional skeletal muscle by freshly isolated satellite cells embedded in a photopolymerizable hydrogel. *FASEB J* 25: 2296-304

Sampson HM, Lam H, Chen PC, Zhang D, Mottillo C, Mirza M, Qasim K, Shrier A, Shyng SL, Hanrahan JW, Thomas DY (2013) Compounds that correct F508del-CFTR trafficking can also correct other protein trafficking diseases: an in vitro study using cell lines. *Orphanet J Rare Dis* 8: 11

Sandona D, Betto R (2009) Sarcoglycanopathies: molecular pathogenesis and therapeutic prospects. *Expert Rev Mol Med* 11: e28

Sandona D, Gastaldello S, Martinello T, Betto R (2004) Characterization of the ATP-hydrolysing activity of alpha-sarcoglycan. *Biochem J* 381: 105-12

Scano M, Benetollo A, Nogara L, Bondi M, Dalla Barba F, Soardi M, Furlan S, Akyurek EE, Caccin P, Carotti M, Sacchetto R, Blaauw B, Sandona D (2021) CFTR corrector C17 is effective in muscular dystrophy, in vivo proof of concept in LGMDR3. *Hum Mol Genet*

Shakya AK, Al-Najjar BO, Deb PK, Naik RR, Tekade RK (2018) First-Pass Metabolism Considerations in Pharmaceutical Product Development. In *Dosage Form Design Considerations*, pp 259-286.

Sheikh MO, Halmo SM, Wells L (2017) Recent advancements in understanding mammalian O-mannosylation. *Glycobiology* 27: 806-819

Shi W, Chen Z, Schottenfeld J, Stahl RC, Kunkel LM, Chan YM (2004) Specific assembly pathway of sarcoglycans is dependent on beta- and delta-sarcoglycan. *Muscle Nerve* 29: 409-19

Soheili T, Gicquel E, Poupiot J, N'Guyen L, Le Roy F, Bartoli M, Richard I (2012) Rescue of sarcoglycan mutations by inhibition of endoplasmic reticulum quality control is associated with minimal structural modifications. *Hum Mutat* 33: 429-39

Spracklin DK, Kalgutkar AS, Nedderman ANR (2013) The Role of Biotransformation Studies in Reducing Drug Attrition. In *Reducing Drug Attrition*, pp 97-137.

Springer M, Moco S (2019) Resveratrol and Its Human Metabolites-Effects on Metabolic Health and Obesity. *Nutrients* 11

Straub V, Campbell KP (1997) Muscular dystrophies and the dystrophin-glycoprotein complex. *Curr Opin Neurol* 10: 168-75

Straub V, Murphy A, Udd B, group Lws (2018) 229th ENMC international workshop: Limb girdle muscular dystrophies - Nomenclature and reformed classification Naarden, the Netherlands, 17-19 March 2017. *Neuromuscul Disord* 28: 702-710

Szultka-Mlynska M, Buszewski B (2016) Study of in-vitro metabolism of selected antibiotic drugs in human liver microsomes by liquid chromatography coupled with tandem mass spectrometry. *Anal Bioanal Chem* 408: 8273-8287

Takano A, Bonnemann CG, Honda H, Sakai M, Feener CA, Kunkel LM, Sobue G (2000) Intrafamilial phenotypic variation in limb-girdle muscular dystrophy type 2C with compound heterozygous mutations. *Muscle Nerve* 23: 807-10

Tarakci H, Berger J (2016) The sarcoglycan complex in skeletal muscle. *Front Biosci (Landmark Ed)* 21: 744-56

Thompson R, Straub V (2016) Limb-girdle muscular dystrophies - international collaborations for translational research. *Nat Rev Neurol* 12: 294-309

Ueda K, Valdivia C, Medeiros-Domingo A, Tester DJ, Vatta M, Farrugia G, Ackerman MJ, Makielski JC (2008) Syntrophin mutation associated with long QT syndrome through activation of the nNOS-SCN5A macromolecular complex. *Proc Natl Acad Sci U S A* 105: 9355-60

Vainzof M, Passos-Bueno MR, Pavanello RC, Marie SK, Oliveira AS, Zatz M (1999) Sarcoglycanopathies are responsible for 68% of severe autosomal recessive limb-girdle muscular dystrophy in the Brazilian population. *J Neurol Sci* 164: 44-9

Vainzof M, Souza LS, Gurgel-Giannetti J, Zatz M (2021) Sarcoglycanopathies: an update. *Neuromuscul Disord*

Valastyan JS, Lindquist S (2014) Mechanisms of protein-folding diseases at a glance. *Dis Model Mech* 7: 9-14

van der Woerd WL, Wichers CG, Vestergaard AL, Andersen JP, Paulusma CC, Houwen RH, van de Graaf SF (2016) Rescue of defective ATP8B1 trafficking by CFTR correctors as a therapeutic strategy for familial intrahepatic cholestasis. *J Hepatol* 64: 1339-47

Veit G, Avramescu RG, Chiang AN, Houck SA, Cai Z, Peters KW, Hong JS, Pollard HB, Guggino WB, Balch WE, Skach WR, Cutting GR, Frizzell RA, Sheppard DN, Cyr DM, Sorscher EJ, Brodsky JL, Lukacs GL (2016) From CFTR biology toward combinatorial pharmacotherapy: expanded classification of cystic fibrosis mutations. *Mol Biol Cell* 27: 424-33

Vertex (2017) Vertex Announces Positive Phase 1 & Phase 2 Data from Three Different Triple Combination Regimens in People with Cystic Fibrosis Who Have One F508del Mutation and One Minimal Function Mutation. In https://investors.vrtx.com/news-releases/news-release-details/vertex-announces-positive-phase-1-phase-2-data-three-different

Vitiello C, Faraso S, Sorrentino NC, Di Salvo G, Nusco E, Nigro G, Cutillo L, Calabro R, Auricchio A, Nigro V (2009) Disease rescue and increased lifespan in a model of cardiomyopathy and muscular dystrophy by combined AAV treatments. *PLoS One* 4: e5051

Vrbanac J, Slauter R (2017) ADME in Drug Discovery. In *A Comprehensive Guide to Toxicology in Nonclinical Drug Development*, pp 39-67.

Walton JN, Nattrass FJ (1954) On the classification, natural history and treatment of the myopathies. *Brain* 77: 169-231

Wang YJ, Di XJ, Mu TW (2014) Using pharmacological chaperones to restore proteostasis. *Pharmacol Res* 83: 3-9

Wheeler MT, Zarnegar S, McNally EM (2002) Zeta-sarcoglycan, a novel component of the sarcoglycan complex, is reduced in muscular dystrophy. *Hum Mol Genet* 11: 2147-54

Winder SJ (2001) The complexities of dystroglycan. *Trends Biochem Sci* 26: 118-24

Wu G, Ai T, Kim JJ, Mohapatra B, Xi Y, Li Z, Abbasi S, Purevjav E, Samani K, Ackerman MJ, Qi M, Moss AJ, Shimizu W, Towbin JA, Cheng J, Vatta M (2008) alpha-1-syntrophin mutation and the long-QT syndrome: a disease of sodium channel disruption. *Circ Arrhythm Electrophysiol* 1: 193-201

Yagishita N, Aratani S, Leach C, Amano T, Yamano Y, Nakatani K, Nishioka K, Nakajima T (2012) RING-finger type E3 ubiquitin ligase inhibitors as novel candidates for the treatment of rheumatoid arthritis. *Int J Mol Med* 30: 1281-6

Yoo CL, Yu GJ, Yang B, Robins LI, Verkman AS, Kurth MJ (2008) 4 '-methyl-4,5 '-bithiazole-based correctors of defective Delta F508-CFTR cellular processing. *Bioorg Med Chem Lett* 18: 2610-2614

Zhang D, Luo G, Ding X, Lu C (2012) Preclinical experimental models of drug metabolism and disposition in drug discovery and development. *Acta Pharmaceutica Sinica B* 2: 549-561

Zhao J, Yang HT, Wasala L, Zhang K, Yue Y, Duan D, Lai Y (2019) Dystrophin R16/17 protein therapy restores sarcolemmal nNOS in trans and improves muscle perfusion and function. *Mol Med* 25: 31

Zincarelli C, Soltys S, Rengo G, Rabinowitz JE (2008) Analysis of AAV serotypes 1-9 mediated gene expression and tropism in mice after systemic injection. *Mol Ther* 16: 1073-80